

Modelling and Efficient Numerical Solution
of Hydrogeochemical Multicomponent
Transport Problems
by Process–Preserving Decoupling Techniques

Den Naturwissenschaftlichen Fakultäten
der Friedrich–Alexander–Universität Erlangen–Nürnberg
zur
Erlangung des Doktorgrades

vorgelegt von
Alexander Prechtel
aus Kulmbach

Als Dissertation genehmigt von den Naturwissenschaftlichen Fakultäten
der Universität Erlangen–Nürnberg

Tag der mündlichen Prüfung:	18. Mai 2005
Vorsitzender der Prüfungskommission:	Prof. Dr. D.-P. Häder
Erstberichterstatter:	Prof. Dr. P. Knabner
Zweitberichterstatter:	PD Dr. W. Merz, PD Dr. K. U. Totsche

Acknowledgements

First of all I want to thank my supervisor Prof. Dr. Peter Knabner for creating the possibility for me to work on this fascinating subject at the interface of mathematics and geosciences, for teaching me at the same time theoretical foundations and appreciating their transfer to applications. He kept me on the track when necessary and continuously supported me by sharing his knowledge. I am also grateful to PD Dr. Wilhelm Merz for providing his evaluation of this thesis – without complaining about time constraints. Next I am glad to express my gratitude to PD Dr. Kai Totsche, for many stimulating and encouraging discussions about models and much more, and for sharing his commitment to science with me.

Finally all my colleagues at the Institute of Applied Mathematics in Erlangen deserve my warmest gratitude, it always has been a pleasure to work in this convenient atmosphere. In particular, I want to thank Dr. Eckhard Schneid who was a patient tutor in the beginning of my work. Many thanks also to Dr. Markus Bause, Dr. Christof Eck, Dr. Serge Kräutle, and Dr. Florin Radu, whose doors were never closed – whether I sought a discussion about numerical analysis, software issues, reaction systems, or ... football.

I cannot proceed without thanking Alexandra, my parents, and all my friends for being there, and Monty Python for the dead parrot sketch. And now for something completely different.

*Erlangen, March 2005,
Alexander Prechtel*

Contents

Acknowledgements	iii
List of Figures	viii
List of Tables	xi
1 Introduction	1
1.1 Motivation	1
1.2 Previous Work	3
1.3 Objectives	5
1.4 Structure of the Work	5
2 The Mathematical Model of Reactive Transport in Porous Media	7
2.1 Starting Point: The General Transport Equation	8
2.2 Stoichiometric Reaction Mechanisms	9
2.3 Sorption Processes	16
2.3.1 Equilibrium Reaction	17
2.3.2 Reaction Kinetics (Non Equilibrium)	17
2.3.3 Carrier Facilitation	18
2.4 Biodegradation	19
2.4.1 Zeroth Order Kinetics	20
2.4.2 First Order Kinetics	20
2.4.3 Monod Kinetics	21
2.4.4 The Dual Monod Model	22
2.4.5 A General Multiplicative Monod Model	23
2.5 Kinetic Reactions: Mass Action Law	26
2.6 Thermodynamic Equilibrium Reactions	26
2.7 Scales of Transport and Reaction Processes	29
2.8 Regularisation of Reaction Terms	29

3	Reduction Schemes for the Multicomponent Problem	31
3.1	Elimination of Reaction Rates	31
3.2	General Reduction Schemes	33
4	Discretization of the Hydrogeochemical Multicomponent Model	37
4.1	Preliminaries	37
4.2	Variational Formulation of the Multicomponent Problem . . .	38
4.3	Conforming Finite Element Discretization	41
5	Solution Strategies – Algorithms	49
5.1	Operator Splitting	50
5.1.1	General Schemes	50
5.1.2	Commuting Operators	53
5.1.3	Splitting of ADR Equations	58
5.2	Fully Implicit Solution Strategy	65
5.2.1	Newton’s Method and Variants	66
5.2.2	Structure of the Jacobian	68
5.2.3	Process Preserving Decoupling Strategies	73
6	Numerical Examples of Reactive Multicomponent Transport	81
6.1	The EDTA Example Problem	81
6.2	Efficiency of Solution Strategies	85
6.2.1	Selective Coupling: Academic Examples	85
6.2.2	Selective Coupling: EDTA Example	88
6.3	An Experimental Study: Degradation of Propylene Glycol . .	90
6.3.1	Problem Description	90
6.3.2	Data	90
6.3.3	Modelling Approach	93
6.3.4	Simulations	95
6.3.5	Discussion and Conclusion	101
A	Implementation Issues	105
A.1	Componentwise Linear Sparse Matrix Solver	105
A.2	Compressed Data Storage and Efficient Assembling of the Ja- cobian	108
B	Notations	111
	Summary	113
	Zusammenfassung	115

Bibliography	118
Curriculum vitae	131

List of Figures

2.1	Carrier facilitated transport in a porous medium.	18
5.1	Algorithmic scheme for sequential iterative transport / reaction splitting.	65
5.2	Concentration profiles at selected time points ($t = 0, 10, 20, 30$) for the solute in the nonlinear model problem.	68
5.3	Comparison of computational effort for assembling and linear solving with growing number of coupled species for a nonlinear model problem.	76
5.4	l_2 -norm of the residual for the Newton iterations, left: timestep $\tau = 0.5$, right: $\tau = 0.7$	78
5.5	Summary of the maximum speed-up factors (CPU time fully coupled : CPU time decoupled) of several test cases.	79
6.1	Results for the EDTA-example of [CGS98]. Concentrations [mM/l] of species Co(II)-EDTA, Fe(III)-EDTA, EDTA, and biomass over time [h].	83
6.2	Results for the EDTA-example of [CGS98]. Concentrations [mM/l] of species over time [h].	84
6.3	Flux $q_{in}(t)$ at inflow $x = 0$ for PG experiments with columns S1 and S2.	92
6.4	Experimental breakthrough concentrations of PG at the outlet $x = 1.5$ dm of column S1 (left) and column S2 (right).	93
6.5	Simulation results and experimental breakthrough concentrations of PG at the outlet of column S1, see Table 6.6 for the corresponding biodegradation parameters, left: undamped reaction rate, right: damped by smaller growth rate and maximum biomass concentration.	97

6.6	Simulation results and experimental breakthrough concentrations of PG at the outlet of column S1 (cf. Table 6.6 for biodegradation parameters), left: unchanged parameters taken over from results of S2, right: same set with adjusted initial biomass and growth rate, compared to set Sim02.	97
6.7	Left: Biomass concentrations in S1 at the end ($t = 305$ h) of simulations Sim02 and Sim04; Right: Fe_o concentrations, data: at the end of all conducted experiments, simulations: after 900 h of simulated single experiment in S2.	98
6.8	Simulation results and experimental breakthrough concentrations of PG at the outlet of column S2; left: unchanged parameter set of S1 (Sim02); right: Sim06 and Sim07, similar breakthrough curves – different parameter sets.	100
6.9	PG data and simulation in S2, left: including sudden biomass decrease at $t = 150$ h, right: Sim07, and adjustments to flow reduction by linear flow decline (Sim10), or biomass decrease (Sim11).	101

List of Tables

5.1	Algorithm for the damped version of Newton's method with monotonicity test and Armijo's rule.	67
5.2	CPU time [s] for solving a nonlinear model problem with 16 uncoupled species.	69
5.3	Simplification of Jacobian: neglecting off-diagonal terms. Effect on number of Newton steps and time for solving.	77
6.1	Performance of the six species example for different decouplings and Damköhler numbers.	86
6.2	Performance of the twelve species example for different decouplings and Damköhler numbers.	87
6.3	Performance of three different coupling strategies for the EDTA example. CPU times in [s].	89
6.4	Soil and transport parameters of the PG degradation experiments.	91
6.5	Boundary conditions for the PG experiments with columns S1 and S2.	91
6.6	Degradation parameters of the simulations of soil column S1.	96
6.7	Degradation parameters of the simulations of soil column S2.	99

Chapter 1

Introduction

The background that motivates the investigation of hydrogeochemical transport problems is presented in Section 1.1. Section 1.2 gives a brief overview of previous work in the water resources and mathematical literature that is closely related to the subject of this thesis, the objectives of which are precised in Section 1.3. The chapter ends with Section 1.4 that contains an outline of the structure of the work.

1.1 Motivation

Water is the major constituent of almost all life forms on earth, without it life probably had never developed on our planet.

Although less than 3 % of the earth's water supply is freshwater, this portion is the decisive part that has to nourish not only mankind. While people in industrialized countries consume on average amounts of 130 liters per day in Germany, or almost 300 liters per day in the USA, less than five liters are actually used for drinking or cooking¹. The rest is spent for irrigation (65 %), industrial use (26 %), and in the household [dM95]. Water also serves as a 'means of transport' to dispose waste. In this case it returns to the hydrologic cycle in more or less polluted form. Less than 1 % of the global volume of water is groundwater, however, it is the most important resource for our drinking water.

The protection of the aquifers is indispensable to safeguard the groundwater and the surface waters and rivers that are fed by it. Nevertheless, groundwater and soil pollution has become a major environmental threat in the last century in particular in the industrialized countries. In Germany, more than 230 000 sites are suspect to contaminations, while more than 10 000 are

¹source: Bundesverband der deutschen Gas- und Wasserwirtschaft, www.bgw.de, 2004

officially classified as contaminated². A major challenge of water resources research in the 21st century will be the (de)contamination of water in general, and groundwater and natural soils in particular [dM95].

A spectrum of substances has been identified as contaminants in groundwater and soils, including solutes and (non aqueous phase) liquids, organic and anorganic chemicals as, e.g., petroleum and tar oils, phenols, metal complexes, radionuclides, and others. Risk assessment of the long term persistence, spreading, and toxicity of chemicals in the subsoil has thus to take into consideration a variety of physicochemical and biological processes.

The fate of chemicals in the soil/groundwater system, their repartition between different forms (ionic, as a complex, in solution, sorbed, etc.) depends on various factors as the pH value, temperature, the present mineral phases, the chemical interaction with other substances, or the presence of microorganisms [Fet99, SY98].

The contamination itself is often hardly accessible in the underground, and an evaluation of the hazardous potential has to be made on the basis of few measurements. Here, quantitative mathematical models of reactive subsurface transport can be a highly valuable tool. The description and formalisation of these processes as conceptual and mathematical models is a challenge in the geosciences and has evolved in the last decades. However, to be of practical use, it is compulsory that they are

- **comprehensive**, in the sense that they include all relevant processes of contaminant propagation and transformation,
- **accurate**, because the coupled highly nonlinear processes are highly sensitive to conceptual and numerical errors, and
- **efficient**, because the complexity of the problems makes their numerical solution very demanding, and thus requires advanced, sophisticated solution techniques.

Meeting these requirements a simulation tool may allow to study the interaction of complex processes, identify geochemical and hydrological factors that determine the fate of the contaminant, evaluate the risk potential of a site, transfer experimental results to the field scale, or optimize reclamation strategies [HWvC98].

Thus they can be of paramount importance – in conjunction with experiments – for the comprehension of the processes and to support site remediation, as also note Islam et al. (2001) in their review [ISO01]:

²source: Drucksache 15/3743, Antwort der Bundesregierung auf eine Kleine Anfrage, www.bmu.de/de/1024/js/download/b_kleine_anfrage_15_3743, 2004

A simulation model that couples the biogeochemical processes to the physical transport processes, [...], can be the key to understanding the movement of leachate and effectively managing the problem.

In particular assessing the potential of contaminated sites for natural attenuation in relevant orders of magnitude and time scales needs an estimation of future developments. The present work is closely related to that question due to several research projects (see p. 132).

The complexity of these problems is considerably high, in particular when multiple species and their various interactions are taken into account, and requires mathematically sound, efficient and accurate solution techniques. The mathematical treatment of the differential equation systems in this interdisciplinary field also aims at providing useful tools to handle environmental real world problems. In this sense geosciences should profit from the use of mathematical models and efficient implementations, and the work hopefully is a contribution to mathematics as a key technology to the future, as postulated by Jäger and Krebs (2003):

Direct, unfiltered access to the results of mathematical research and to the problems and data in real applications are equally important. [...] Experts are needed to translate relevant problems [...] into a mathematical setting. [...] prospecting for areas that can be better and faster explored using mathematical ideas and methods is an important but much neglected task. It is often forgotten that problems can be solved using computers and that mathematical modelling and new mathematical tools could provide better solutions faster and at less expense [JK03, page V].

Nevertheless it should be kept in mind that mathematical models are tools to solve problems, however they are not the solution itself, i.e., they cannot give answers to insufficiently defined problems [SM96a].

1.2 Previous Work

Along with the exponential increase of computational power in the seventies and eighties of the last century large complex simulations became feasible and the field of modelling and simulation of reactive transport in porous media flourished. As this domain of interest is highly interdisciplinary, involving expert knowledge from mathematics, computer science, physics, chemistry and biology, so is the literature widespread. This section is not intended to

give a broad literature review, but only cites some influential key publications closely related to the presented work.

The volume edited by Lichtner et al. (1996) on reactive transport in porous media [LSO96] gives a good overview on multicomponent transport modelling [Lic96] and solution approaches [SM96b], as well as microbial processes [RV96]. An earlier review on hydrological and hydrochemical models is [MT91].

However, there is a lack of adequate simulation tools that meet all the necessary requirements for reliable predictions. US EPA's BIOPLUME III, e.g., simulates aerobic and anaerobic biodegradation processes with predefined electron acceptors, but neglects microbial growth in Monod kinetics [RNG⁺98]. PHREEQC, on the other hand, is a complex geochemical reaction code, but lacks an appropriate flow description and biodegradation models [PA99]. These shortcomings of specialized codes are quite typical, as it is also stated in the review already cited in Section 1.1 [ISO01]:

Relatively few models include the interaction between biodegradation and inorganic geochemical reactions in soils.

The complexity of such comprehensive models is high, thus techniques become necessary to reduce the computational burden. The transformation of the species equations in order to decrease the number of coupled partial differential equations goes back to transformations in batch systems [AM63], has been depicted in the context of hydrogeochemical transport models in [Rub83], and later in [Fri91, FR92, CGS98]. Recent work in this domain is [KKar, MCAS04], but a general algorithm for all reaction types is still missing.

From the algorithmic point of view most complex multicomponent models are based on the operator splitting technique, as existing modules can easily be combined, e.g. [YT91, EK92, Saa96, SY98, SSK98, XPB99, CYSM00, vdLDLG03]. Several authors investigate the inherent splitting errors, mostly for simple reaction terms, and comparisons to analytical solutions or reference solutions on fine grids [VM92, MK95, BMCH96, KMK03, CMB04]. The accuracy of splitting schemes depends on the commutativity of the operators, it can be analyzed by a Lie operator formalism what has been demonstrated by Lanser and Verwer (1999) for a three-term Strang splitting scheme in air pollution problems [LV99], this concept is also presented in [HV03]. Yeh and Tripathi (1989) attempt to compare the algorithmic aspects of different solution approaches, namely the global implicit or one-step method, the direct substitution approach, and sequential methods [YT89]. Very few authors have up to date developed transport models with complex chemistry including heterogeneous reactions (phase transfer) and biodegradation all being

solved simultaneously, among them [Hol00] and [MFB02], both using a finite volume discretization.

A solution strategy based on the simultaneous treatment of strongly coupled subsets only has been described in [RVV00] so far.

Field and laboratory experiments together with advanced model applications can be found for a variety of specific problems. If biodegradation is involved, however, often simple first order decay is assumed. Schirmer et al. (2000) investigated the biodegradation of BTEX, a group of organic contaminants, and showed in a well defined experimental setting the value of identifying model parameters through laboratory experiments and transferred the data to the field scale. The modelling results were in excellent agreement with the measured plumes without further fitting of the parameters to field data, thus demonstrating the predictive capability of complex reactive transport models [Sch98, SMFB00].

1.3 Objectives

The scope of this work is the development and investigation of a versatile multicomponent contaminant transport model that incorporates a comprehensive treatment of the relevant hydraulic, chemical and biological processes in soils. For the coupled nonlinear systems of partial differential equations, discretized with a Finite Element Method, different algorithmic solution strategies have to be evaluated, in particular operator splitting errors assessed and efficiency improvements of the process-preserving one-step approach elaborated. This should yield a valuable tool for practical simulation studies dealing with the fate of contaminants in subsoils.

1.4 Structure of the Work

Following the introduction, which motivates and defines the objectives of the thesis and gives a brief overview on previous related work, a comprehensive description of the mathematical model components to quantify hydrogeochemical multicomponent transport in porous media is presented in Chapter 2.

Starting point is the general, scalar transport equation with advection and diffusion–dispersion in Section 2.1. An introduction to the formalism of chemical reaction systems is given in Section 2.2, together with the definitions of a canonical form for such systems, and an abstract formulation of a multicomponent model is given. The reaction rates are specified after-

wards, including sorption processes represented by isotherms (Section 2.3), biodegradation (Section 2.4), and kinetic and equilibrium reactions according to the law of mass action (Sections 2.5 and 2.6). Microbial processes are emphasized, and a general ansatz is presented based on Monod terms that allows to account for arbitrary reaction partners and also inhibitory substances.

Reduction approaches for general multicomponent models on the level of the mixed partial differential / algebraic equation system are briefly introduced in Chapter 3, which aim at simplifying the formulation through transformations of the equations.

The conforming finite element discretization of the hydrogeochemical transport model is depicted in Chapter 4 in general form, and precised for the implemented 1D situation with linear ansatz functions.

Chapter 5 concentrates on the solution approaches for the resulting coupled nonlinear equation system, which can be divided in splitting techniques and the global implicit approach. Operator splitting schemes are presented in Section 5.1, along with an investigation of the accuracy with the help of commutators and the Lie operator formalism. Section 5.2 focusses on the global implicit approach, that solves the coupled nonlinear system with a variant of Newton's method. The structure of the Jacobian matrix is depicted in detail, and simplifications are discussed that allow a decoupling of the differential equations what implies an essential reduction of the computational effort.

Numerical examples succeed in Chapter 6 with various purposes. First, a complex reaction system for EDTA transformation including fast and slow chemical kinetics and biodegradation is set up to verify the implementation (Section 6.1). It has already been used in the literature to test two other implementations of multicomponent models. Section 6.2 presents efficiency studies of the decoupling techniques for academic examples and the EDTA system. Finally the application of the simulation tool in a case study of anaerobic propylene glycol degradation demonstrates the use for analysing column experiments, and enhancing process comprehension (Section 6.3).

The appendix contains some technical information about the implementation in Chapter A, in particular of the linear sparse matrix solver (Section A.1), that is able to handle arbitrary combinations of subsets flexibly in each time step, and furthermore some notes about the assembling of the Jacobian are given in Section A.2. After gathering the notations in Appendix B, a summary in English and German concludes the work.

Chapter 2

The Mathematical Model of Reactive Transport in Porous Media

The governing equations describing reactive transport in porous media belong to the class of advection–dispersion–reaction equations. The basic form is presented in Section 2.1, and will be extended successively by different reaction or source and sink terms. Concerning reaction terms various processes can be taken into account, which result in linear or nonlinear models that may arbitrarily couple the equation systems. General chemical reaction systems will be introduced in Section 2.2. Sorption isotherms and degradation models can be interpreted as special cases of such general multicomponent models, but because of their self-contained development in the scientific literature they will be presented separately in Sections 2.3 and 2.4. Those are further on the crucial processes for the evaluation of the natural attenuation potential of a soil–groundwater system, together with geochemical reactions proceeding slowly with respect to the transport scale (Section 2.5), or fast (Section 2.6). The interaction of such nonlinear processes rises key questions, for which the application of mathematical models in the simulation of case studies comes into play as a valuable tool. For the risk assessment and the quantification of the hazardous potential of organic contaminants it is of special importance to apply an adequate model coupling chemical reactions and microbial degradation of these contaminants, because their propagation is not only retarded by degradation, but their total mass is actually reduced. Section 2.7 briefly comments on relevant scales of the processes, while in Section 2.8 the C^0 -regularization of kinetic reaction rates is given, which is needed for the proposed numerical solution of the problem.

2.1 Starting Point: The General Transport Equation

The following considerations deal with the basic type of a conservation law in the unknown c , the concentration of a chemical species, that reflects the fact that according to the law of mass conservation temporal changes of the concentration are only due to diffusive, dispersive or convective fluxes, or external sources and sinks. Detailed derivations can be found, e.g., in [DS98] or [dM86]. A general transport equation in a porous medium with variable water content can thus be formulated as

$$\partial_t(\Theta(x, t)c(x, t)) - \nabla \cdot (\mathbf{D}(x, t)\nabla c(x, t) - \mathbf{q}(x, t)c(x, t)) = R. \quad (2.1)$$

The notations are

$t \in (0, T)$	the time variable [T],
$x \in \Omega$	the space variable [L^d], $\Omega \subset \mathbb{R}^d$, $d \in \{1, 2, 3\}$,
Θ	the volumetric water content [-],
c	the solute concentration [M/L ³],
\mathbf{D}	the $d \times d$ diffusion–dispersion–tensor [L ² /T], and
\mathbf{q}	the vector of specific discharge (or Darcy velocity) in \mathbb{R}^d [L/T].

The general term R represents various sources or sinks in the domain, and any reactive processes (like sorption or decay). The specific functional form of this rate expression will not be fixed for the moment. It may be linear or nonlinear relationships that often have empirical roots and may depend on arbitrary other variables, in particular the concentrations of other chemical species, temperature, or the pH value. Sorption terms and decay functions can also be understood as such reaction rates. Thus R may be constant in special cases, but in general, it is a nonlinear, time and space dependent function:

$$R = R(c_1, \dots, c_{N_S}, x, t, T, \dots).$$

To include sorption mechanisms in this description, we allow R to contain the time derivative ∂_t of (sorbed) concentrations, however, we assume that it is not a function of a spatial derivative of c . Thus nonlinearities in the time derivative may also occur. Various kinds of rate expressions will be specified in the following sections for several relevant processes.

Water content Θ and water flux \mathbf{q} are in principle also functions of space and time. When we deal with stationary flow regimes both parameters may be given as constant values, but in general they are variable and are often determined by solving the Richards equation for flow in the vadose zone of soils (cf. [Bea72, DS98]).

For the calculation of particular solutions for the differential equation (2.1) we have to provide an appropriate initial condition $c(x, 0)$ for $x \in \Omega$, and corresponding boundary conditions on $\partial\Omega \times (0, T)$. These boundary conditions can prescribe

- the unknown c itself (*Dirichlet boundary condition*):

$$c = g_1 \quad \text{on } \Gamma_1 \times (0, T), \quad (2.2)$$

- the gradient of the unknown (*Neumann boundary condition*):

$$\mathbf{D}\nabla c \cdot \nu = g_2 \quad \text{on } \Gamma_2 \times (0, T), \quad (2.3)$$

- the normal component of the total flux (*flux boundary condition*):

$$(\mathbf{D}\nabla c - \mathbf{q}c) \cdot \nu = g_3 \quad \text{on } \Gamma_3 \times (0, T), \quad (2.4)$$

where ν denotes the outer unit normal, or

- a linear combination of the normal flux and the unknown (*mixed boundary condition*):

$$(\mathbf{D}\nabla c - \mathbf{q}c) \cdot \nu + \alpha c = g_4 \quad \text{on } \Gamma_4 \times (0, T). \quad (2.5)$$

We suppose that $\Gamma_1, \dots, \Gamma_4$ form a disjoint decomposition of $\partial\Omega$:

$$\partial\Omega = \Gamma_1 \cup \Gamma_2 \cup \Gamma_3 \cup \Gamma_4. \quad (2.6)$$

g_i and α in general depend on $x \in \partial\Omega$ and $t \in (0, T)$ (see also [KA03, Section 0.5]).

2.2 Stoichiometric Reaction Mechanisms

In the following the mathematical model of transport will be extended with rate expressions that correspond to chemical reaction mechanisms and can be formulated in terms of a stoichiometric equation.

A chemical reaction causes a redistribution of the (molar) masses in the system. We want to consider reactions of arbitrary type, the only restriction in this section being that they can be expressed in form of a stoichiometric equation. This includes, e.g., redox reactions (where electron transfers), acid-base reactions (with proton migrations), ion exchange or complexation. Basically we must distinguish different classes of reactions, that we have to

treat differently in the mathematical model (and the solution algorithm). Concerning the velocity of a reaction, sufficiently fast, reversible reactions have to be distinguished of slow and/or irreversible reactions (a comprehensive presentation can be found in [Rub83], see also Section 2.7).

We suppose that the reactions under consideration can be assigned uniquely to one of these two types, and that they do not change their type (due to strong temperature variations or other reasons).

Concerning the resulting differential equation systems we can also distinguish the group of heterogeneous reactions from the homogeneous reactions which only occur in one single phase (normally the aqueous one). In the field of hydrogeochemistry phase transitions between the liquid phase and solids (e.g. sorption phenomena) are of particular importance. But we may also think of transitions from the gaseous to the fluid phase.

First some concepts and definitions will be introduced, the presentation basically follows work of [AM63, SM96c] and [Saa96].

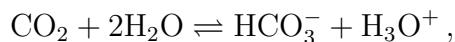
Definition 2.1 A *chemical species* is a chemical entity that can be characterized uniquely by

1. its molecular formula,
2. its molecular structure, and
3. the phase to which it belongs.

With the help of this definition we classify different isomers (as *cis*-1,2-dichloroethene and *trans*-1,2-DCE), or different states of the same substance (like gaseous carbon dioxide CO₂ and dissolved CO₂) as different species. A chemical system is thus a collection of N_S species and the N_E elements from which they are formed. To describe this system we can use the formula matrix.

Definition 2.2 The *formula matrix* A consists of column vectors $a_i, i = 1, \dots, N_S$ which contain the indices of the elements in the chemical formula of the i th species; $A = (a_1, \dots, a_{N_S}) \in \mathbb{R}^{N_E \times N_S}$.

Example 2.3 The formula matrix for a system that describes the reaction of dissolved CO₂ with H₂O to HCO₃⁻ and H₃O⁺,



a system with four species and three elements H, C and O, reads

$$\begin{array}{c} \text{C} \\ \text{O} \\ \text{H} \end{array} \begin{pmatrix} 1 & 0 & 1 & 0 \\ 2 & 1 & 3 & 1 \\ 0 & 2 & 1 & 3 \end{pmatrix} \cdot$$

$$\begin{array}{cccc} \text{CO}_2 & \text{H}_2\text{O} & \text{HCO}_3^- & \text{H}_3\text{O}^+ \end{array}$$

Thus we see that the formula matrix reflects the representation of the species by the chemical elements. For a consistent formulation of the system it is necessary that an element is understood as a unity that conserves its characteristics throughout all reactive transformations, i.e., in particular its oxidation state. This implies that an 'electron element' is being introduced, when redox reactions (electron transfers) occur, analogously proton elements for acid–base–reactions, and eventually neutrons for radioactive decay [Saa96]. The j th chemical reaction equation consists of the species including their stoichiometric coefficients $\nu_{ij}, i \in \{1, \dots, N_S\}, j \in \{1, \dots, N_R\}$:

$$\sum_{i=1}^{N_S} \nu_{ij} X_i \rightleftharpoons 0.$$

By convention the stoichiometric coefficients of products and reactants (the educts) differ in their sign, we choose $\nu_{ij} < 0$ for the products. They are uniquely defined only up to a constant factor, and there is no general agreement about a standard normalisation [AM63]. According to the convention chosen, the sign of the rate term must correspond to it. The relation between species and reaction equations is given by means of the stoichiometric matrix:

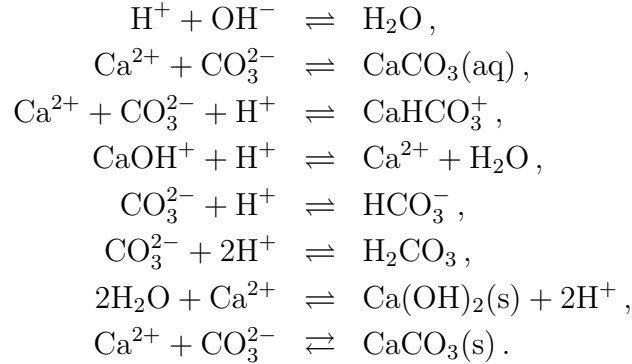
Definition 2.4 The *stoichiometric matrix* $V \in \mathbb{R}^{N_S \times N_R}$ consists of N_R column vectors that lie in the kernel (or null-space) of the formula matrix $\ker(A)$; the entries v_{ij} are the stoichiometric coefficients of the i th species X_i in the j th reaction.

Reactions have to leave the (molar) mass of elements unchanged.

Example 2.5 The simple system of Example 2.3 owns the following stoichiometric matrix $V \in \mathbb{R}^{4 \times 1}$:

$$V^T = \begin{pmatrix} 1 & 2 & -1 & -1 \\ \text{CO}_2 & \text{H}_2\text{O} & \text{HCO}_3^- & \text{H}_3\text{O}^+ \end{pmatrix}.$$

Example 2.6 The distribution of dissolved carbonate species plays a fundamental role in the aquatic geochemical system. It influences decisively the pH value calibration and thus the chemical composition of the ground water [SM96c]. The following example of calcite (CaCO_3) dissolution forms a part of this complex. We consider a system composed of $N_S = 12$ species that are built of $N_E = 4$ chemical elements, and $N_R = 8$ independent reactions, including one kinetic reaction (the last one in the following list):



So the formula matrix reads

$$\begin{array}{c} \text{H} \\ \text{O} \\ \text{Ca} \\ \text{C} \end{array} \begin{pmatrix} 1 & 2 & 0 & 0 & 1 & 0 & 1 & 1 & 1 & 2 & 2 & 0 \\ 0 & 1 & 0 & 3 & 1 & 3 & 3 & 1 & 3 & 3 & 2 & 3 \\ 0 & 0 & 1 & 0 & 0 & 1 & 1 & 1 & 0 & 0 & 1 & 1 \\ 0 & 0 & 0 & 1 & 0 & 1 & 1 & 0 & 1 & 1 & 0 & 1 \end{pmatrix}.$$

The columns correspond to the species $\text{H}^+, \text{H}_2\text{O}, \text{Ca}^{2+}, \text{CO}_3^{2-}, \text{OH}^-, \text{CaCO}_3(\text{aq}), \text{CaHCO}_3^+, \text{CaOH}^+, \text{HCO}_3^-, \text{H}_2\text{CO}_3, \text{Ca}(\text{OH})_2(\text{s}), \text{CaCO}_3(\text{s})$. The stoichiometric matrix $V \in \mathbb{R}^{12 \times 8}$ with rows attributed to those species in the same order can be given as

$$V = \begin{pmatrix} 1 & 0 & 1 & 1 & 1 & 2 & 2 & 0 \\ -1 & 0 & 0 & -1 & 0 & 0 & -2 & 0 \\ 0 & 1 & 1 & -1 & 0 & 0 & -1 & 1 \\ 0 & 1 & 1 & 0 & 1 & 1 & 0 & 1 \\ 1 & 0 & 0 & 0 & 0 & 0 & 0 & 0 \\ 0 & -1 & 0 & 0 & 0 & 0 & 0 & 0 \\ 0 & 0 & -1 & 0 & 0 & 0 & 0 & 0 \\ 0 & 0 & 0 & 1 & 0 & 0 & 0 & 0 \\ 0 & 0 & 0 & 0 & -1 & 0 & 0 & 0 \\ 0 & 0 & 0 & 0 & 0 & -1 & 0 & 0 \\ 0 & 0 & 0 & 0 & 0 & 0 & 1 & 0 \\ 0 & 0 & 0 & 0 & 0 & 0 & 0 & -1 \end{pmatrix}.$$

Defining $N_C := \text{rank}(A)$, the so-called (*basis*) *components* represent the minimum number N_C of building blocks which are necessary to express every species in the system. Evidently we have $N_C \leq N_E$, because we can represent every species by the N_E elements. $N_R = \dim(\ker(A))$ is thus the number of independent chemical reactions that can occur in the system, and we have from $N_S = \dim(\ker(A)) + \text{rank}(A) \Rightarrow N_R = N_S - N_C$. For an arbitrary chemical system we want to guarantee that the reactions we deal with are linearly independent, this reduces the effort for solving the system and eliminates redundant information. This can be achieved by a Gauss–Jordan transformation (cf. [Str03]) with elementary row and column operations on the stoichiometric matrix to obtain the reduced row echelon form (this is equivalent to the so-called tableaux form according to [MH93]). Thus the number of reactions can be reduced to a minimum by linear algebra without specific knowledge of the chemistry at hand [AM63]. This transformation results in

Definition 2.7 The *canonical form* of the formula matrix $A \in \mathbb{R}^{N_E \times N_S}$ and the stoichiometric matrix $V \in \mathbb{R}^{N_S \times N_R}$ is given by

$$A = \begin{pmatrix} I_{N_C} & \hat{A} \\ 0 & 0 \end{pmatrix}, \quad V = \begin{pmatrix} -\hat{A} \\ I_{N_R} \end{pmatrix}. \quad (2.7)$$

The dimensions are $N_C \times (N_S - N_C)$ for \hat{A} . We omit additionally the $(N_E - N_C)$ zero rows of A and want to refer in the following to these canonical forms as they constitute an efficient formulation for a chemical reaction system.

The submatrix $-\hat{A}$ in V is obtained by the requirement

$$AV = (I_{N_C} \hat{A}) \begin{pmatrix} \hat{V} \\ I_{N_R} \end{pmatrix} \stackrel{!}{=} 0 \Leftrightarrow \hat{V} = -\hat{A}. \quad (2.8)$$

Note that each reaction is composed of basis components and exactly one additional species which thus can be assigned to one specific reaction. This species is also called *product species* of this reaction, and it appears in exactly one reaction rate expression. A formal derivation of the canonical form is also given in [Hol00].

Example 2.8 The canonical form of the formula matrix of Example 2.3 is given by

$$A = \begin{pmatrix} 1 & 0 & 0 & 1 \\ 0 & 1 & 0 & 2 \\ 0 & 0 & 1 & -1 \end{pmatrix}.$$

As we obtained the canonical form in this case without interchanging columns, we can choose the species CO_2 , H_2O , and HCO_3^- as basis components. This

choice of course is not unique. Furthermore we have $\hat{V} = (-1, -2, 1)^T$, and $V = (-1, -2, 1, 1)^T$, $N_R = 1$.

Example 2.9 For the calcite example 2.6 possible basis components are given by H^+ , H_2O , Ca^{2+} , and CO_3^{2-} :

$$A = \begin{pmatrix} 1 & 0 & 0 & 0 & -1 & 0 & 1 & -1 & 1 & 2 & -2 & 0 \\ 0 & 1 & 0 & 0 & 1 & 0 & 0 & 1 & 0 & 0 & 2 & 0 \\ 0 & 0 & 1 & 0 & 0 & 1 & 1 & 1 & 0 & 0 & 1 & 1 \\ 0 & 0 & 0 & 1 & 0 & 1 & 1 & 0 & 1 & 1 & 0 & 1 \end{pmatrix},$$

$$V = \begin{pmatrix} 1 & 0 & -1 & 1 & -1 & -2 & 2 & 0 \\ -1 & 0 & 0 & -1 & 0 & 0 & 2 & 0 \\ 0 & -1 & -1 & -1 & 0 & 0 & -1 & -1 \\ 0 & -1 & -1 & 0 & -1 & -1 & 0 & -1 \\ 1 & 0 & 0 & 0 & 0 & 0 & 0 & 0 \\ 0 & 1 & 0 & 0 & 0 & 0 & 0 & 0 \\ 0 & 0 & 1 & 0 & 0 & 0 & 0 & 0 \\ 0 & 0 & 0 & 1 & 0 & 0 & 0 & 0 \\ 0 & 0 & 0 & 0 & 1 & 0 & 0 & 0 \\ 0 & 0 & 0 & 0 & 0 & 1 & 0 & 0 \\ 0 & 0 & 0 & 0 & 0 & 0 & 1 & 0 \\ 0 & 0 & 0 & 0 & 0 & 0 & 0 & 1 \end{pmatrix}.$$

With independent reactions the columns of V span the null-space of A , $\dim(\ker(A)) = N_R$, and $\dim(\text{Im}(A)) = \text{rank}(A) = N_C$. As

$$\ker(A) \oplus \ker(A)^\perp = \ker(A) \oplus \text{Im}(A^T) = \mathbb{R}^{N_s},$$

any composition (say any vector of species concentrations \mathbf{c}) of the system can be written in the form

$$\mathbf{c} = A^T \boldsymbol{\eta} + V \boldsymbol{\xi},$$

where the vector $\boldsymbol{\eta}$ consists of the reaction invariants of the system [Saa96]. In a closed (batch) system only the variations in $\boldsymbol{\xi}$ (the changes by reaction) are the determining factor. There we have $\mathbf{c} = \mathbf{c}_0 + V \boldsymbol{\xi}$ with a particular solution $\mathbf{c}_0 \in \mathbb{R}^{N_s}$ of $A \mathbf{c}_0 = \mathbf{e}$ (where \mathbf{e} is the element mole vector that consists of the total number of moles for each element in the system, cf. [Saa96]).

The transformed amount per time of a species X_i in the j th reaction is equal to $\nu_{ij} R_j$ with the reaction rate R_j [M/(L³T)] (the reaction rate should not be confounded with the rate constant of a reaction, which is also called

the velocity constant of the reaction and is given in units of $[1/T]$ for an elementary reaction). R represents the net rate of exchange in the reaction, this means in the case of reversible reactions forward – backward reaction rates.

Now we can state the following transport equation as a general reactive multicomponent model for the i th mobile species:

$$\partial_t(\Theta c_i) - \nabla \cdot (D \nabla c_i - \mathbf{q} c_i) = \Theta \sum_{j=1}^{N_R} \nu_{ij} R_j. \quad (2.9)$$

For immobile species the transport terms must be omitted and also the factor Θ that has related the solute concentration to the fluid volume. It remains

$$\partial_t c_i = \sum_{j=1}^{N_R} \nu_{ij} R_j. \quad (2.10)$$

Note that the concentrations of the immobile species (including microbial species) are also defined in units of $[M/L^3]$, and thus the conversion factor ρ_b (the bulk density) is not needed. To simplify the notation we introduce the transport operator $\mathcal{L} := \nabla \cdot (D \nabla - \mathbf{q})$ for $N_{S_{\text{mob}}}$ mobile species, and set $\mathcal{L} \equiv 0$ for the $N_{S_{\text{im}}}$ immobile species. By \mathcal{R} we denote a general reaction operator. Then for the complete system we can write

$$\partial_t \mathbf{c} - \mathcal{L}(\mathbf{c}) = V \mathcal{R}(\mathbf{c}^T), \quad (2.11)$$

or, if we include the stoichiometric factors in the reaction operator,

$$\partial_t \mathbf{c} - \mathcal{L}(\mathbf{c}) = \mathcal{R}(\mathbf{c}^T), \quad (2.12)$$

where $\mathbf{c} = (\Theta \mathbf{c}_{\text{mob}}, \mathbf{c}_{\text{im}})^T \in \mathbb{R}^{N_{S_{\text{mob}}}} \times \mathbb{R}^{N_{S_{\text{im}}}}$ comprises the mobile and immobile species.

Remark 2.10 Based on Definition 2.1 of the species and the choice of the basis and product components from the set of species (and not, e.g., from the chemical elements), it is guaranteed that every component X_i with associated concentration c_i can be uniquely identified as mobile or immobile. The choice of the basis is not unique, however (see also [Bet96] for basis changes). This formulation does not lead to linear combinations of species or elements, as other approaches may do (cf. Chapter 3), what can lead to linear combinations of unknowns under the transport operator.

For the efficient solution of a general multicomponent problem the system above should be reduced further. A crucial role plays the character of the rate expressions R , in particular their functional dependency upon other species concentrations. Another difficulty is the strong variability of the parameters and unknowns. Xu et al. [XPB99], e.g., report of variations in the concentration of more than *90 orders of magnitude* in an example of pyrite oxidation in the unsaturated zone.

For an efficient solution strategy of the resulting system the following aspects are promising:

- elimination of the explicitly unknown rate expressions of the equilibrium reactions;
- reduction of the number of coupled transport equations;
- limitation of the rate expressions to few transport equations;
- formation of the coupling of the PDEs as local as possible;
- simplification of the system by elimination of negligible coupling terms.

For the moment we refer to the species based forms (2.9) with (2.10), and (2.11).

2.3 Sorption Processes

On the one hand the ad- and desorption of a substance between the liquid phase and the solid matrix may be described in detail in form of a stoichiometric equation, and thus the formalism of Section 2.2 can be applied. On the other hand it can be modelled with the help of sorption isotherms that renounce the detailed description of the interaction of the relevant species and subsume the mechanism in describing the relation of sorbed mass to dissolved mass. This sorption isotherm is then incorporated in the conservation equation of the solute, and acts there as a (possibly nonlinear) retardation term. In this sense one can still speak of a single component model, that only accounts for the transition of a substance to another phase in form of a source/sink term in the equation of the solute. Remind, however, that the sorbed substance is a different species, conforming to Definition 2.1. According to the speed of this exchange process in relation to the time scales of the transport we distinguish equilibrium sorption (Section 2.3.1) and kinetic processes (Section 2.3.2). An extension of these sorption models is the consideration of carrier facilitated transport, where the sorbent additionally

may attach to a mobile carrier substance. This results in a so-called effective isotherm that will be introduced in Section 2.3.3.

2.3.1 Equilibrium Reaction

Standard modelling prescribes, at a given temperature and specific solute concentration c_i , an instantaneously sorbed concentration s_i by a relationship defined as so-called sorption isotherms ϕ of different functional forms:

$$\phi(c_i(x, t)) = s_i(x, t). \quad (2.13)$$

The functional dependence may be linear, but there are also widespread nonlinear formulations of so-called Freundlich or Langmuir types (cf., e.g., [Kna91, Fet99]). Another interesting approach is the representation by spline functions [IK98], which is of particular interest for parameter identification algorithms (inverse modelling). For a detailed description we refer to the given references. In general a sink (or more precisely retardation) term of the following type is added in the transport equation of the mobile species:

$$\partial_t(\Theta c_i) - \nabla \cdot (\mathbf{D}\nabla c_i - \mathbf{q}c_i) = -\rho_b \partial_t(\phi(c_i)). \quad (2.14)$$

This may lead to a nonlinearity of the concentration under the temporal derivative. Note that the sorbed concentration s_i usually is given in units of mass of sorbate per total mass [M/M]. For the appropriate relation in the volume related conservation equation it has to be multiplied with the bulk density ρ_b [M/L³].

2.3.2 Reaction Kinetics (Non Equilibrium)

A temporal evolution can be modelled, e.g., by a linear rate function to describe the transfer from the solid to the aqueous phase. We assume that the corresponding (limit) equilibrium state can be represented by an isotherm. The difference between the isotherm of the nonequilibrium reaction φ (describing the mass that can potentially be sorbed) and the actually sorbed concentration s_i is the driving force for the kinetics with the rate parameter k_i [1/T]:

$$\partial_t(\Theta c_i) - \nabla \cdot (\mathbf{D}\nabla c_i - \mathbf{q}c_i) = -\rho_b (k_i(\varphi(c_i) - s_i)), \quad \partial_t s_i = k_i(\varphi(c_i) - s_i). \quad (2.15)$$

Of course more complex forms of sorption isotherms are possible, and also have been realized in the simulation tool RICHY1D [Ins05] by the author and others, e.g. to account for multiple sorption sites, or the phenomenon of carrier facilitated transport, which will be treated in the following section.

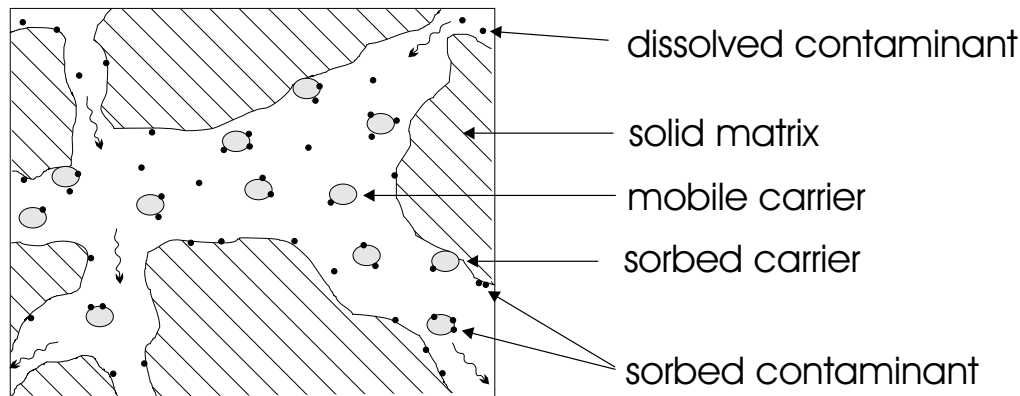


Figure 2.1: Carrier facilitated transport in a porous medium.

2.3.3 Carrier Facilitation

Carrier facilitated transport can represent the dominant mechanism for the migration of strongly sorbing contaminants as radionuclids or hydrophobic organic compounds (HOC). Here the additional sorption of a dissolved substance to macro molecules (mobile sorbents) in the liquid phase is being considered (see the schematic presentation in Figure 2.1). In the context of soils the most prominent carrier substance is dissolved organic matter. Abundant experimental evidence shows the potential of DOC to enhance [MZ89, DJTM92, JA95] or reduce the mobility of contaminants [SH96, TDKK97]. Thus neglecting the effect of carriers can result in strongly misleading predictions of the fate of a contaminant plume [PKST02].

Knabner et al. (1996) established a general, appropriate model [KTKK96, TKKK96] that is slightly simplified here to cope with a majority of relevant field situations. Prechtel et al. (2002) applied it for a simulation study with phenanthrene in a layered, unsaturated soil column to demonstrate the effects on contaminant migration [PKST02].

The contaminant's equilibrium isotherm (2.13) is replaced by an effective sorption isotherm ϕ_{eff} , including a linear model for the partitioning of contaminant and carrier, and consisting of a term for the sorption of the free contaminant and a term for the sorption of the carrier bound contaminant:

$$\psi_{\text{eff}}(c_i, c_c) = \underbrace{f_{\phi_f} \phi_f \left(\frac{1}{1 + c_c K} c_i \right)}_{\text{sorption of free solute}} + \underbrace{f_{\phi_c} \phi_c \left(\frac{c_c K}{1 + c_c K} c_i \right)}_{\text{sorption of carrier bound solute}} \quad . \quad (2.16)$$

Here, c_i is the total (free + carrier bound) dissolved concentration of the

contaminant, f_{ϕ_f} and f_{ϕ_c} are the mass fractions of the solid matrix providing equilibrium sorption sites for free HOC and for the carrier, respectively, ϕ_f and ϕ_c are the equilibrium sorption isotherms for free solute and for the carrier, c_c is the current solute concentration of the carrier, and K is the partition coefficient for the linear sorption of HOC to the carrier. Note that the term describing the sorption of carrier bound HOC only takes cumulative sorption into account, i.e., the binding of dissolved HOC to sorbed carrier. This effect is formally different from co-sorption, i.e., the sorption of HOC-loaded carrier particles. An additional model term could be easily added, however, the experimental distinction between the two effects is still questionable. Furthermore it is assumed that the transport of the contaminant has no influence on the transport behaviour of the carrier. In this sense the coupling of the partial differential equations is unidirectional.

For the derivation, further discussion and properties of the model, we refer to [KTKK96, TKKK96, KS96].

2.4 Biodegradation

The persistence and spreading of many organic contaminants is influenced decisively by the microbial activity in the soil. Microorganisms enable the degradation of these substances, and the rates of this transformation process depend on the nature of the contaminant, its concentration, the microorganisms, and a number of physicochemical factors. From the chemical point of view, the microbial degradation is mostly related to redox reactions. For energetic reasons these redox reactions proceed while sequentially consuming different electron acceptors present in the aquifers and thus lead to the formation of characteristic redox zones [HWvC98]. In the last decades several models for the description of biological decay processes have been developed. As a consequence of the sometimes rudimentary knowledge about the activity of microbial populations in the natural subsurface many of these formulations have been derived purely on an empirical basis, and thus the model parameters are just fitting parameters without a physical meaning. An overview can be found for example in [AS89]. In the following the renowned models will be presented (Sections 2.4.1–2.4.4), and a very general formulation that covers the preceding models as simplifications, but extends to arbitrary complex combinations of reaction partners, is finally derived in Section 2.4.5.

2.4.1 Zeroth Order Kinetics

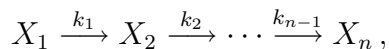
Zero order kinetics mathematically represents the simplest model for degradation processes. When we consider it as the r th reactive term in the equations (2.9) and (2.10), then we write

$$R_r = -S_r \quad [\text{M}/(\text{L}^3\text{T})], \quad r \in \{1, \dots, N_R\}, \quad (2.17)$$

i.e., a constant amount of the substance is lost per unit time. Note that (non-physical) negative concentrations may result from this model. Such a model should only be used for descriptive purposes. Predictive statements have to be reviewed very critically, in particular if a prognosis is given for concentration ranges where no measurements have been made [BWG98]. Nevertheless in the literature authors can be found that use this model for the description of field and laboratory data [RSK⁺97]. Under special circumstances it can be theoretically justified and be derived from the Monod model that is introduced in Section 2.4.3 [AS89], e.g. in the case of constant biomass, and substrate concentrations c_i that are distinctively higher than the Monod concentrations K_M : $c_i \gg K_M$.

2.4.2 First Order Kinetics

Degradation according to kinetics of first order corresponds to a loss of substance subject to an exponential decay, as it can occur for radioactive substances but also organic contaminants. The decay is determined only by the concentration itself and a constant factor. Kinetics of first order are widespread also because of their simple mathematical formulation. In comparison to the Monod model an approximation of first order can be valid or admissible for substrate concentrations $c_i \ll K_M$ and constant biomass concentrations. However several authors [AS89, RV96, BWG98] point out that due to their simplicity models of first order are often applied even when the necessary assumptions do not hold and the experimental situation does not justify it. The representation of the decay in form of first order kinetics in an elementary, irreversible reaction chain,



implies rate expressions of the following form in the equation of species X_i :

$$R_r = R_r(c_{i-1}, c_i) = Y_{i-1}k_{i-1}c_{i-1} - k_i c_i. \quad (2.18)$$

The mass balance equation for a product of such a decay reaction consequently contains a source term of the form $Y_{i-1}k_{i-1}c_{i-1}$ including a stoichiometric yield factor Y_{i-1} which characterizes the ratio of degraded substance

to generated substance. The rate constants k_i are determined empirically, but they depend strongly upon the specific site conditions and are not unique for one substance. These irreversible decay chains are also special cases of the considered general reaction problems (2.11).

2.4.3 Monod Kinetics

A more detailed analysis of microbial degradation mechanisms in soil–groundwater–systems shows that mostly redox reactions (i.e. electron transfers) are involved, and the biomass acts as a catalyst for these reactions [Cha01]. The activity and the growth of the biomass is essentially depending on the availability of an organic substrate, which besides the electrons also provides nutrients for the biomass, and a terminal electron acceptor (for details cf. [Cha01] or [RV96]). If – in a first stage – only the dependence of the degradation on substrate and biomass is considered the following holds: the consumption of the substrate first increases linearly for low contaminant concentrations c_i , before it attains a maximum rate which cannot be further augmented with higher concentrations and thus asymptotically rests at this maximum rate $\mu_{\max_r} c_{B_r}$. Monod (1949) observed this behaviour in work concerning bacterial growth and gave it a mathematical formulation, the following equation is therefore known as Monod model or Michaelis–Menten equation:

$$R_r = -\mu_{\max_r} \left(\frac{c_i}{K_{M_i} + c_i} \right) c_{B_r}. \quad (2.19)$$

μ_{\max_r} is the maximum specific substrate consumption rate [1/T], K_{M_i} the so-called Monod constant, i.e. the concentration value where the rate equals $\mu_{\max_r}/2$ (also known as half saturation concentration), and c_{B_r} is the biomass concentration. In its simplest form c_{B_r} is a constant, and therefore (2.19) is also called no-growth-kinetics. The biomass is considered in most cases as immobile. If the fact should be taken into account that the substrate can have a toxic effect on the microorganisms at higher concentrations, then the so-called Haldane model [AS89] can be applied that additionally incorporates an inhibition term:

$$R_r = -\mu_{\max_r} \left(\frac{c_i}{K_{M_i} + c_i + \frac{c_i^2}{K_{I_i}}} \right) c_{B_r}. \quad (2.20)$$

K_{I_i} denotes the Haldane inhibition concentration [M/L³]. This approach has already been used by Haldane in 1930 in work about enzyme kinetics [SMFB00]. The above degradation rates (2.19) and (2.20) enter analogously

with opposite sign as production (source) terms in the conservation equation of the biomass, with the slight correction of a yield factor Y_r [M/M] that takes into account the ratio of generated biomass per mass of consumed substrate, which of course needs not to be 1. The rate expression then reads

$$R_r = \mu_{\max,r} Y_r \left(\frac{c_i}{K_{M_i} + c_i} \right) c_{B_r}, \text{ or } R_r = \mu_{\max,r} Y_r \left(\frac{c_i}{K_{M_i} + c_i + \frac{c_i^2}{K_{I_i}}} \right) c_{B_r}. \quad (2.21)$$

2.4.4 The Dual Monod Model

Redox processes are responsible for the degradation of organic contaminants. If not only the availability of substrate and biomass, but also the limitation of the reaction by the necessary terminal electron acceptor should be taken into account in the mathematical model, another Monod term is being added. This results in the so-called double or dual Monod model that thus represents a three component system of electron donor (often an organic carbon species, index D), electron acceptor (e.g. oxygen, nitrate, index A), and immobile biomass (index B), which enables the oxidation of the substrate. The resulting degradation products are not considered explicitly in the Monod model, but of course it is possible to include a source term of Monod type, together with a stoichiometric factor, in a species' equation. The reaction rates R_r for donor and acceptor are then given by

$$R_r = -\mu_{\max,r} \left(\frac{c_D}{K_{M_D} + c_D + \frac{c_D^2}{K_{I_D}}} \right) \left(\frac{c_A}{K_{M_A} + c_A + \frac{c_A^2}{K_{I_A}}} \right) c_{B_r}. \quad (2.22)$$

The immobile biomass profits from the transformation, so here a source term results:

$$R_r = R_r(c_D, c_A, c_{B_r}) = Y_r \left(1 - \frac{c_{B_r}}{c_{B_{\max}}} \right) \mu_{\max,r} \left(\frac{c_D}{K_{M_D} + c_D + \frac{c_D^2}{K_{I_D}}} \right) \left(\frac{c_A}{K_{M_A} + c_A + \frac{c_A^2}{K_{I_A}}} \right) c_{B_r}. \quad (2.23)$$

This source term is supplemented by the penalty term $(1 - c_{B_r}/c_{B_{\max}})$, which inhibits the growth for $c_{B_r} \rightarrow c_{B_{\max}}$, and sets a maximum biomass concentration at $c_{B_{\max}}$. This corresponds to the observation that biomass does not grow in an unlimited, exponential fashion under natural site conditions, due

to limitations, e.g., of the available pore space, the production of inhibiting metabolites, or lack of nutrients [SMFB00]. In natural soils a variety of substrates and electron acceptors is available, but for energetic reasons there exists a sequence of preferred reactions: Supposing the corresponding substances are present, in the first place aerobic consumption occurs, then denitrification, reduction of manganese, reduction of ferric iron, sulfate reduction, and finally fermentation. The most important terminal electron acceptors of these transformations are, e.g., O_2 , NO_3^- , Fe(III) or SO_4^{2-} [HWvC98].

2.4.5 A General Multiplicative Monod Model

The three component model with rate expressions (2.22) and (2.23) can be generalized to account for the specific microbial reactions that take place in the different redox zones simultaneously: one should consider N_{Sbio} different microbial populations or species (index B_r , $r = 1, \dots, N_{\text{Sbio}}$). These may be characteristic for a specific decay chain (for example iron reducing microbes), but also the participation at several reactions is admitted (e.g. in the case of microorganisms that are able to perform aerobic degradation as well as nitrate reduction). Let N_{Rbio} denote the number of biochemical reactions in the system. We want to formulate a degradation term globally for all redox zones that respects that a microbial species may dominate the degradation of a substance in one redox zone, but in another region remains inactive due to unfavourable conditions. This must be controlled by inhibition functions that depend on the concentrations c_i of arbitrary species characteristic or at least influencing the processes in a redox zone.

The presented model (2.22) and (2.23) of Section 2.4.4 is not suitable for a generalization in this form, because it is not possible to reproduce the exclusively inhibiting effect of a species on a degradation pathway. In (2.22) an inhibiting substance with concentration $c_i = 0$ will always result in a rate R of zero, but in this case, degradation should be possible.

Therefore a generalization of the biological decay expression must separate Monod terms (i.e. growth terms) of the form $\frac{c_i}{K_{M_i} + c_i}$, and inhibition terms $h(c_j)$. One well-known proposal for the functional form of these inhibition terms according to [WMB88] is the following:

$$h(c_j) = \frac{K_{I_j}}{K_{I_j} + c_j}. \quad (2.24)$$

Thus a substance may either exclusively enhance or inhibit a reaction, but also do both simultaneously in different concentration ranges. This would not be possible by means of the proposed Haldane term in (2.20) and (2.21), or

in (2.22) and (2.23), there the exclusively inhibiting behaviour of a substance cannot be reflected by the model.

With (2.24) it follows the subsequent general reaction term in the equation of a chemical species that undergoes microbiological transformations, where we refer to a single biochemical reaction $r \in \{1, \dots, N_{\text{Rbio}}\}$:

$$\begin{aligned} R_r &= R_r(c_1, \dots, c_{N_S}, c_{B_r}) \\ &= -\mu_{\max_r} c_{B_r} \prod_{i \in I_r^1 \subset \{1, \dots, N_S\}} \left(\frac{c_i}{K_{M_i} + c_i} \right) \prod_{j \in I_r^2 \subset \{1, \dots, N_S\}} h(c_j). \end{aligned} \quad (2.25)$$

Here we want to use

Definition 2.11 In relation with biochemical degradation reactions we define the following index sets:

$$\begin{aligned} I_r^1 &:= \{i \in \{1, \dots, N_S\} \mid \text{species } X_i \text{ is being transformed in reaction } r\}, \\ I_r^2 &:= \{i \in \{1, \dots, N_S\} \mid \text{species } X_i \text{ inhibits reaction } r\}, \text{ and} \\ I^3 &:= \{i \in \{1, \dots, N_S\} \mid \text{species } X_i \text{ is a microbial species}\}. \end{aligned}$$

Furthermore let species X_{B_r} be the microbial species that catalyses the r th reaction ($B_r \in I^3$). The index set I_r^1 contains the indices of those chemical species that are being transformed in the r th reaction, i.e., in a simple case the indices of one electron donor and one acceptor.

For the complete biological reaction term of one species we have to sum over the single biochemical reactions where this species takes part. For the sake of a general formulation we sum over all N_{Rbio} reactions, and by means of the sign of the stoichiometric factor we see, if the substance is being consumed, is generated, or does not even take part in the r th reaction. The stoichiometric factor also corresponds to the so-called yield factor when dealing with biogeochemical reactions (Y in equations (2.22) and (2.21)).

Thus it results the following biochemical reaction rate in the differential equation for one specific species concentration c_l , $l \notin I^3$:

$$\begin{aligned} R_{\text{bio}} &= \sum_{r=1}^{N_{\text{Rbio}}} \nu_{lr} R_r(c_1, \dots, c_{N_S}) = \\ &= \sum_{r=1}^{N_{\text{Rbio}}} \nu_{lr} \mu_{\max_r} c_{B_r} \prod_{i \in I_r^1 \subset \{1, \dots, N_S\}} \left(\frac{c_i}{K_{M_i} + c_i} \right) \prod_{j \in I_r^2 \subset \{1, \dots, N_S\}} h(c_j). \end{aligned} \quad (2.26)$$

Considering now the rate expression for an arbitrary microbial species X_{B_m} (now $B_m \in I^3$), analogous terms will occur (and stoichiometric factors $\nu_{mr} \neq$

0 will have positive sign, as we deal with growth terms here). Additionally the penalty term will be added, which limits the growth of the biomass up to a maximum concentration of total biomass $c_{B_{\max}}$ (cf. (2.23)). For the microbial species X_{B_m} we thus get the rate expression

$$\begin{aligned}
R_{\text{bio}} &= \left(1 - \frac{\sum_{B_j \in I^3} c_{B_j}}{c_{B_{\max}}}\right) \sum_{r=1}^{N_{\text{Rbio}}} \nu_{mr} R_r(c_1, \dots, c_{N_S}) = \\
&= \left(1 - \frac{\sum_{B_j \in I^3} c_{B_j}}{c_{B_{\max}}}\right) \left(\sum_{r=1}^{N_{\text{Rbio}}} \nu_{mr} \mu_{\max_r} c_{B_m} \right. \\
&\quad \left. \prod_{i \in I_r^1 \subset \{1, \dots, N_S\}} \left(\frac{c_i}{K_{M_i} + c_i} \right) \prod_{j \in I_r^2 \subset \{1, \dots, N_S\}} h(c_j) \right).
\end{aligned} \tag{2.27}$$

As the (immobile) biomass species only take part in the reactions described in this section, we can immediately formulate their conservation equation:

$$\begin{aligned}
\partial_t c_{B_m} &= \left(1 - \frac{\sum_{B_j \in I^3} c_{B_j}}{c_{B_{\max}}}\right) \sum_{r=1}^{N_{\text{Rbio}}} \nu_{mr} R_r(c_1, \dots, c_{N_S}) = \\
&= \left(1 - \frac{\sum_{B_j \in I^3} c_{B_j}}{c_{B_{\max}}}\right) \left(\sum_{r=1}^{N_{\text{Rbio}}} \nu_{mr} \mu_{\max_r} c_{B_m} \right. \\
&\quad \left. \prod_{i \in I_r^1} \left(\frac{c_i}{K_{M_i} + c_i} \right) \prod_{j \in I_r^2} h(c_j) \right) - k_m c_{B_m},
\end{aligned} \tag{2.28}$$

where we added a decay rate of first order $k_m c_{B_m}$ for the microorganisms. Another possibility to account for the microbially mediated processes consists in the description of an equilibrium reaction between substrate and electrone acceptor [RV96, HWvC98]. In this case it is supposed that the decay depends essentially on the availability of the reaction partners, and not – as in the Monod model – on the microbially dominated kinetics of that reaction. Formally this yields to a type of model that is treated in Section 2.6, but also kinetic stoichiometric formulations as in Section 2.5 can be given. Such microbial degradation reactions could be described in even more details by explicitly including particular substeps and interacting processes for the overall reactions of the transformation process in the model formulation (e.g. fermentation, redox half-reactions, interacting inorganic chemistry [MN94, Cur03, BE02]), what also can be realized with the help of the concepts and building blocks of Chapter 2.

2.5 Kinetic Reactions: Mass Action Law

The general reaction rate of the r th elementary kinetic reaction of the form

$$\sum_{i=1}^{N_S} \nu_{ir} X_i \rightleftharpoons 0 \quad (2.29)$$

is given as the net rate between forward and backward reaction rates, which can be formulated by the rate constants of forward and backward reaction, k_r^f and k_r^b :

$$R_r = \left(k_r^b \prod_{\{i|\nu_{ir}<0\}} c_i^{-\nu_{ir}} - k_r^f \prod_{\{i|\nu_{ir}>0\}} c_i^{\nu_{ir}} \right). \quad (2.30)$$

The first product refers to the product species, where by convention for the stoichiometric coefficients $\nu_{ir} < 0$, the second to the reactants. The units of the rate constants k_r^f and k_r^b depend on the number of species participating in the reaction [SM96c, Chapter 2.14]. For a so-called first-order reaction with one reactant and one product, they have units of [1/T].

More precisely, we should replace the concentrations c_i by their activities a_i because due to electrostatical effects, the reaction may not proceed at its theoretical rate. Therefore the concentration is multiplied by an activity coefficient $\gamma_i \leq 1$ that accounts for these non-ideal effects [Bet96, SM96c] of an aqueous solution and leads, loosely speaking, to an 'active' concentration. For this activity coefficient different parametrizations exist, and it is in general a function of the ionic strength of a solution. A common model is the Debye–Hückel equation, and a variant of it is the Davies approximation (see, e.g., [Bet96, Chapter 7.1]) that reads

$$\log \gamma_i = -Az_i^2 \left(\frac{\sqrt{I}}{1 + \sqrt{I}} - 0.2I \right),$$

with the charge of the ion z_i , a temperature depending function $A = A(T)$, and the ionic strength of the solution, $I = I(c_1, \dots, c_{N_S})$.

However, we want to make the common assumption of ideal activity that holds for dilute solutions with low ion concentrations, i.e. $\gamma_i = 1$, and thus $c_i = a_i$.

2.6 Thermodynamic Equilibrium Reactions

Reactions that proceed very fast in comparison with the time scales of transport processes (see Section 2.7) can be treated as being in equilibrium. In

thermodynamic equilibrium, the net reaction rate R_r equals zero, such that the well known law of mass action results from (2.30):

$$0 = \left(k_r^b \prod_{\{i|\nu_{ir}<0\}} c_i^{-\nu_{ir}} - k_r^f \prod_{\{i|\nu_{ir}>0\}} c_i^{\nu_{ir}} \right), \quad (2.31)$$

$$\Rightarrow K_r = \frac{k_r^f}{k_r^b} = \prod_{i=1}^{N_S} c_i^{-\nu_{ir}}. \quad (2.32)$$

Thus the differential equation (2.30) has been replaced in this case by the algebraic equation (2.32). Species that take part at those equilibrium reactions implicitly obey the law of mass action, independent of other effects like transport of these species. So in general it is not possible to define rates explicitly, the local equilibrium assumption supposes an infinitely fast rate to attain equilibrium, whereas the net rate then is zero (cf. [Rub83]). Due to this difficulty, the rates of the equilibrium reactions have to be eliminated from the set of coupled partial differential equations. This can be done by taking into account not only species concentrations, but also their linear combinations, which leads to the consideration of conservation quantities. This aspect will be pursued further in Chapter 3. The model equations that have been implemented deal with kinetic formulations of the rates and do not take equilibrium reactions (algebraic equations) into account explicitly. So we refuse to the local equilibrium assumption and impose fast kinetic reactions for such a case instead, keeping in mind that this requires small time steps of the numerical scheme.

If we assume the canonical form (2.7) the equilibrium reaction can be written in terms of the N_C component species and exactly one product species,

$$c_{N_C+r} = K_r \prod_{i=1}^{N_C} c_i^{\nu_{ir}}, \quad r \in \{1, \dots, N_R\}, \quad (2.33)$$

assuming that the first N_C species are the component species.

The equilibrium constants K_r may vary for different reactions by several orders of magnitude, what makes the numerical treatment of these equations very demanding. They are in general temperature dependent, the influence of the pressure is negligible here.

An alternative method to treat reactions is the minimization of the total GIBBS free energy of the system, where equilibrium and kinetic reactions can be treated more flexibly [Saa96]. The GIBBS free energy comprises the chemical potential μ_i of a species, which is defined [SM96c, Bet96] by

$$\mu_i = \mu_i^0 + RT \ln a_i, \quad (2.34)$$

and simplifies – in the case of an ideal solution – to

$$\mu_i = \mu_i^0 + RT \ln c_i. \quad (2.35)$$

The chemical reference potential μ_i^0 is a fixed quantity at a given temperature and pressure, R is the universal gas constant, and T the temperature. Now we can establish the relation for the change of the GIBBS free energy ΔG_r of the system, which is composed of the sum of its constituents:

$$\Delta G_r = \sum_{i=1}^{N_S} \nu_{ir} \mu_i = \sum_i \nu_{ir} (\mu_i^0 + RT \ln c_i) = \quad (2.36)$$

$$= \sum_i \nu_{ir} \mu_i^0 + RT \ln \left(\prod_i c_i^{-\nu_{ir}} \right) = \Delta G_r^0 + RT \ln Q_r, \quad (2.37)$$

with the standard GIBBS free energy change of the r th reaction ΔG_r^0 and the reaction quotient Q_r [SM96c]. While Q_r describes the actual composition of the solution, the equilibrium constant K_r describes the equilibrium composition,

$$\ln K_r = -\frac{\Delta G_r^0}{RT}, \quad (2.38)$$

and thus it follows

$$\Delta G_r = RT \ln \frac{Q_r}{K_r}, \quad (2.39)$$

and

$$\Delta G_r = 0 \quad (2.40)$$

in equilibrium.

The coupling of the species through an equilibrium reaction via equation (2.32) would not only comprise the species directly involved in that reaction, but all ions of an aqueous solution if we would take into account their activity. This correction of the concentration as a function of the ionic strength has already been mentioned in Section 2.5 and will not be pursued further here.

2.7 Scales of Transport and Reaction Processes

An important criterion for the classification of reactive transport problems is the *Damköhler number* Da , which relates the typical time scale of the reaction in form of a rate constant k [1/T] to the transport time scale $\|q\|/L$ (with L being loosely defined as some characteristic length of the domain), i.e.,

$$Da = \frac{kL}{\|q\|}.$$

The classification of a reaction into kinetic or equilibrium type is not a strict one and should be seen in context with the time scale of the transport. As a rule of thumb, a reaction is in (quasi) equilibrium, if $Da \gg 1$, and kinetic for $Da \leq 1$.

In the majority of the practical cases the homogeneous reactions in the aqueous phase proceed in time scales of seconds or minutes (and are thus often treated as equilibrium reactions). Ad- or desorption processes on the other hand mostly have rate constants in the order of days, whereas mineral dissolution or precipitation processes occur over days up to thousands of years until an equilibrium would be attained [DS98].

In the model implementation we will not make the local equilibrium assumption, hence only consider kinetic reactions, eventually with large rate constants. This in fact is a more appropriate approach from the chemical point of view, as the fast transitions of species are also part of the model. This can be important, if some reactions only proceed at transient concentration ranges of the 'quasi equilibrium' species, which are missed by the equilibrium assumption, where we have no transition but an instantaneous switching [CGS98]. The disadvantage is the resulting stiffness of the system that can render the problem hard to solve numerically.

2.8 Regularisation of Reaction Terms

The partial derivatives of the reaction rate for a chemical kinetic reaction presented in (2.30) are given by

$$\frac{\partial R_r}{\partial c_j} = -k_r^f \nu_{jr} c_j^{(\nu_{jr}-1)} \prod_{j \neq k} c_k^{\nu_{kr}}, \quad (2.41)$$

if $\nu_{jr} > 0$ (reactant), and by

$$\frac{\partial R_r}{\partial c_j} = -k_r^b \nu_{jr} c_j^{(-\nu_{jr}-1)} \prod_{j \neq k} c_k^{-\nu_{kr}}, \quad (2.42)$$

if $\nu_{jr} < 0$ (product). Thus

$$\frac{\partial R_r}{\partial c_j} \rightarrow \mp \infty \text{ for } |\nu_{jr}| < 1 \wedge c_j \rightarrow 0. \quad (2.43)$$

This situation has to be avoided as we have to calculate those derivatives when solving the system with Newton's method that is presented in Section 5.2. Therefore we introduce a C^0 -regularisation whenever $c_k < \tilde{c}$ and $|\nu_{kr}| < 1$. Using the abbreviations

$$\begin{aligned} M_1 &:= \{k \in \{1, \dots, N_S\} | \nu_{kr} \geq 1 \vee c_k > \tilde{c}\}, \quad M_2 := \{k | 0 < \nu_{kr} < 1 \wedge c_k \leq \tilde{c}\}, \\ M_3 &:= \{k | \nu_{kr} \leq -1 \vee c_k > \tilde{c}\}, \quad M_4 := \{k | -1 < \nu_{kr} < 0 \wedge c_k \leq \tilde{c}\}, \end{aligned} \quad (2.44)$$

results in the following rate

$$R_r = -k_r^f \prod_{k \in M_1} c_k^{\nu_{kr}} \prod_{k \in M_2} \tilde{c}^{\nu_{kr}} \frac{c_k}{\tilde{c}} + k_r^b \prod_{k \in M_3} c_k^{-\nu_{kr}} \prod_{k \in M_4} \tilde{c}^{-\nu_{kr}} \frac{c_k}{\tilde{c}}. \quad (2.45)$$

This yields four cases of partial derivatives with finite limits for $c_j \rightarrow 0$:

$$\frac{\partial R_r}{\partial c_j} = -k_r^f \nu_{jr} c_j^{(\nu_{jr}-1)} \prod_{k \in M_1, k \neq j} c_k^{\nu_{kr}} \prod_{k \in M_2} \tilde{c}^{\nu_{kr}} \frac{c_k}{\tilde{c}}, \text{ for } j \in M_1, \quad (2.46)$$

$$\frac{\partial R_r}{\partial c_j} = -k_r^f \tilde{c}^{\nu_{jr}} \frac{1}{\tilde{c}} \prod_{k \in M_1} c_k^{\nu_{kr}} \prod_{k \in M_2, k \neq j} \tilde{c}^{\nu_{kr}} \frac{c_k}{\tilde{c}}, \text{ for } j \in M_2, \quad (2.47)$$

$$\frac{\partial R_r}{\partial c_j} = -k_r^b \nu_{jr} c_j^{(-\nu_{jr}-1)} \prod_{k \in M_3, k \neq j} c_k^{-\nu_{kr}} \prod_{k \in M_4} \tilde{c}^{-\nu_{kr}} \frac{c_k}{\tilde{c}}, \text{ for } j \in M_3, \quad (2.48)$$

$$\frac{\partial R_r}{\partial c_j} = -k_r^b \tilde{c}^{\nu_{jr}} \frac{1}{\tilde{c}} \prod_{k \in M_3} c_k^{-\nu_{kr}} \prod_{k \in M_4, k \neq j} \tilde{c}^{-\nu_{kr}} \frac{c_k}{\tilde{c}}, \text{ for } j \in M_4. \quad (2.49)$$

Chapter 3

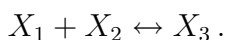
Reduction Schemes for the Multicomponent Problem

While the sheer transport of different solutes in the porous medium is independent from each other, the reactions make the simultaneous solution of the partial differential equations necessary. We have already noted in Section 2.6 that the reaction rates for infinitely fast equilibrium reactions cannot be quantified explicitly and thus have to be eliminated from the PDEs. Although we do not include such reactions in the discretized and implemented model formulation of Chapters 4 et seq. the general idea of combining the equations is presented briefly in this chapter.

Moreover, the effort for solving those coupled systems increases substantially and can limit – in particular in higher dimensions – the feasibility of large simulations. Although not in the focus of this work a glimpse of approaches is presented which transform the given equation systems in order to decouple a number of PDEs from each other.

3.1 Elimination of Reaction Rates

The formulation of equilibrium reactions yields algebraic equations that the species obey while being transported, in this case the unknown 'equilibrium rates' *have to* be eliminated from the partial differential equations, and an algebraic equation is to be solved instead that describes the equilibrium state (cf. Section 2.6, [Rub83]). Kinetic reaction terms may also be eliminated in some partial differential equations, but the number of PDEs will not be reduced in this case. The idea is demonstrated by a simple prototype, consider the homogeneous reaction in the liquid phase



To dispose of equations of the kind $\partial_t c_i - \mathcal{L}(c_i) = \pm R$ linear combinations of the species yield conservation quantities that do not change their molar mass in the system, and are only subject to transport. For consistency, the algebraic equilibrium equation completes the system:

$$\partial_t(c_1 + c_3) - \mathcal{L}(c_1 + c_3) = 0, \quad (3.1)$$

$$\partial_t(c_2 + c_3) - \mathcal{L}(c_2 + c_3) = 0, \quad (3.2)$$

$$K = \frac{c_3}{c_1 c_2}. \quad (3.3)$$

Note that in this special case, due to the linearity of the operators on the left-hand side and the fact that all species are of the same type, i.e., mobile, a variable transformation $u_1 := c_1 + c_3$, and $u_2 := c_2 + c_3$ can be made and (3.2) and (3.3) can be solved completely in these new variables, equations decouple. This is not possible when \mathcal{L} is different, e.g. one species is immobile. Note that in this situation, we could also completely replace c_3 in (3.2) and (3.3) via $c_3 = K c_1 c_2$. This is the so-called direct substitution approach [YT89] yielding in general nonlinear terms under the transport operator, what should be avoided.

This idea can also be pursued in the case of kinetic reactions, however the number of PDEs is not reduced:

$$\partial_t(c_1 + c_3) - \mathcal{L}(c_1 + c_3) = 0, \quad (3.4)$$

$$\partial_t(c_2 + c_3) - \mathcal{L}(c_2 + c_3) = 0, \quad (3.5)$$

$$\partial_t c_3 + \mathcal{L}(c_3) = -R(c_1, c_2, c_3). \quad (3.6)$$

In passing we remark that for all transformations, initial and boundary conditions have to be transformed equally. Though the above examples are very simple, they demonstrate the basic principles of any reduction scheme:

- decoupling of transport equations,
- elimination of equilibrium rates and replacement by algebraic equations,
- restriction of kinetic rates to as few equations as possible.

A general approach for the elimination of the equilibrium rates is given in the following. We refer to the general system $\partial_t \mathbf{c} - \mathcal{L}(\mathbf{c}) = V\mathcal{R}$, where we have split the stoichiometric matrix off the reaction term and recall that it is given in canonical form (Definition 2.7). Furthermore arrange the equations such that equilibrium and kinetic reactions are grouped together, and denote parts corresponding to the equilibrium reactions with superscript q and to

the kinetic reactions with superscript k :

$$V = \begin{pmatrix} \hat{V} \\ I_{N_R} \end{pmatrix} = \begin{pmatrix} \hat{V}^k & \hat{V}^q \\ I_{N_R^k} & 0 \\ 0 & I_{N_R^q} \end{pmatrix}, \quad (3.7)$$

where the matrices have dimensions $\hat{V} \in \mathbb{R}^{N_C \times N_R}$, $\hat{V}^k \in \mathbb{R}^{N_C \times N_R^k}$, and $\hat{V}^q \in \mathbb{R}^{N_C \times N_R^q}$. Now multiply the system with a matrix M that is orthogonal to the last N_R^q columns of V . M exists, as the columns of V are linearly independent for the canonical form. In fact, it is easy to write

$$M = \begin{pmatrix} I_{N_C} & 0 & -\hat{V}^q \\ 0 & I_{N_R^k} & 0 \end{pmatrix}, \quad (3.8)$$

and the equation system gets

$$\partial_t M \mathbf{c} - M \mathcal{L}(\mathbf{c}) = M V \mathcal{R} = \begin{pmatrix} \hat{V}^k & 0 \\ I_{N_R^k} & 0 \end{pmatrix} \begin{pmatrix} \mathcal{R}^k \\ \mathcal{R}^q \end{pmatrix} = \begin{pmatrix} \hat{V}^k \mathcal{R}^k \\ \mathcal{R}^k \end{pmatrix}. \quad (3.9)$$

For the left-hand side we recall that $\mathcal{L} \equiv 0$ for the immobile species, and thus we do not necessarily get the same linear combination under the time derivative as under the transport operator. In fact, we get only mobile species contributions, denoted with $\tilde{\mathbf{c}}$:

$$M \mathcal{L}(\mathbf{c}) = \begin{pmatrix} \mathcal{L}(\tilde{\mathbf{c}}^c - \hat{V}^q \tilde{\mathbf{c}}^q) \\ \mathcal{L}(\tilde{\mathbf{c}}^k) \end{pmatrix}. \quad (3.10)$$

Thus the equilibrium rates have been eliminated, the number of PDEs is now $N_C + N_R^k$, and the remaining N_R^q equations to solve the system are the algebraic equations of the type (2.32). This approach is rather classical (cf. [AM63]), a general formal derivation starting from an arbitrary reaction network including dependent reactions is also given in [Hol00]. By this transformation the number of PDEs has been reduced, but in fact no decoupling or reduction of the unknowns has been achieved. This is the subject of the following section.

3.2 General Reduction Schemes

Several authors investigate schemes for general multicomponent problems with the purpose to reduce systems of type (3.9) with (2.32) further, in the sense that equations decouple, and reaction rates occur in as few equations as possible [FR92, MCAS04, KKar].

Remark 3.1 In the special case of exclusively aqueous species undergoing equilibrium reactions, the PDEs in (3.9) read

$$\partial_t(\mathbf{c}^c - \hat{V}^q \mathbf{c}^q) - \mathcal{L}(\mathbf{c}^c - \hat{V}^q \mathbf{c}^q) = 0, \quad (3.11)$$

and this completely decoupled system can be solved in the N_C transformed variables $\boldsymbol{\psi} := \mathbf{c}^c - \hat{V}^q \mathbf{c}^q$. Afterwards, the N_R^q equilibrium product species are determined with the help of the (coupled) equilibrium equations (cf., e.g., [Hol00] for algebraic equilibrium equations, or [Saa96] for the ansatz minimizing the free energy).

As the nature of the underlying problem is quite heterogeneous, and the used matrix transformations and the choice of basis components are not unique, the approaches become cumbersome to compare. We only comment on some general approaches that do not make restrictive assumptions.

Friedly and Rubin (1992) start with the stoichiometric matrix, ordered according to lines for mobile and immobile species:

$$V = \begin{pmatrix} \tilde{V}_{\text{mob}}^k & \tilde{V}_{\text{mob}}^q \\ \tilde{V}_{\text{im}}^k & \tilde{V}_{\text{im}}^q \end{pmatrix}. \quad (3.12)$$

They construct a matrix W_1 , consisting of linearly independent columns of $(\tilde{V}_{\text{mob}}^k, \tilde{V}_{\text{mob}}^q) =: W_2$, and get with orthogonal matrices the following transformation to new variables:

$$\begin{pmatrix} \mathbf{c}_{\text{mob}} \\ \mathbf{c}_{\text{im}} \end{pmatrix} = V\xi + V^\perp \eta + \begin{pmatrix} W_1 \xi_m + W_2^\perp \eta_m \\ 0 \end{pmatrix}. \quad (3.13)$$

The η are the so-called reaction invariants, and are constants. From the remaining unknowns the η_m can be solved independently of the others in linear PDEs, then there are still ξ and ξ_m to determine by coupled nonlinear algebraic and/or kinetic equations together with PDEs, all consisting of linear combinations of the unknowns. This last system has the size $N_R + N_W$, $N_W = \text{rank of } W_1$ [FR92]. It is not clear, when $N_S > N_R + N_W$, such that there is a net efficiency gain. However, rates have been isolated from the PDEs. On the other hand, linear combinations under the transport operator come into play, what generates couplings and new entries in a Jacobian, if Newton's method is applied.

Kräutle and Knabner (2005) propose a further reduction of the above system, transforming the mobile and immobile blocks separately. The method is void of coupling terms under the transport operator, and with a maximum of N_R^k coupled PDEs, which own, however, rate expressions also [KKar]. Systematic comparisons of the approaches are lacking up to date.

On the transformed systems the decoupling strategies of Section 5.2.3 can be applied, but it is expected that the transformed systems and matrices are less sparse than the original ones, and thus the neglect of couplings will rarely entail a reducible matrix. These aspects have not been investigated yet.

Chapter 4

Discretization of the Hydrogeochemical Multicomponent Model

4.1 Preliminaries

We introduce some notions of functional analysis that will be used in the following. For a more comprehensive treatment we refer to textbooks on finite element methods and the literature cited therein, e.g. [Bra97, KA03, QV94, RG94]. Finite element methods for parabolic problems are treated in [KA03, Tho97, Ž90]. The weak formulation of the multicomponent problem is presented in general form, for the fully discrete calculations we restrict ourselves, however, to the 1D case that has been implemented in RICHY [Ins05].

Let $\Omega \subset \mathbb{R}^d$ be an open, bounded Lipschitz domain. A scalar product on $L^2(\Omega)$ is given by

$$(u, v)_0 := \int_{\Omega} uv dx$$

for $u, v \in L^2(\Omega)$.

Definition 4.1 The well-known *Sobolev spaces* $H^1(\Omega)$ and $H_0^1(\Omega)$ are defined as

$$\begin{aligned} H^1(\Omega) &:= \{u : \Omega \rightarrow \mathbb{R} \mid u \in L^2(\Omega), \\ &\quad u \text{ has weak derivatives } \partial_i u \in L^2(\Omega) \forall i = 1, \dots, d\}, \\ H_0^1(\Omega) &:= \{u \in H^1(\Omega) \mid u = 0 \text{ in the sense of a trace on } \partial\Omega\}. \end{aligned}$$

Additionally we define the spaces

$$\begin{aligned} H_{\Gamma_1,0}^1(\Omega) &:= \{u \in H^1(\Omega) | u = 0 \text{ on } \Gamma_1 \subset \partial\Omega\}, \text{ and} \\ H_{\Gamma_1,\text{Dir}}^1(\Omega) &:= \{u \in H^1(\Omega) | u = g_1 \text{ on } \Gamma_1 \subset \partial\Omega\}. \end{aligned}$$

Note that $H_{\Gamma_1,\text{Dir}}^1(\Omega)$ is no longer a linear space. In slight modification of the standard notation (see, e.g., [Eva98]) the dual space of $H_{\Gamma_1,0}^1(\Omega)$ is denoted by $H_{\Gamma_1}^{-1}(\Omega)$, and the dual space of $H^1(\Omega)$ by $H^{-1,*}(\Omega)$.

4.2 Variational Formulation of the Multicomponent Problem

The general multicomponent problem (2.12) for the vector of unknown concentrations $\mathbf{c} \in \mathbb{R}^{N_s}$ consists of a coupled system of partial and ordinary differential equations for the mobile and immobile species. We recall the abstract formulation

$$\partial_t \mathbf{c} - \mathcal{L}(\mathbf{c}) = \mathcal{R}(\mathbf{c}^T) \text{ in } \Omega \times (0, T), \quad (4.1)$$

with $\mathbf{c} = (\Theta \mathbf{c}_{\text{mob}}, \mathbf{c}_{\text{im}})^T \in \mathbb{R}^{N_{s_{\text{mob}}}} \times \mathbb{R}^{N_{s_{\text{im}}}}$, and the differential operator \mathcal{L} that is non-vanishing only for the mobile species. Concretely, the implemented problem formulation includes rate expressions of zeroth and first order (cf. (2.17) and (2.18)), the general Monod model with inhibition and growth restriction (see (2.26) and (2.27)), and the kinetic reaction term (2.30) with regularisation (2.45). Sorption isotherms of equilibrium and kinetic type as shown in (2.14) and (2.15) are incorporated but not presented here, this has already been shown in [Kas02].

The problem is completed by initial conditions $\mathbf{c}(x, 0) = \mathbf{c}_0(x)$ for $x \in \Omega$, and appropriate boundary conditions for the mobile species $c_i, i \in \{1, \dots, N_{s_{\text{mob}}}\}$ of the following types:

$$- \text{Dirichlet boundary condition } c_i = g_{i1} \text{ on } \Gamma_{i1} \times (0, T), \quad (4.2)$$

$$- \text{Neumann boundary condition } \mathbf{D}\nabla c_i \cdot \nu = g_{i2} \text{ on } \Gamma_{i2} \times (0, T), \text{ and } (4.3)$$

$$- \text{flux boundary condition } (\mathbf{D}\nabla c_i - \mathbf{q}c_i) \cdot \nu = g_{i3} \text{ on } \Gamma_{i3} \times (0, T) \quad (4.4)$$

with the outer unit normal ν .

$\Gamma_{i1}, \Gamma_{i2}, \Gamma_{i3}$ form a disjoint decomposition of $\partial\Omega$, and the boundary conditions in general depend on $x \in \partial\Omega$ and $t \in (0, T)$. We allow arbitrary of the above boundary conditions for each of the (mobile) species, and also $\Gamma_{ik} \neq \Gamma_{jk}$

for $i \neq j$. The following presentation is restricted to homogeneous Dirichlet conditions, the incorporation of nonhomogeneous values in the fully discrete problem is done in the standard way, we refer to [KA03, Chapter 3.5].

The investigation of such systems of quasilinear, parabolic differential equations with nonhomogeneous boundary conditions still leaves open questions and is an active field of research, e.g. concerning the global existence or blow up of solutions [CHL03, Cui01, LLX03, LX03]. Merz (2005) has recently shown a global existence result for the Monod model [Mer05].

The Variational Formulation of the Multicomponent Problem

It is formally derived by integration over the domain Ω and multiplication of the system of differential equations with vectorial test functions $\mathbf{v} \in V$. Then integrate by parts while taking into account the boundary conditions. For the test functions we require $V = (H_{\Gamma_1,0}^1(\Omega))^{N_{S_{\text{mob}}}} \times (L^2(\Omega))^{N_{S_{\text{im}}}}$. However, we will embed the immobile species also in the variational formulation of the mobile species, which is H^1 -conforming. Therefore we write throughout the presentation $V = (H_{\Gamma_1,0}^1(\Omega))^{N_{S_{\text{mob}}}} \times (H^1(\Omega))^{N_{S_{\text{im}}}}$, although this higher regularity for the immobile species would not be necessary from the continuous point of view. Note that the boundaries Γ_{i1} in fact may vary for every species, but we suppress the additional index i to facilitate the notation when writing $(H_{\Gamma_1,0}^1(\Omega))^{N_{S_{\text{mob}}}}$. The following derivation is meant to illustrate formally the origin of the variational formulation, it is not rigorous in the mathematical sense. We assume that the functions possess the necessary regularity and operations are well-defined. The weak formulation will be defined precisely at the end of the section. So let us start from the strong formulation. The multiplications "o" in (4.5) refer to the Hadamard product, i.e. they should be interpreted componentwise:

$$\int_{\Omega} \partial_t \mathbf{c}(x, t) \circ \mathbf{v}(x) dx - \int_{\Omega} \mathcal{L}(\mathbf{c}(x, t)) \circ \mathbf{v}(x) dx = \int_{\Omega} \mathcal{R}(\mathbf{c}^T(x, t)) \circ \mathbf{v}(x) dx \quad (4.5)$$

$$\forall \mathbf{v} \in (H_{\Gamma_1,0}^1(\Omega))^{N_{S_{\text{mob}}}} \times (H^1(\Omega))^{N_{S_{\text{im}}}},$$

for almost every $t \in (0, T)$, and with $\mathbf{c}(x, 0) = \mathbf{c}_0 \in L^2(\Omega)$ for $x \in \Omega$.

For a better understanding we rewrite the formulations for a single species. Let $i \in \{1, \dots, N_{S_{\text{mob}}}\}$. For the i th mobile species \mathcal{L}_i is the convection-diffusion operator, and here integrating $\nabla \cdot (\mathbf{D} \nabla c_i) v_i$ by parts results in the scalar equation

$$\int_{\Omega} \partial_t (\Theta c_i) v_i dx + \int_{\Omega} \mathbf{D} \nabla c_i \cdot \nabla v_i dx - \int_{\partial \Omega} \mathbf{D} \nabla c_i \cdot \nu v_i d\sigma + \int_{\Omega} \nabla \cdot (\mathbf{q} c_i) v_i dx =$$

$$= \int_{\Omega} \mathcal{R}_i(\mathbf{c}^T) v_i dx, \quad (4.6)$$

and, after accounting for the given boundary conditions,

$$\begin{aligned} \Leftrightarrow \int_{\Omega} \partial_t(\Theta c_i) v_i dx + \int_{\Omega} \mathbf{D} \nabla c_i \cdot \nabla v_i dx - \int_{\Gamma_{i3}} \nu \cdot (\mathbf{q} c_i) v_i d\sigma + \int_{\Omega} \nabla \cdot (\mathbf{q} c_i) v_i dx &= \\ &= \int_{\Gamma_{i2}} g_{i2} v_i d\sigma + \int_{\Gamma_{i3}} g_{i3} v_i d\sigma + \int_{\Omega} \mathcal{R}_i(\mathbf{c}^T) v_i dx \\ &\quad \forall v_i \in H_{\Gamma_{i1},0}^1(\Omega). \end{aligned}$$

In this formulation the Neumann boundary condition (4.3) is the natural boundary condition as it corresponds exactly to the boundary term in (4.6). Depending on the nature of the reaction operator \mathcal{R} , the partial differential equation is of linear (e.g. for rates of the type (2.17) or (2.18)), or semilinear type (e.g. for Monod terms (2.20) or (2.26)), or quasilinear, if we have nonlinearities in the time derivative as with nonlinear isotherms in (2.14) or (2.15). However the derivatives of second order are always linear in the c_i 's in the strong formulation. For the reaction operator \mathcal{R} we suppose that the reaction rates are continuously differentiable functions $R \in \mathcal{C}^1(\mathbb{R}^{N_s}, \mathbb{R})$, and the operator \mathcal{R} induced by these rate functions maps $(H^1(\Omega))^{N_s} \rightarrow L^2(\Omega)$ (cf. [Ama95]). In Section 2.8 we have seen that kinetic rate terms may not be differentiable in 0. Although from the above theoretical reasons we would require a \mathcal{C}^1 -regularisation, e.g. with a quadratic spline, we choose a \mathcal{C}^0 -regularisation in Section 2.8 from pragmatic reasons that did not deteriorate the performance of the algorithm in practice.

For immobile species (now $i \in \{N_{S_{\text{mob}}} + 1, \dots, N_{S_{\text{mob}}} + N_{S_{\text{im}}} = N_S\}$) we only have

$$\int_{\Omega} \partial_t c_i v_i dx - \int_{\Omega} \mathcal{R}_i(\mathbf{c}^T) v_i dx = 0 \quad \forall v_i \in H^1(\Omega).$$

To rewrite the variational problem with the help of nonlinear and linear forms, we use

Definition 4.2 For a mobile species, we define the mapping $a_i^{\text{mob}} : H^1(\Omega) \times H^1(\Omega) \rightarrow \mathbb{R}$, and the linear form $b_i^{\text{mob}} : H^1(\Omega) \rightarrow \mathbb{R}$, for every fixed $t \in (0, T)$:

$$\begin{aligned} a_i^{\text{mob}}(c_i, v_i) &:= \int_{\Omega} \mathbf{D} \nabla c_i \cdot \nabla v_i dx - \int_{\Gamma_{i3}} \nu \cdot (\mathbf{q} c_i) v_i d\sigma + \int_{\Omega} \nabla \cdot (\mathbf{q} c_i) v_i dx \\ &\quad - \int_{\Omega} \mathcal{R}_i(\mathbf{c}^T) v_i dx, \end{aligned} \tag{4.7}$$

$$b_i^{\text{mob}}(v_i) := \int_{\Gamma_{i2}} g_{i2} v_i d\sigma + \int_{\Gamma_{i3}} g_{i3} v_i d\sigma. \tag{4.8}$$

Analogously, for the immobile species we define $a_i^{\text{im}} : H^1(\Omega) \times H^1(\Omega) \rightarrow \mathbb{R}$, and $b_i^{\text{im}} : H^1(\Omega) \rightarrow \mathbb{R}$:

$$a_i^{\text{im}}(c_i, v_i) := - \int_{\Omega} \mathcal{R}_i(\mathbf{c}^T) v_i dx, \quad (4.9)$$

$$b_i^{\text{im}}(v_i) := 0. \quad (4.10)$$

Now the shorthand notations $\mathbf{a} = (\mathbf{a}^{\text{mob}}, \mathbf{a}^{\text{im}})^T$ and $\mathbf{b} = (\mathbf{b}^{\text{mob}}, \mathbf{0})^T$ are introduced. In this notation we state the

Weak Formulation of the Hydrogeochemical Multicomponent Problem

Let $V := (H_{\Gamma_1,0}^1(\Omega))^{N_{S_{\text{mob}}}} \times (H^1(\Omega))^{N_{S_{\text{im}}}}$. Find $\mathbf{c} : \Omega \times (0, T) \rightarrow \mathbb{R}^{N_S}$ such that $\mathbf{c} \in L^2((0, T); (H_{\Gamma_1,0}^1(\Omega))^{N_{S_{\text{mob}}}} \times (H^1(\Omega))^{N_{S_{\text{im}}}})$, weak derivatives $\partial_t \mathbf{c} \in L^2((0, T); (H_{\Gamma_1}^{-1}(\Omega))^{N_{S_{\text{mob}}}} \times (H^{-1,*}(\Omega))^{N_{S_{\text{im}}}})$, and with Definition 4.2:

$$(\partial_t \mathbf{c}, \mathbf{v})_0 + \mathbf{a}(\mathbf{c}, \mathbf{v}) = \mathbf{b}(\mathbf{v}) \forall \mathbf{v} \in V, \quad (4.11)$$

for almost every $t \in (0, T)$, together with $\mathbf{c}(x, 0) = \mathbf{c}_0(x) \in L^2(\Omega)$ for $x \in \Omega$. Note that the Dirichlet boundary condition for the mobile species is accounted for in the definition of the space of admissible solutions, while the others are included in the variational equation. In general, \mathbf{a} is not a linear form, and thus the Lax–Milgram Theorem (see, e.g., [KA03]) can no longer be applied. At this point it is assumed that the problem admits a unique, sufficiently smooth solution.

Remark 4.3 From $\mathbf{c} \in L^2((0, T); (H_{\Gamma_1,0}^1(\Omega))^{N_{S_{\text{mob}}}} \times (H^1(\Omega))^{N_{S_{\text{im}}}})$ and $\partial_t \mathbf{c} \in L^2((0, T); (H_{\Gamma_1}^{-1}(\Omega))^{N_{S_{\text{mob}}}} \times (H^{-1,*}(\Omega))^{N_{S_{\text{im}}}})$ we have $\mathbf{c} \in \mathcal{C}([0, T]; (L^2(\Omega))^{N_S})$ [Eva98].

In the following section the spatial and temporal discretization of the problem (4.11) is depicted.

4.3 Conforming Finite Element Discretization

To derive the Galerkin approximation of the variational problem (4.11) let a regular triangulation \mathcal{T}_h of the domain Ω be given, and time levels $t_0 = 0, \dots, t_N = T$. Loosely spoken we need to determine a numerical approximation \mathbf{c}^h that satisfies the (semi)discrete version of (4.11):

$$(\partial_t \mathbf{c}^h(t), \mathbf{v}^h)_0 + \mathbf{a}(\mathbf{c}^h(t), \mathbf{v}^h) = \mathbf{b}(\mathbf{v}^h) \forall \mathbf{v} \in (V^h)^{N_S}. \quad (4.12)$$

We apply Galerkin's method (see, e.g., [KA03, QV94]) with a finite dimensional ansatz space V^h that consists of piecewise linear functions:

$$V^h(\Omega) := \{u \in \mathcal{C}(\bar{\Omega}) \mid u|_{\Omega_i} \in \mathcal{P}_1(\Omega_i) \text{ for } \Omega_i \in \mathcal{T}_h\}.$$

Analogously to Definition 4.1 we introduce the finite dimensional counterparts

$$\begin{aligned} V_{\Gamma_1, \text{Dir}}^h(\Omega) &:= \{u \in V^h \mid u = g_1 \text{ on } \Gamma_1 \subset \partial\Omega\}, \text{ and} \\ V_{\Gamma_1, 0}^h(\Omega) &:= \{u \in V^h \mid u = 0 \text{ on } \Gamma_1 \subset \partial\Omega\}. \end{aligned}$$

Now represent the elements in V^h by means of basis functions Φ_j as

$$c_i^h(x, t) = \sum_{j=0}^N \xi_{i,j}(t) \Phi_j(x).$$

In the same way the initial conditions are represented as an approximation of c_i^0 : $c_i^{0,h}(x) = \sum_{j=0}^N \xi_{i,j}^0 \Phi_j(x)$. To gain a fully discrete formulation, the time derivative $\partial_t c_i$ is approximated by the application of a one step method, the implicit Euler scheme:

$$\partial_t c_i(t_n) \approx \frac{c_i(t_n) - c_i(t_{n-1})}{t_n - t_{n-1}}.$$

It is of first order convergence (with respect to the time step size) and absolutely stable for linear problems, however it may tend to damp the solution (cf., e.g., [KA03]). Recalling the definitions (4.7) – (4.10), and setting $\tau_n := t_n - t_{n-1}$ we can write down the fully discrete equations:

The Fully Discrete Multicomponent Problem

For all $n = 1, \dots, \mathcal{N}$, find $\mathbf{c}^h(t_n) \in (V_{\Gamma_1, 0}^h(\Omega))^{N_{S_{\text{mob}}}} \times (V^h(\Omega))^{N_{S_{\text{im}}}}$ such that

$$(\mathbf{c}^h(t_n), \mathbf{v}^h)_0 - (\mathbf{c}^h(t_{n-1}), \mathbf{v}^h)_0 + \tau_n \mathbf{a}(\mathbf{c}^h(t_n), \mathbf{v}^h) = \tau_n \mathbf{b}(\mathbf{v}^h) \quad (4.13)$$

$$\forall \mathbf{v}^h \in (V_{\Gamma_1, 0}^h(\Omega))^{N_{S_{\text{mob}}}} \times (V^h(\Omega))^{N_{S_{\text{im}}}},$$

$$\text{and } \mathbf{c}^h(t_0) = \mathbf{c}^{0,h}. \quad (4.14)$$

Again, to be precise, we note that the Dirichlet boundary Γ_{i1} may vary for every mobile species, but we omit the additional index i in $(V_{\Gamma_1, 0}^h(\Omega))^{N_{S_{\text{mob}}}}$. The integrals over Ω can be calculated as the sum over the elements Ω_k of the triangulation \mathcal{T}_h , and as test functions we choose the basis functions Φ_k ,

$k = 0, \dots, N$. Finally, the integrals are evaluated with the help of quadrature rules. A system of nonlinear equations in the unknowns $(\xi_{i,j})_{j=0,\dots,N}$ remains to solve for every species ($i = 1, \dots, N_S$), where the systems of different species are coupled by the reaction rates. The concrete calculation of the terms is presented in greater detail for the 1D case in the following paragraphs.

Evaluation in the 1D Case

In the 1D case, the triangulation \mathcal{T}_h consists of intervals $\Omega_k = [x_{k-1}, x_k]$, $k = 1, \dots, N$. The hat functions $\{\Phi_k\}_{k=0,\dots,N}$ with support $[x_{k-1}, x_{k+1}]$ form a basis of V^h :

$$\begin{aligned} \Phi_0(x) &:= \begin{cases} \frac{x_1-x}{x_1-x_0} & \text{for } x \in \Omega_1 := [x_0, x_1], \\ 0 & \text{else.} \end{cases} \\ \Phi_k(x) &:= \begin{cases} \frac{x-x_{k-1}}{x_k-x_{k-1}} & \text{for } x \in \Omega_k := [x_{k-1}, x_k], \\ \frac{x_{k+1}-x}{x_{k+1}-x_k} & \text{for } x \in \Omega_{k+1}, \\ 0 & \text{else, } k = 1, \dots, N-1. \end{cases} \\ \Phi_N(x) &:= \begin{cases} \frac{x-x_{N-1}}{x_N-x_{N-1}} & \text{for } x \in \Omega_N := [x_{N-1}, x_N], \\ 0 & \text{else.} \end{cases} \end{aligned} \quad (4.15)$$

Clearly, $\Phi_k(x_l) = \delta_{kl}$.

We present the single terms that result for the i th species from (4.13) while using quadrature rules for the approximation of the integrals. The gradient notation ∇ is kept, although it reduces of course to one spatial derivative. We start with the mobile species, i.e. $i \in \{1, \dots, N_{S_{\text{mob}}}\}$, and use the abbreviation $\xi_{i,j}(t_n) =: \xi_{i,j}^n$. The test function is Φ_k , with $k = 0, \dots, N$. Of course, for $k = 0$, or $k = N$, the terms for the integrals over Ω_{k-1} and Ω_k , or Ω_{k+1} , are obsolete, respectively. The following integrals are calculated with the trapezoidal rule, what leads to stronger diagonal entries and zeros in the nondiagonal terms (of the so-called mass matrix). Θ is given as a piecewise constant approximation on the elements, and q is piecewise linear and continuous. They can be calculated in a preceding step by solving the Richards equation for flow by means of a mixed hybrid finite element discretization using Raviart-Thomas elements of lowest order [Sch00]. As we then deal with at most linear functions here, the trapezoidal rule is exact in this case. Due to the local support of the Φ_k , only few elements are relevant.

$$(\Theta^n c_i^h(t_n), \Phi_k)_0 = \int_{\Omega_k} \Theta^n \sum_{j=0}^N \xi_{i,j}^n \Phi_j \Phi_k dx + \int_{\Omega_{k+1}} \Theta^n \sum_{j=0}^N \xi_{i,j}^n \Phi_j \Phi_k dx$$

$$\begin{aligned}
&= \int_{\Omega_k} \Theta^n \sum_{j=k-1}^k \xi_{i,j}^n \Phi_j \Phi_k dx + \int_{\Omega_{k+1}} \Theta^n \sum_{j=k}^{k+1} \xi_{i,j}^n \Phi_j \Phi_k dx \\
&= \int_{\Omega_k} \Theta^n \xi_{i,k-1}^n \Phi_{k-1} \Phi_k dx + \int_{\Omega_k} \Theta^n \xi_{i,k}^n \Phi_k \Phi_k dx + \\
&\quad + \int_{\Omega_{k+1}} \Theta^n \xi_{i,k}^n \Phi_k \Phi_k dx + \int_{\Omega_{k+1}} \Theta^n \xi_{i,k+1}^n \Phi_{k+1} \Phi_k dx \\
&\stackrel{\text{trapez. rule}}{=} 0 + \Theta^n \frac{|\Omega_k|}{2} \xi_{i,k}^n + \Theta^n \frac{|\Omega_{k+1}|}{2} \xi_{i,k}^n + 0. \tag{4.16}
\end{aligned}$$

Analogously,

$$(\Theta^{n-1} c_i^h(t_{n-1}), \Phi_k)_0 = \Theta^{n-1} \frac{|\Omega_k|}{2} \xi_{i,k}^{n-1} + \Theta^{n-1} \frac{|\Omega_{k+1}|}{2} \xi_{i,k}^{n-1}, \tag{4.17}$$

which is known at time t_n and thus will enter the right hand side of our equation system. The diffusion–dispersion in Ω_k is again linear, specified as $D = \frac{1}{2}(q(x_{k-1}) - q(x_k))\alpha_l + d\Theta$. The terms derived from the form $a_i^{\text{mob}}(c_i^h(t_n), \Phi_k)$ (cf. (4.7)) will become

$$\begin{aligned}
&\int_{\Omega} D \nabla \sum_{j=0}^N \xi_{i,j}^n \Phi_j \cdot \nabla \Phi_k dx = \\
&= \int_{\Omega_k} D \sum_{j=k-1}^k \xi_{i,j}^n \nabla \Phi_j \cdot \nabla \Phi_k dx + \int_{\Omega_{k+1}} D \sum_{j=k}^{k+1} \xi_{i,j}^n \nabla \Phi_j \cdot \nabla \Phi_k dx = \\
&= -\frac{D}{|\Omega_k|} \xi_{i,k-1}^n + \frac{D}{|\Omega_k|} \xi_{i,k}^n + \frac{D}{|\Omega_{k+1}|} \xi_{i,k}^n - \frac{D}{|\Omega_{k+1}|} \xi_{i,k+1}^n. \tag{4.18}
\end{aligned}$$

Now consider the case of flux boundary conditions (4.4) on $\partial\Omega = \Gamma_{i3}$. In 1D the boundary term that stems from the partial integration reduces to the difference of the function values at the two boundary points:

$$-\int_{\partial\Omega} \nu \cdot (q \sum_{j=0}^N \xi_{i,j}^n \Phi_j) \Phi_0 d\sigma = q(x_0) \xi_{i,0}^n, \tag{4.19}$$

$$\text{and } -\int_{\partial\Omega} \nu \cdot (q \sum_{j=0}^N \xi_{i,j}^n \Phi_j) \Phi_N d\sigma = -q(x_N) \xi_{i,N}^n. \tag{4.20}$$

For the convection term, Simpson's rule is applied for the numerical quadrature after integrating by parts, which is exact for polynomials of second degree:

$$\int_a^b f(x) dx \approx \frac{b-a}{6} \left(f(a) + 4f\left(\frac{a+b}{2}\right) + f(b) \right).$$

Using that the flux is also piecewise linear and continuous (see above), the integral is in \mathcal{P}_2 and thus Simpson's rule is exact. We have to deal with terms of the following kind:

$$\begin{aligned}
\int_{\Omega_k} \nabla \cdot (q\Phi_k)\Phi_k dx &= q\Phi_k\Phi_k|_{x_{k-1}}^{x_k} - \int_{\Omega_k} q\Phi_k \nabla \Phi_k = \\
&= q(x_k) - \frac{1}{|\Omega_k|} \int_{\Omega_k} q \frac{x - x_{k-1}}{|\Omega_k|} dx = q(x_k) - \frac{1}{|\Omega_k|^2} \frac{|\Omega_k|}{2 \cdot 3} \\
&\quad \left(q(x_{k-1}) \cdot 0 + 4 \frac{q(x_{k-1}) + q(x_k)}{2} \left(\frac{x_{k-1} + x_k}{2} - x_{k-1} \right) + q(x_k)|\Omega_k| \right) = \\
&= \frac{2}{3}q(x_k) - \frac{1}{6}q(x_{k-1}).
\end{aligned}$$

Analogously, for the whole convective part we thus get

$$\begin{aligned}
\int_{\Omega} \nabla \cdot (q \sum_{j=0}^N \xi_{i,j}^n \Phi_j) \Phi_k dx &= \\
&= \int_{\Omega_k} \sum_{j=k-1}^k \xi_{i,j}^n \nabla \cdot (q\Phi_j)\Phi_k dx + \int_{\Omega_{k+1}} \sum_{j=k}^{k+1} \xi_{i,j}^n \nabla \cdot (q\Phi_j)\Phi_k dx = \\
&= \left(-\frac{1}{3}q(x_{k-1}) - \frac{1}{6}q(x_k) \right) \xi_{i,k-1}^n + \left(-\frac{1}{6}q(x_{k-1}) + \frac{2}{3}q(x_k) \right) \xi_{i,k}^n + \\
&\quad + \left(-\frac{2}{3}q(x_k) + \frac{1}{6}q(x_{k+1}) \right) \xi_{i,k}^n + \left(\frac{1}{6}q(x_k) + \frac{1}{3}q(x_{k+1}) \right) \xi_{i,k+1}^n.
\end{aligned} \tag{4.21}$$

For the potentially nonlinear reactive terms we apply the trapezoidal rule, what results in a diagonalisation (cf. [KA03, Chapter 8.3]):

Because

$$\mathcal{R}_i((\mathbf{c}^h(x_k))^T) = \mathcal{R}_i \left(\sum_{j=0}^N \xi_{i,j}^n \Phi_j(x_k), i = 1, \dots, N_S \right) = \mathcal{R}_i(\boldsymbol{\xi}_k^T)$$

from $\Phi_j(x_k) = \delta_{jk}$, this leaves us with

$$\begin{aligned}
\int_{\Omega} \mathcal{R}_i((\mathbf{c}^h)^T) \Phi_k dx &= \int_{\Omega_k} \mathcal{R}_i((\mathbf{c}^h)^T) \Phi_k dx + \int_{\Omega_{k+1}} \mathcal{R}_i((\mathbf{c}^h)^T) \Phi_k dx \approx \\
&\approx \frac{|\Omega_k|}{2} \mathcal{R}_i(\boldsymbol{\xi}_k^T) + \frac{|\Omega_{k+1}|}{2} \mathcal{R}_i(\boldsymbol{\xi}_k^T).
\end{aligned} \tag{4.22}$$

Here, the vectorial writing should not be confounded, $\boldsymbol{\xi}_k^T$ means $(\xi_{1,k}, \dots, \xi_{N_S,k})$, i.e., the unknowns of all species concentrations at the node x_k . Note that

this means that – due to the trapezoidal rule and the linear ansatz – the immobile species contributions are evaluated pointwise (cf. 4.22). This does not necessarily hold true with ansatz functions of higher degrees being evaluated on a larger support, where the incorporation of the immobile species in the variational formulation of the mobile species may lead to instabilities [BK04]. Note further that despite the fact that only diagonal entries at node x_k occur this does not necessarily imply that the diagonal is strengthened. This depends on the signs of the reactive terms. In the case sorption isotherms are considered, additional time derivatives occur (cf. (2.14) and (2.15)). We do not focus on these model parts here, the incorporation in the discretization in the scalar case has been described in detail in [Kas02] and can be transferred to the multicomponent problem straightforward. Finally, the (nonhomogeneous) boundary terms in \mathbf{b} lead to

$$\int_{\Gamma_{i2}} g_{i2} \Phi_0 d\sigma = -g_{i2}(x_0), \text{ and } \int_{\Gamma_{i2}} g_{i2} \Phi_N d\sigma = g_{i2}(x_N), \quad (4.23)$$

$$\int_{\Gamma_{i3}} g_{i3} \Phi_0 d\sigma = -g_{i3}(x_0), \text{ and } \int_{\Gamma_{i3}} g_{i3} \Phi_N d\sigma = g_{i3}(x_N). \quad (4.24)$$

For immobile species ($i \in \{N_{S_{\text{mob}}} + 1, \dots, N_S\}$) the terms (4.16) and (4.17) become

$$(c_i^h(t_n), \Phi_k)_0 = \frac{|\Omega_k|}{2} \xi_{i,k}^n + \frac{|\Omega_{k+1}|}{2} \xi_{i,k}^n, \text{ and} \quad (4.25)$$

$$(c_i^h(t_{n-1}), \Phi_k)_0 = \frac{|\Omega_k|}{2} \xi_{i,k}^{n-1} + \frac{|\Omega_{k+1}|}{2} \xi_{i,k}^{n-1}, \quad (4.26)$$

respectively, by using the trapezoidal rule. Furthermore, only the reactive terms (4.22) arise.

Remark 4.4 Of course the assembling of the matrix and right-hand sides in the finite element code is organised elementwise. Therefore the contributions of different elements in the final lines of the above calculations are not subsumed further.

The fully discrete system (4.13) has thus led to terms (4.16) – (4.26) that constitute a coupled nonlinear equation system in the vector of unknowns $(\xi_{i,j}^n)_{j=0,\dots,N}$ for every species ($i = 1, \dots, N_S$), thus in total we have $(N+1) \times N_S$ degrees of freedom. We choose the following ordering of the degrees of freedom: we group together all species at one node, and then increment the node index, i.e.,

$$\boldsymbol{\xi} := (\xi_{1,0}, \dots, \xi_{N_S,0}, \dots, \xi_{1,N}, \dots, \xi_{N_S,N})^T.$$

It can be written in general form as

$$A\xi^n + \mathbf{g}(\xi^{n,T}) = \mathbf{r} \quad (4.27)$$

with a linear part A , a nonlinear part \mathbf{g} , and the right-hand side \mathbf{r} . It is solved with a variant of Newton's method, which will be presented in Section 5.2. Note that nonhomogeneous Dirichlet conditions for some $\xi_{i,0}$, $\xi_{i,N}$ will be set directly through $\xi_{i,0}^n = g_{i1}(x_0, t_n)$, and $\xi_{i,N}^n = g_{i1}(x_N, t_n)$, (and modifying the corresponding matrix parts on the left to unit vectors, cf. [KA03]).

Chapter 5

Solution Strategies – Algorithms

The solution of a multicomponent advection-dispersion-reaction problem is demanding from several points of view. The different nature of the physical processes and their corresponding equation parts has led to the spreading of two principal techniques: Algorithms that solve the complete, fully coupled system simultaneously (also known as global implicit or one-step methods), and algorithms that apply a variant of the so-called operator splitting method to treat subproblems separately [SM96b].

However, only recently Kanney et al. (2003) stated that *“the lack of broad and detailed comparisons among different combinations of solution algorithms and methods [...] indicates a general lack of guidance to aid in the selection of efficient approaches”* [KMB03].

The principal approaches of this chapter are not restricted to a concrete discretization that is chosen, therefore many ideas are presented in a more general framework. In Section 5.1 we give an overview of some relevant results concerning the operator splitting technique, including an introduction to popular approaches, the concept of commuting operators to assess the accuracy of splitting, and the concrete case of advection-dispersion-reaction problems. In Section 5.2 the fully implicit solution strategy is depicted, with an emphasis on Newton’s method for solving the nonlinear problem at hand, and modifications of it for enhancing the efficiency of the method while not destroying the process-preserving character of the global implicit approach.

5.1 Operator Splitting

The general idea of the operator splitting technique is the decomposition of the full problem into subproblems that are easier to solve. This idea can be applied in various ways, e.g., by splitting a time step according to spatial dimensions or with respect to different physical properties of the differential operators (see, e.g., [Mar90, HV03]). Solution of the subproblems should then be facilitated, and specific discretization schemes or even analytical solutions for the split problems may be applied.

Furthermore the (necessary) recombination of the subproblems (and the time steps for which they are solved) gives rise to a variety of solution strategies. It is beyond the scope of this work to depict all those approaches in detail. We restrict ourselves to the general concept of the most important ones for reactive transport problems in Section 5.1.1, and assess the question of accuracy with the help of a Lie operator formalism in Section 5.1.2. Finally we give some important results for the class of advection–dispersion–reaction problems in Section 5.1.3.

5.1.1 General Schemes

Standard Non-Iterative Splitting

Let us first consider the simplest, non-iterative operator splitting scheme of an abstract PDE problem. We split the general differential operator \mathbf{F} :

$$\partial_t \mathbf{c}(x, t) = \mathbf{F}(x, t, \mathbf{c}(x, t)) = \mathbf{F}_1(x, t, \mathbf{c}(t)) + \mathbf{F}_2(x, t, \mathbf{c}(t)), \quad (5.1)$$

with appropriate initial and boundary conditions according to the type of differential operator. Now, instead of (5.1), the following subproblems are solved sequentially in each time step,

$$\partial_t \mathbf{c}^*(x, t) = \mathbf{F}_1(x, t, \mathbf{c}^*(x, t)); \quad t_n < t \leq t_{n+1}; \quad \mathbf{c}^*(x, t_n) = \mathbf{c}_n, \quad (5.2)$$

$$\partial_t \mathbf{c}^{**}(x, t) = \mathbf{F}_2(x, t, \mathbf{c}^{**}(x, t)); \quad t_n < t \leq t_{n+1}; \quad \mathbf{c}^{**}(x, t_n) = \mathbf{c}^*(x, t_{n+1}), \quad (5.3)$$

and then $\mathbf{c}_{n+1} := \mathbf{c}^{**}(x, t_{n+1})$ is set as the solution for time t_{n+1} . Note that here each subproblem is solved for the full timestep. This scheme has been named sequential non-iterative approach [YT89, SM96b] and has been widely applied (see the citations from the field of hydrogeochemical models in Section 5.1.3).

The advantage of this technique consists in the decomposition of a complex problem into easier subproblems. As the characters of these subproblems may differ substantially from each other, their solution is sought with specific algorithms that account for their special structure each. One may think, e.g.,

of a combination of implicit and explicit methods, where appropriate. Moreover, existing codes for the subproblems can easily be combined to tackle the complex problem, and parallel implementations may become easier [WD87]. If the individual steps are not calculated for the whole time interval each, but only for fractions of it, the technique is also known as the method of fractional steps (see [Mar90]). Furthermore, there is no need that the time steps of the subproblems must be the same. It may be an advantage to take smaller time steps only for one subproblem, where the time scales are fast compared to the other one(s).

The splitting schemes must satisfy the conditions of approximation and stability on the whole. In (5.2) and (5.3) an error has been committed, the so-called *splitting error*, which is independent of the numerical scheme we use to solve the subproblems, and even is present, if they can be solved analytically [VM92, LV99]. This error is due to the fact that coupled, simultaneous processes are represented by subproblems which are solved independently of each other, we will speak of a scheme that in this sense is not *process-preserving*. The splitting error can be quantified in simple cases, as we will see in Section 5.1.2 by comparing the exact solutions of the full and the subproblems. There we also demonstrate that this splitting scheme can even lead to the correct solution with zero splitting error.

Hundsdorfer and Verwer (2003) give the following truncation error ρ_n (see Definition 5.2) of order one for general nonlinear ODE systems (which can be regarded as the result of the semidiscretization of a PDE problem). Via Taylor expansion they get (cf. (IV.1.9) in [HV03])

$$\rho_n = \frac{1}{2}\tau \left[\frac{\partial F_1}{\partial c} F_2 - \frac{\partial F_2}{\partial c} F_1 \right] (t_n, c(t_n)) + \mathcal{O}(\tau^2).$$

We present a more detailed derivation of this error in Section 5.1.2 with the help of a Lie operator formalism.

Alternate Non-Iterative Splitting

Variants of the non-iterative approach use different lengths and schemes of the timesteps, e.g. a symmetrical Strang splitting scheme [Str68], where two half-steps are performed with reversed sequence of the operators:

$$\partial_t \mathbf{c}^* = \mathbf{F}_1(\mathbf{c}^*); \quad t_n < t \leq t_{n+1/2}; \quad \mathbf{c}^*(x, t_n) = \mathbf{c}_n, \quad (5.4)$$

$$\partial_t \mathbf{c}^{**} = \mathbf{F}_2(\mathbf{c}^{**}); \quad t_n < t \leq t_{n+1}; \quad \mathbf{c}^{**}(x, t_n) = \mathbf{c}^*(x, t_{n+1/2}), \quad (5.5)$$

$$\partial_t \mathbf{c}^{***} = \mathbf{F}_1(\mathbf{c}^{***}); \quad t_{n+1/2} < t \leq t_{n+1}; \quad \mathbf{c}^{***}(x, t_{n+1/2}) = \mathbf{c}^{**}(x, t_{n+1}). \quad (5.6)$$

This scheme can also be applied for full timesteps (set t_{n+1} for $t_{n+1/2}$ and t_{n+2} for t_{n+1} in (5.4) – (5.6)), as proposed in [VM92]. They termed the

method alternate operator splitting technique. Reversing of the sequence of the operators can enhance the approximation properties of the algorithm. We analyze some cases in Section 5.1.3. However, they are mostly not of practical use for complex advection-diffusion-reaction problems. We will derive the local truncation error ρ_n of order two in Section 5.1.2 via a Lie operator formalism. For non-autonomous systems Hundsdorfer and Verwer (2003) claim that the method is still of order two [HV03].

Iterative Splitting

To improve the accuracy of the operator splitting approach Yeh and Tripathi (1989) and others proposed to seek a solution of the fully coupled problem, but without the need to assemble and solve the large, fully coupled system. The idea is to iterate between the subproblems while including in every subproblem the terms of the other one at the previous iteration:

$$\partial_t \mathbf{c}^{(i+1)} = \mathbf{F}_1(\mathbf{c}^{(i+1)}) + \mathbf{F}_2(\mathbf{c}^{(i)}); \quad t_n < t \leq t_{n+1}; \quad \mathbf{c}^{(0)}(x, t_n) = \mathbf{c}_n, \quad (5.7)$$

$$\partial_t \mathbf{c}^{(i+2)} = \mathbf{F}_1(\mathbf{c}^{(i+1)}) + \mathbf{F}_2(\mathbf{c}^{(i+2)}); \quad t_n < t \leq t_{n+1}. \quad (5.8)$$

The iteration stops, when some tolerance criterion is met, e.g.,

$$|\mathbf{c}^{(i+2)} - \mathbf{c}^{(i+1)}| < \epsilon, \quad \text{or} \quad \frac{|\mathbf{c}^{(i+2)} - \mathbf{c}^{(i+1)}|}{|\mathbf{c}^{(i+2)}|} < \epsilon.$$

Thus the term $\mathbf{F}_2(\mathbf{c}^{(i)})$ in (5.7), and the term $\mathbf{F}_1(\mathbf{c}^{(i+1)})$ in (5.8), respectively, are known from the previous iteration and just have to be evaluated. They will enter the right-hand side of the equation system as a source term. The subproblems are solved for a full timestep each. The scheme is illustrated for a transport/reaction splitting in Figure 5.1 of Section 5.1.3.

As also pointed out by Barry et al. (1996), the accuracy of the scheme strongly depends on the problem considered [BMCH96].

Yeh and Tripathi (1989) advocated in their often cited paper [YT89] that “*only the sequential iterative approach can be used for realistic applications*”. However, this statement was based merely on theoretical considerations, not taking into account the number of iterations needed by the approaches, and seems to be outdated, as also note [vdLD01] in their review. Several authors point out that the benefit of dealing with smaller, decoupled systems of equations may be outweighed by the inferior convergence of the overall algorithm [EK92, SM96b, RVV00, SCA00]. Van der Lee et al. (2003) note that “*the iterative sequential approach is notorious for failing to converge, even for moderately complex systems*” [vdLDLG03].

The accuracy of the coupling scheme can be addressed in several ways, many authors use heuristic arguments by, e.g., calculating a reference solution c_{ref} in specific situations, which might be derived from an analytical solution in simple cases, but often is a numerical solution calculated for the fully coupled problem on a fine grid.

Definition 5.1 The *mass balance error* $E(t_n)$ of the solution $\mathbf{c}_{\text{OS}}(x, t_n)$ obtained by an operator splitting scheme at time t_n is defined as

$$E(t_n) := 1 - \frac{\int_{\Omega} \mathbf{c}_{\text{OS}}(x, t_n) dx}{\int_{\Omega} \mathbf{c}_{\text{ref}}(x, t_n) dx}.$$

Thus a mass loss corresponds to $E > 0$.

Most schemes are only first-order approximations $\mathcal{O}(\tau)$, but in special cases the quality of the approximation can be of second order or even better.

5.1.2 Commuting Operators

When dealing with the accuracy of splitting schemes, the question of commutativity of operators arises. With the help of a Lie operator formalism the operators can be analyzed and the splitting error studied in a convenient way. Lanser and Verwer (1999) used this concept to elaborate the error of a three-term Strang splitting scheme for air pollution problems [LV99]. We want to follow their methodology and apply it to the two-term splitting of transport and reaction, both for the standard non-iterative splitting, and the Strang splitting. The considerations are independent of the underlying spatial discretizations used. The concept is also presented in [HV03], for an introduction to the Lie formalism we refer to [SSC94]. For a better understanding, the relevant definitions and properties will also be given in this section.

We want to investigate a two-term splitting for the abstract problem

$$\partial_t \mathbf{c}(x, t) = \mathbf{F}(x, t, \mathbf{c}(x, t)) = \mathbf{F}_1(x, t, \mathbf{c}) + \mathbf{F}_2(x, t, \mathbf{c}). \quad (5.9)$$

This equation may represent any ODE or PDE problem, where for PDE problems we think of an initial value problem in autonomous form without boundary conditions. For convenience we will frequently omit the spatial variable x in the notations. Let \mathcal{S} denote the function space of real, sufficiently often differentiable, vector valued functions \mathbf{c} on \mathbb{R}^d . We now define the solution (semigroup) operator S_τ acting on \mathcal{S} such that the exact solution \mathbf{c} of (5.9) at time $t + \tau$ can be given as

$$\mathbf{c}(t + \tau) = S_\tau(\mathbf{c}(t)).$$

Analogously we define the solution operators $S_{k,\tau}$, $k \in \{1, 2\}$, for the sub-problems $\partial_t \mathbf{c} = \mathbf{F}_k(\mathbf{c})$.

Thus we can write the standard non-iterative and the alternating splitting scheme (see Section 5.1.1) as

$$\tilde{\mathbf{c}}(t + \tau) = \tilde{S}_\tau(\tilde{\mathbf{c}}(t)), \quad (5.10)$$

with $\tilde{S}_\tau = S_{2,\tau} \circ S_{1,\tau}$, or $\tilde{S}_\tau = S_{1,\tau/2} \circ S_{2,\tau} \circ S_{1,\tau/2}$, respectively. Here, $\tilde{\mathbf{c}} \in \mathcal{S}$ denotes the approximation of the exact solution \mathbf{c} .

Definition 5.2 The *local truncation error* ρ_n , i.e. the splitting error introduced per time step $\tau_n := t_{n+1} - t_n$, is given by inserting the exact solution \mathbf{c} of (5.9) in the approximation scheme (5.10). This results in

$$\mathbf{c}(t + \tau) = \tilde{S}_\tau(\mathbf{c}(t)) + \tau \rho_n,$$

for any of the two schemes.

This splitting error can be analysed by Taylor expansion, however, we will employ a Lie operator formalism that provides insight in the dependence between the subprocesses and the consequences on the splitting error [LV99]. The composition of (differential) operators in general is noncommutative. The following notation is useful in this context.

Definition 5.3 The *commutator* of two operators F_1, F_2 , acting on the same space \mathcal{S} , is defined as

$$[F_1, F_2] := F_1 F_2 - F_2 F_1.$$

Remark 5.4 The commutator bracket $[\cdot, \cdot]$ is bilinear, skew-symmetric, and satisfies the Jacobi condition

$$[F_1, [F_2, F_3]] + [F_2, [F_3, F_1]] + [F_3, [F_1, F_2]] = 0.$$

Due to these properties, the space of operators endowed with the product operation $[\cdot, \cdot]$ forms a *Lie algebra*. For iterated commutators we will also use the following notation:

$$\begin{aligned} [F_1, F_2, F_3] &= [F_1, [F_2, F_3]], \\ [F_1, F_2, F_3, F_4] &= [F_1, [F_2, [F_3, F_4]]] \text{ etc.} \end{aligned}$$

Definition 5.5 Let F be an operator acting on the function space \mathcal{S} . The *Lie operator* \mathcal{F} is a linear operator on the space of operators acting on \mathcal{S} . It is defined such that, for *any* operator G acting on \mathcal{S} , it holds

$$\mathcal{F}G(\mathbf{c}) := G'(\mathbf{c})F(\mathbf{c}) \text{ for any } \mathbf{c} \in \mathcal{S}.$$

Here, the prime denotes the differentiation w.r.t. \mathbf{c} .

Let us depict some consequences of this definition and apply it to our problem. As the solution \mathbf{c} of $\partial_t \mathbf{c} = F(\mathbf{c})$ is a function of t , with the chain rule it holds then

$$\mathcal{F}G(\mathbf{c}) = G'(\mathbf{c}(t))F(\mathbf{c}(t)) = \frac{\partial G}{\partial t}(\mathbf{c}(t)).$$

So $\mathcal{F}G(\mathbf{c})$ can be interpreted as a measure for the rate of change of G along the solution of $\partial_t \mathbf{c} = F(\mathbf{c})$. Analogously we get for $k \geq 1$

$$\mathcal{F}^k G(\mathbf{c}(t)) = \frac{\partial^k}{\partial t^k} G(\mathbf{c}(t)).$$

Now we want to use the notion of the exponential form of an operator A

$$e^{\tau A} := I + \tau A + \frac{\tau^2}{2} A^2 + \dots + \frac{\tau^k}{k!} A^k + \dots$$

This definition should be seen in a formal way, without considering convergence properties of this series.

With $G \equiv I$ we can write

$$e^{\tau \mathcal{F}} I(\mathbf{c}(t)) = \sum_{k=0}^{\infty} \frac{\tau^k}{k!} \mathcal{F}^k I(\mathbf{c}(t)) = \sum_{k=0}^{\infty} \frac{\tau^k}{k!} \frac{\partial^k}{\partial t^k} I(\mathbf{c}(t)).$$

The last term is the Taylor series of $\mathbf{c}(t+\tau) = S_\tau(\mathbf{c}(t))$. Thus we have gained a representation of the solution operator S_τ by the Lie–Taylor series operator $e^{\tau \mathcal{F}} I$:

$$\mathbf{c}(t + \tau) = e^{\tau \mathcal{F}} I(\mathbf{c}(t)). \quad (5.11)$$

Recall that \mathbf{c} is the exact solution. If we proceed analogously for the sub-problems $\partial_t \mathbf{c} = F_k(\mathbf{c})$, we can write the non-iterative splitting scheme as

$$\tilde{\mathbf{c}}(t + \tau) = e^{\tau \mathcal{F}_1} e^{\tau \mathcal{F}_2} I(\tilde{\mathbf{c}}(t)). \quad (5.12)$$

Note that the composition of the solution operators results in an reversed order of the exponentials (see also [HV03, p. 334]).

For the alternating splitting we get

$$\tilde{\mathbf{c}}(t + \tau) = e^{\frac{\tau}{2} \mathcal{F}_1} e^{\tau \mathcal{F}_2} e^{\frac{\tau}{2} \mathcal{F}_1} I(\tilde{\mathbf{c}}(t)). \quad (5.13)$$

To evaluate the splitting errors we have to compare the exponential series in (5.11) with those in (5.12) and (5.13). Therefore, the *Baker–Campbell–Hausdorff formula* [SSC94] to express the product of two exponentials e^X, e^Y

as a new exponential e^Z is useful:

$$\begin{aligned}
e^X e^Y &= e^Z, \text{ where} \\
Z &= X + Y + \frac{1}{2}[X, Y] + \frac{1}{12}([X, X, Y] + [Y, Y, X]) + \frac{1}{24}[X, Y, Y, X] \\
&\quad - \frac{1}{720}([Y, Y, Y, Y, X] + [X, X, X, X, Y]) \\
&\quad + \frac{1}{360}([Y, X, X, X, Y] + [X, Y, Y, Y, X]) + \dots
\end{aligned}$$

We will make use of this formula in the proofs of the following two theorems, which are the main results of this section.

Theorem 5.6 *Consider the abstract problem $\partial_t \mathbf{c}(x, t) = F(x, t, \mathbf{c}(x, t))$ with the solution operator $\mathbf{c}(t_n + \tau) = S_\tau(\mathbf{c}(t_n))$.*

The accuracy of operator splitting for the standard non-iterative splitting scheme (5.2) and (5.3) is of first order in time, and for the splitting error ρ_n per time step τ it holds

$$\begin{aligned}
\rho_n &= \frac{1}{2}\tau (F_2'F_1 - F_1'F_2)(\mathbf{c}(t_n)) + \frac{1}{12}\tau^2 \left((F_1'F_2)'F_2 - 2(F_2'F_1)'F_2 + (F_2'F_2)'F_1 \right. \\
&\quad \left. + (F_2'F_1)'F_1 - 2(F_1'F_2)'F_1 + (F_1'F_1)'F_2 \right)(\mathbf{c}(t_n)) + \mathcal{O}(\tau^3). \quad (5.14)
\end{aligned}$$

' denotes differentiation with respect to \mathbf{c} : $F_i' = \frac{\partial F_i}{\partial \mathbf{c}}$.

If the subprocesses commute, i.e. $(F_2'F_1)(\mathbf{c}) = (F_1'F_2)(\mathbf{c})$, the splitting error equals zero.

Proof: Recall that the Lie operator is a *linear* operator. The splitting error can be assessed inserting the exact solution in the operator splitting scheme (5.12). We have

$$\mathbf{c}(t_n + \tau) = \tilde{S}_\tau(\mathbf{c}(t_n)) + \tau\rho_n = e^{\tau\tilde{\mathcal{F}}}I(\mathbf{c}(t_n)) + \tau\rho_n = e^{\tau\mathcal{F}_1}e^{\tau\mathcal{F}_2}I(\mathbf{c}(t_n)) + \tau\rho_n.$$

Now evaluate the right-hand side of the following expression:

$$\rho_n = \frac{1}{\tau} (e^{\tau\tilde{\mathcal{F}}} - e^{\tau\mathcal{F}_1}e^{\tau\mathcal{F}_2}) I(\mathbf{c}(t_n)).$$

Applying the Baker–Campbell–Hausdorff formula we get

$$\begin{aligned}
\tau\tilde{\mathcal{F}} &= \tau\mathcal{F}_1 + \tau\mathcal{F}_2 + \frac{1}{2}\tau^2[\mathcal{F}_1, \mathcal{F}_2] + \frac{1}{12}\tau^3([\mathcal{F}_1, \mathcal{F}_1, \mathcal{F}_2] + [\mathcal{F}_2, \mathcal{F}_2, \mathcal{F}_1]) \\
&\quad + \frac{1}{24}\tau^4[\mathcal{F}_1, \mathcal{F}_2, \mathcal{F}_2, \mathcal{F}_1] + \mathcal{O}(\tau^5).
\end{aligned}$$

Now divide by τ , evaluate the iterated commutators and transform the Lie operators \mathcal{F}_i to the original operators F_i . Let $i, j \in \{1, 2\}$, and $i \neq j$.

$$\begin{aligned} [\mathcal{F}_i, \mathcal{F}_j]I(\mathbf{c}) &= (\mathcal{F}_i\mathcal{F}_j - \mathcal{F}_j\mathcal{F}_i)I(\mathbf{c}) = \\ &= (I'(\mathbf{c})F_j(\mathbf{c}))'F_i(\mathbf{c}) - (I'(\mathbf{c})F_i(\mathbf{c}))'F_j(\mathbf{c}) = \\ &= F_j'(\mathbf{c})F_i(\mathbf{c}) - F_i'(\mathbf{c})F_j(\mathbf{c}), \end{aligned}$$

$$\begin{aligned} [\mathcal{F}_i, \mathcal{F}_i, \mathcal{F}_j]I(\mathbf{c}) &= [\mathcal{F}_i, \mathcal{F}_i\mathcal{F}_j - \mathcal{F}_j\mathcal{F}_i]I(\mathbf{c}) = \\ &= (\mathcal{F}_i\mathcal{F}_i\mathcal{F}_j)I(\mathbf{c}) - (\mathcal{F}_i\mathcal{F}_j\mathcal{F}_i)I(\mathbf{c}) - (\mathcal{F}_i\mathcal{F}_j\mathcal{F}_i)I(\mathbf{c}) + (\mathcal{F}_j\mathcal{F}_i\mathcal{F}_i)I(\mathbf{c}) \\ &= (F_j'(\mathbf{c})F_i(\mathbf{c}))'F_i(\mathbf{c}) - 2(F_i'(\mathbf{c})F_j(\mathbf{c}))'F_i(\mathbf{c}) + (F_i'(\mathbf{c})F_i(\mathbf{c}))'F_j(\mathbf{c}), \end{aligned}$$

and finally,

$$\begin{aligned} [\mathcal{F}_1, \mathcal{F}_2, \mathcal{F}_2, \mathcal{F}_1]I(\mathbf{c}) &= [\mathcal{F}_1, [\mathcal{F}_2, [\mathcal{F}_2, \mathcal{F}_1]]]I(\mathbf{c}) = \\ &= [\mathcal{F}_1, [\mathcal{F}_2, \mathcal{F}_2\mathcal{F}_1]]I(\mathbf{c}) - [\mathcal{F}_1, [\mathcal{F}_2, \mathcal{F}_1\mathcal{F}_2]]I(\mathbf{c}) = \\ &= [\mathcal{F}_1, \mathcal{F}_2\mathcal{F}_2\mathcal{F}_1]I(\mathbf{c}) - 2[\mathcal{F}_1, \mathcal{F}_2\mathcal{F}_1\mathcal{F}_2]I(\mathbf{c}) + [\mathcal{F}_1, \mathcal{F}_1\mathcal{F}_2\mathcal{F}_2]I(\mathbf{c}) = \\ &= (\mathcal{F}_1\mathcal{F}_1\mathcal{F}_2\mathcal{F}_2)I(\mathbf{c}) - 2(\mathcal{F}_1\mathcal{F}_2\mathcal{F}_1\mathcal{F}_2)I(\mathbf{c}) + \\ &\quad + 2(\mathcal{F}_2\mathcal{F}_1\mathcal{F}_2\mathcal{F}_1)I(\mathbf{c}) - (\mathcal{F}_2\mathcal{F}_2\mathcal{F}_1\mathcal{F}_1)I(\mathbf{c}) = \\ &= ((F_2'(\mathbf{c})F_2(\mathbf{c}))'F_1(\mathbf{c}))'F_1(\mathbf{c}) - 2((F_2'(\mathbf{c})F_1(\mathbf{c}))'F_2(\mathbf{c}))'F_1(\mathbf{c}) + \\ &\quad + 2((F_1'(\mathbf{c})F_2(\mathbf{c}))'F_1(\mathbf{c}))'F_2(\mathbf{c}) - ((F_1'(\mathbf{c})F_1(\mathbf{c}))'F_2(\mathbf{c}))'F_2(\mathbf{c})). \end{aligned}$$

Clearly, from $\tilde{\mathcal{F}} = \mathcal{F}_1 + \mathcal{F}_2 = \mathcal{F}$ we have $\rho_n = 0$. As can be seen, all the commutators vanish, if $[\mathcal{F}_1, \mathcal{F}_2]$ equals the zero operator. This is equivalent to $(F_2'F_1)(\mathbf{c}) - (F_1'F_2)(\mathbf{c}) = 0$, what completes the proof. \square

We proceed with the result for the Strang splitting.

Theorem 5.7 *Consider the abstract problem $\partial_t \mathbf{c}(x, t) = F(x, t, \mathbf{c}(x, t))$ with the solution operator $\mathbf{c}(t_n + \tau) = S_\tau(\mathbf{c}(t_n))$.*

The accuracy of operator splitting for the alternating non-iterative splitting scheme (5.4) – (5.6) (Strang splitting) is of second order in time, and for the splitting error ρ_n per time step τ it holds

$$\begin{aligned} \rho_n &= \frac{1}{24}\tau^2 \left(2(F_1'F_2)'F_2 - 4(F_2'F_1)'F_2 + 2(F_2'F_2)'F_1 \right. \\ &\quad \left. - (F_2'F_1)'F_1 + 2(F_1'F_2)'F_1 - (F_1'F_1)'F_2 \right) (\mathbf{c}(t_n)) + \mathcal{O}(\tau^4). \end{aligned} \quad (5.15)$$

If the subprocesses commute, i.e. $(F_2'F_1)(\mathbf{c}) = (F_1'F_2)(\mathbf{c})$, the splitting error equals zero.

Proof: We proceed analogously to the proof of Theorem 5.6. Applying the Baker–Campbell–Hausdorff formula twice yields

$$\tau\tilde{\mathcal{F}} = \tau\mathcal{F}_1 + \tau\mathcal{F}_2 + \frac{1}{24}\tau^3(2[\mathcal{F}_2, \mathcal{F}_2, \mathcal{F}_1] - [\mathcal{F}_1, \mathcal{F}_1, \mathcal{F}_2]) + \mathcal{O}(\tau^5).$$

Division by τ already shows the second order accuracy in time. The corresponding commutators have been calculated in the preceding proof, this leads directly to (5.15). Again, due to the iterated formulation of the commutators it becomes evident that all the error terms vanish, if $[\mathcal{F}_1, \mathcal{F}_2]$ equals the zero operator. \square

We will analyze the meaning of commutativity of the processes in some concrete cases relevant for reactive hydrogeochemical transport models in the next section.

5.1.3 Splitting of ADR Equations

Now let us deal with advection–diffusion–reaction systems of the type (2.11) and algorithms that separate the transport problem from the (geochemical) reaction problem. This is the most important configuration, although some authors also consider splitting of advection and diffusion processes [Saa96, HV03]. We will present the approaches of the previous section in this concrete case and summarize briefly the results of the literature, which differ mainly in the reaction terms under consideration. An overview of the techniques is also given in [SM96b]. The coupled equation system can thus be written as

$$\partial_t \mathbf{c}(x, t) = \mathcal{L}(x, t, \mathbf{c}(x, t)) + \mathcal{R}(x, t, \mathbf{c}(t)), \quad (5.16)$$

with the general transport operator $\mathcal{L} = \nabla \cdot (D\nabla - \mathbf{q})$, and a reaction operator \mathcal{R} , cf. (2.12).

First we observe that we are left with linear PDEs of second order for the transport part and algebraic and/or ordinary differential equations for the reactive part. The PDEs then have only couplings in space, not among different species, whereas the reactive part in general entails local (pointwise) equations with coupling among the species. Specific implementations of codes on parallel machines can take advantage of this fact.

Standard Non-Iterative Splitting

As this scheme allows for the easiest connection of existing codes for the subproblems to solve the coupled transport–reaction problem, it has become

very popular in the water resources literature. Analogously to (5.2) and (5.3) the scheme reads

$$\partial_t \mathbf{c}^*(x, t) = \mathcal{L}(x, t, \mathbf{c}^*(x, t)); \quad t_n < t \leq t_{n+1}; \quad \mathbf{c}^*(x, t_n) = \mathbf{c}_n, \quad (5.17)$$

$$\partial_t \mathbf{c}^{**}(x, t) = \mathcal{R}(x, t, \mathbf{c}^{**}(x, t)); \quad t_n < t \leq t_{n+1}; \quad \mathbf{c}^{**}(x, t_n) = \mathbf{c}^*(x, t_{n+1}), \quad (5.18)$$

with $\mathbf{c}_{n+1} := \mathbf{c}^{**}(x, t_{n+1})$ as the solution for time t_{n+1} . We will call this solution also the operator splitting solution \mathbf{c}_{OS} . In the case of a single species $\mathbf{c} = c$ and first order decay $\mathcal{R}(c) = -kc$ with the rate constant k [1/T], analytical solutions exist for the subproblems as well as for the coupled problem. Valocchi and Malmstead (1992) investigate this case (for constant flux boundary conditions, zero initial condition) in 1D with a semiinfinite domain Ω [VM92], and derive the following mass balance error (Definition 5.1) for one time step τ :

$$E(\tau) = 1 - \frac{k\tau e^{-k\tau}}{1 - e^{-k\tau}}. \quad (5.19)$$

It can be directly seen that the error is controlled by the rate constant and the time step in $k\tau$, and that it is of first order $\mathcal{O}(\tau)$. Kaluarachchi and Morshed (1995) consider additionally Dirichlet $c(0, T) = e^{-\lambda^* T}$, and flux type boundary conditions $(D\partial_x c - qc)_{x=0} = e^{-\lambda^* T}$. The corresponding analytical solutions can be found, e.g., in [vGA82]. The mass balance error reads for the flux type condition

$$E(t_n) = 1 - \frac{1 - e^{-\lambda^* \tau}}{1 - e^{-(\lambda^* - k)\tau}} \left(1 - \frac{k}{\lambda^*} \right) \quad \text{for } k \neq \lambda^*, \lambda^* \neq 0. \quad (5.20)$$

For the Dirichlet condition, an error that shows similar behaviour is derived (see [KM95]). A sensitivity analysis shows the strong dependence of the error on $k\tau$.

Reaction terms of the Monod type corresponding to biodegradation problems are considered in [BB86, WD87, MK95]. Wheeler and Dawson (1987) show the convergence of the scheme for N_S species coupled by a nonlinear reaction term under certain regularity and coefficient assumptions (see [WD87]). They use a modified method of characteristics and a second order Runge Kutta method for solving the subproblems.

Saaf (1996) splits advection, diffusion, kinetic reaction, and equilibrium reaction for a general multicomponent model, and shows by Taylor expansions the accuracy of first order in time of the operator splitting scheme [Saa96]. These results are of course in accordance with the derivations in Section 5.1.2. Another standard reference within a general framework is the chapter of Marchuk on splitting and alternating direction methods [Mar90].

General sorption mechanisms are included by [MR93], various example calculations with equilibrium and kinetic reactions are given in [ZSD94, Saa96, CYSM00].

A vague statement as given by Chilakapati et al. (2000) “*that time-splitting of the operators as is done here, does not prevent [...] from matching analytic solutions to problems with nonlinear, mixed kinetic-equilibrium systems and nonuniform flows*” [CYSM00] is of little value. Of course any – even an erratic – scheme can, at least by coincidence, meet the true solution in some special configuration, but the quality of the approximation should be guaranteed systematically for all cases.

Alternate Non-Iterative Splitting

Transferring the scheme (5.4)–(5.6) to the transport/reaction splitting yields

$$\partial_t \mathbf{c}^* = \mathcal{L}(\mathbf{c}^*); \quad t_n < t \leq t_{n+1/2}; \quad \mathbf{c}^*(x, t_n) = \mathbf{c}_n, \quad (5.21)$$

$$\partial_t \mathbf{c}^{**} = \mathcal{R}(\mathbf{c}^{**}); \quad t_n < t \leq t_{n+1}; \quad \mathbf{c}^{**}(x, t_n) = \mathbf{c}^*(x, t_{n+1/2}), \quad (5.22)$$

$$\partial_t \mathbf{c}^{***} = \mathcal{L}(\mathbf{c}^{***}); \quad t_{n+1/2} < t \leq t_{n+1}; \quad \mathbf{c}^{***}(x, t_{n+1/2}) = \mathbf{c}^{**}(x, t_{n+1}). \quad (5.23)$$

In the linear 1D situation of [VM92] this reduces the mass-balance error by more than a factor of 10 for a wide range of $k\tau$ values. More specifically, we have already seen that the operator splitting error is now of order $\mathcal{O}(\tau^2)$. Kaluarachchi and Morshed (1995) consider the corresponding mass balance errors for linear decay. E.g., for the flux boundary condition (compare with (5.20)) this results in [KM95]

$$E(t_n) = 1 - (1 - e^{-\lambda^* \tau}) \left(\frac{e^{-2k\tau} + e^{-\lambda^* \tau}}{e^{-2k\tau} - e^{-2\lambda^* \tau}} \right) \left(1 - \frac{k}{\lambda^*} \right) \quad (5.24)$$

for $k \neq \lambda^*, \lambda^* \neq 0$.

The analogous derivations for the Monod type reactions are given in [MK95]. Many of the authors cited in the previous section also apply the Strang splitting for comparisons [VM92, MR93, ZSD94, KM95, MK95, BMCH96, CMB04].

Commuting Operators

We want to evaluate under which conditions a zero splitting error results. As we have seen in Section 5.1.2 for the general case (Theorems 5.6 and 5.7), the local truncation errors are of order $\mathcal{O}(\tau)$, or $\mathcal{O}(\tau^2)$ for the standard or the Strang splitting, respectively.

F_1 will be identified with the transport operator \mathcal{L} , F_2 with the reaction operator \mathcal{R} . The relevant term is

$$[\mathcal{F}_1, \mathcal{F}_2]I(\mathbf{c}) = (F_2'F_1)(\mathbf{c}) - (F_1'F_2)(\mathbf{c}),$$

regarding (componentwise) differentiation with respect to \mathbf{c} . More precisely, the operator defined by the functional matrix $\mathcal{L}'(\mathbf{c})$ (dimensions $N_S \times N_S$) has only (equal) entries on the diagonal, and due to the linearity of the differential operators in \mathcal{L} , we have for an arbitrary function $s \in \mathcal{S}$:

$$F_1'(\mathbf{c})s \equiv F_1(s) = \nabla \cdot (D\nabla s - \mathbf{q}s).$$

$F_2'(\mathbf{c})$ is the $(N_S \times N_S)$ -Jacobian $\mathcal{R}'(\mathbf{c})$ (cf. again [LV99]).

Let us evaluate the leading term of the splitting error for standard non-iterative splitting (5.17) and (5.18) in case of general, space dependent diffusion-dispersion D and convection \mathbf{q} . Reactions normally apply on the whole domain Ω , and thus can be assumed space independent. Note that this excludes local source or sink terms in \mathcal{R} . We are interested in particular in general kinetic reactions of type (2.30) and biodegradation of the general type (2.26).

Theorem 5.8 *Under the above assumptions the leading error term in (5.14) for the standard operator splitting scheme (5.17) and (5.18) is given by*

$$\begin{aligned} & \frac{\tau}{2}[(F_2'F_1)(\mathbf{c}) - (F_1'F_2)(\mathbf{c})] = & (5.25) \\ & = -\frac{\tau}{2} \sum_{i,j=1}^3 (D_{ij}\mathcal{R}''(\mathbf{c})\partial_{x_i}\mathbf{c}\partial_{x_j}\mathbf{c}) + \frac{\tau}{2} \sum_{i=1}^3 \partial_{x_i}q_i(\mathcal{R}(\mathbf{c}) - \mathcal{R}'(\mathbf{c})\mathbf{c}). \end{aligned}$$

Proof: In Theorem 5.6 we have seen that the leading error term is $\frac{\tau}{2}(F_2'F_1)(\mathbf{c}) - (F_1'F_2)(\mathbf{c})$. We denote the vectors with $\mathbf{x} = (x_1, x_2, x_3)^T$ and $\mathbf{q} = (q_1, q_2, q_3)^T$, and recall that \mathbf{c} has N_S components. We occasionally also write c_{x_i} for short, instead of $\frac{\partial \mathbf{c}}{\partial x_i}$. Then we get in detail

$$\begin{aligned} (F_2'F_1)(\mathbf{c}) &= \mathcal{R}'(\mathbf{c})(\nabla \cdot (D\nabla \mathbf{c} - \mathbf{q}\mathbf{c})) = \\ &= \mathcal{R}'(\mathbf{c}) \left(\partial_{x_1}(D_{11}\mathbf{c}_{x_1} + D_{12}\mathbf{c}_{x_2} + D_{13}\mathbf{c}_{x_3} - q_1\mathbf{c}) + \right. \\ &\quad \left. + \partial_{x_2}(D_{21}\mathbf{c}_{x_1} + D_{22}\mathbf{c}_{x_2} + D_{23}\mathbf{c}_{x_3} - q_2\mathbf{c}) + \right. \\ &\quad \left. + \partial_{x_3}(D_{31}\mathbf{c}_{x_1} + D_{32}\mathbf{c}_{x_2} + D_{33}\mathbf{c}_{x_3} - q_3\mathbf{c}) \right), \text{ and} \end{aligned}$$

$$\begin{aligned}
(F_1'F_2)(\mathbf{c}) &= (\nabla \cdot (D\nabla - \mathbf{q}))\mathcal{R}(\mathbf{c}) = \\
&= \partial_{x_1} \left(D_{11}\partial_{x_1}(\mathcal{R}(\mathbf{c})) + D_{12}\partial_{x_2}(\mathcal{R}(\mathbf{c})) + D_{13}\partial_{x_3}(\mathcal{R}(\mathbf{c})) - q_1\mathcal{R}(\mathbf{c}) \right) \\
&\quad + \partial_{x_2} \left(D_{21}\partial_{x_1}(\mathcal{R}(\mathbf{c})) + D_{22}\partial_{x_2}(\mathcal{R}(\mathbf{c})) + D_{23}\partial_{x_3}(\mathcal{R}(\mathbf{c})) - q_2\mathcal{R}(\mathbf{c}) \right) \\
&\quad + \partial_{x_3} \left(D_{31}\partial_{x_1}(\mathcal{R}(\mathbf{c})) + D_{32}\partial_{x_2}(\mathcal{R}(\mathbf{c})) + D_{33}\partial_{x_3}(\mathcal{R}(\mathbf{c})) - q_3\mathcal{R}(\mathbf{c}) \right).
\end{aligned}$$

Remember that $\partial_{x_i}(\mathcal{R}(\mathbf{x}, \mathbf{c}(\mathbf{x}))) = \mathcal{R}_{x_i}(\mathbf{x}, \mathbf{c}(\mathbf{x})) + \mathcal{R}'(\mathbf{x}, \mathbf{c}(\mathbf{x}))\mathbf{c}_{x_i}$ with $i \in \{1, 2, 3\}$. Taking into account the independence of \mathbf{x} for $\mathcal{R}(\mathbf{c})$, this results in

$$\begin{aligned}
(F_2'F_1)(\mathbf{c}) - (F_1'F_2)(\mathbf{c}) &= \mathcal{R}'(\mathbf{c}) \sum_{i,j=1}^3 \partial_{x_i}(D_{ij}\partial_{x_j}\mathbf{c}) - \mathcal{R}'(\mathbf{c}) \sum_{i=1}^3 \partial_{x_i}(q_i\mathbf{c}) \\
&\quad - \sum_{i,j=1}^3 (\partial_{x_i}(D_{ij}\partial_{x_j}(\mathcal{R}(\mathbf{c})))) + \sum_{i=1}^3 \partial_{x_i}(q_i\mathcal{R}(\mathbf{c})) = \\
&= \mathcal{R}'(\mathbf{c}) \sum_{i,j=1}^3 (\cancel{\partial_{x_i}D_{ij}\partial_{x_j}\mathbf{c}} + D_{ij}\partial_{x_ix_j}^2\mathbf{c}) - \mathcal{R}'(\mathbf{c}) \sum_{i=1}^3 (\partial_{x_i}q_i\mathbf{c} + q_i\partial_{x_i}\mathbf{c}) \\
&\quad - \sum_{i,j=1}^3 (\cancel{\partial_{x_i}D_{ij}\mathcal{R}'(\mathbf{c})\partial_{x_j}\mathbf{c}} + D_{ij}\partial_{x_i}(\mathcal{R}'(\mathbf{c})\partial_{x_j}\mathbf{c})) \\
&\quad + \sum_{i=1}^3 (\partial_{x_i}q_i\mathcal{R}(\mathbf{c}) + q_i\partial_{x_i}(\mathcal{R}(\mathbf{c}))) = \\
&= \cancel{\mathcal{R}'(\mathbf{c}) \sum_{i,j=1}^3 (D_{ij}\partial_{x_ix_j}^2\mathbf{c})} - \mathcal{R}'(\mathbf{c}) \sum_{i=1}^3 (\partial_{x_i}q_i\mathbf{c} + q_i\cancel{\partial_{x_i}\mathbf{c}}) \\
&\quad - \sum_{i,j=1}^3 (D_{ij}\partial_{x_i}(\mathcal{R}'(\mathbf{c}))\partial_{x_j}\mathbf{c} + \cancel{D_{ij}\mathcal{R}'(\mathbf{c})\partial_{x_ix_j}^2\mathbf{c}}) + \sum_{i=1}^3 (\partial_{x_i}q_i\mathcal{R}(\mathbf{c}) + \cancel{q_i\mathcal{R}'(\mathbf{c})\partial_{x_i}\mathbf{c}}) \\
&= - \sum_{i,j=1}^3 (D_{ij}\mathcal{R}''(\mathbf{c})\partial_{x_i}\mathbf{c}\partial_{x_j}\mathbf{c}) + \sum_{i=1}^3 \partial_{x_i}q_i(\mathcal{R}(\mathbf{c}) - \mathcal{R}'(\mathbf{c})\mathbf{c}). \tag{5.26}
\end{aligned}$$

This completes the proof. \square

From this result we can easily deduce the following corollary which, however, refers to assumptions rarely met in practical situations.

Corollary 5.9 *Consider equation (5.16) with standard non-iterative splitting (5.17) and (5.18), or Strang splitting (5.21)–(5.23). Let $\mathcal{R}(\mathbf{c}) := \mathbf{A}\mathbf{c} + B$, with constant matrices $A, B \in \mathbb{R}^{N_S \times N_S}$, thus $\mathcal{R}(\mathbf{c})$ being a linear function of*

\mathbf{c} and independent of \mathbf{x} , and let furthermore the velocity field \mathbf{q} be divergence free. Then the splitting error for both schemes is zero.

Proof: From Theorems 5.6 and 5.7 we know that the term to vanish is $(F_2'F_1)(\mathbf{c}) - (F_1'F_2)(\mathbf{c})$. As the tensor $\mathcal{R}''(\mathbf{c}) \equiv \mathbf{0}$ under the given assumptions, the first sum in (5.26) is nil. From

$$\nabla \cdot \mathbf{q} = 0 \Rightarrow \sum_{i=1}^3 \partial_{x_i} q_i (\mathcal{R}(\mathbf{c}) - \mathcal{R}'(\mathbf{c})\mathbf{c}) = 0.$$

Thus we have a sufficient condition for zero splitting errors. \square

Note that – for an incompressible fluid – a stationary flow field (with a constant water flux) is divergence free.

Remark 5.10 Due to the multiplicative character of the rate expressions, second derivatives do not simplify essentially. Rate expressions (2.30) for kinetic chemistry

$$R_r = \left(k_r^b \prod_{\{i|\nu_{ir}<0\}} c_i^{-\nu_{ir}} - k_r^f \prod_{\{i|\nu_{ir}>0\}} c_i^{\nu_{ir}} \right)$$

yield non-zero entries of the following kinds by contributing to $\mathcal{R}''(\mathbf{c})$ in the error term:

$$\begin{aligned} \frac{\partial^2 R_r}{\partial c_k^2} &= -k_r |\nu_{kr}| (|\nu_{kr}| - 1) c_k^{|\nu_{kr}|-2} \prod_{i \neq k} c_i^{|\nu_{ir}|}, \text{ or} \\ \frac{\partial^2 R_r}{\partial c_k c_l} &= -k_r |\nu_{kr}| |\nu_{lr}| c_k^{|\nu_{kr}|-1} c_l^{|\nu_{lr}|-1} \prod_{i \neq k} c_i^{|\nu_{ir}|}, \end{aligned}$$

with k_r being the forward or backward rate constant for c_k, c_l being both educt species, or product species, respectively. Again the terms can be unbounded for some $c_i \rightarrow 0$ with exponent < 1 in the above expressions. If we consider the regularised form of Section 2.8, this is avoided.

Rate (2.26) for biodegradation consists of single reaction terms reading

$$R_r = \mu_{\max_r} c_{B_r} \prod_{i \in I_r^1} \left(\frac{c_i}{K_{M_i} + c_i} \right) \prod_{j \in I_r^2} \left(\frac{K_{I_j}}{K_{I_j} + c_j} \right).$$

According to the role of the species this yields non-zero entries of the following types, for $k \in I_r^1 \setminus I_r^2$ (remember Definition 2.11):

$$\begin{aligned} \frac{\partial^2 R_r}{\partial c_k^2} &= \mu_{\max_r} c_{B_r} \frac{-2K_{M_k}}{(K_{M_k} + c_k)^3} \prod_{i \in I_r^1 \setminus \{k\}} \left(\frac{c_i}{K_{M_i} + c_i} \right) \prod_{j \in I_r^2} \left(\frac{K_{I_j}}{K_{I_j} + c_j} \right) = \\ &= \frac{-2K_{M_k}}{c_k (K_{M_k} + c_k)^2} R_r, \end{aligned}$$

for $k \in I_r^2 \setminus I_r^1$:

$$\begin{aligned} \frac{\partial^2 R_r}{\partial c_k^2} &= \mu_{\max_r} c_{B_r} \frac{2K_{I_k}}{(K_{I_k} + c_k)^3} \prod_{i \in I_r^1} \left(\frac{c_i}{K_{M_i} + c_i} \right) \prod_{j \in I_r^2 \setminus \{k\}} \left(\frac{K_{I_j}}{K_{I_j} + c_j} \right) = \\ &= \frac{2}{(K_{I_k} + c_k)^2} R_r, \end{aligned}$$

and for $k \in I_r^1 \cap I_r^2$:

$$\begin{aligned} \frac{\partial^2 R_r}{\partial c_k^2} &= \frac{\partial}{\partial c_k} \left(R_r \left(\frac{K_{M_k}}{c_k (K_{M_k} + c_k)} - \frac{1}{K_{I_k} + c_k} \right) \right) = \\ &= R_r \left(\frac{1}{(K_{I_k} + c_k)^2} - \frac{K_{M_k}}{c_k^2 (K_{M_k} + c_k)} + \left(\frac{K_{M_k}}{c_k (K_{M_k} + c_k)} - \frac{1}{K_{I_k} + c_k} \right)^2 \right). \end{aligned}$$

Similar terms can be derived for the cross derivative terms. To put it in a nutshell, it can be seen from the above derivations that in the situation of Theorem 5.8 large rates, i.e. stiff chemistry, in combination with large concentration and flux gradients are problematic.

Iterative Splitting

The sequential iterative approach that has been described in Section 5.1.1 is illustrated in Fig. 5.1. In case the iteration loop is omitted, we fall back to the standard non-iterative procedure.

It has been applied, e.g., by [YT91, EK92, HWvC98, XPB99, vdLDLG03, KMK03, CMB04]. [EK92] report cases with slow convergence what limits the size of systems that can be handled even in 1D.

Kanney et al. (2003) show that the theoretical convergence rate of this approach for general nonlinear reactive transport problems is $\mathcal{O}(\tau^2)$ under certain assumptions including Lipschitz continuous transport and reaction operators [KMK03]. This Lipschitz continuity, however, can be violated in practical situations, e.g. in the case of the Freundlich model for sorption.

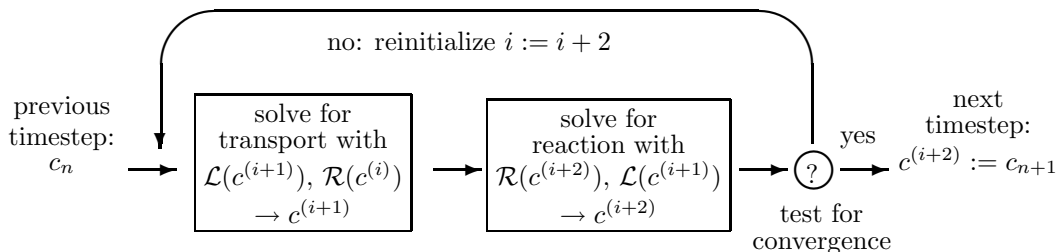


Figure 5.1: Algorithmic scheme for sequential iterative transport / reaction splitting. Subscript indicates the timestep, superscript the iteration count. The substeps are calculated for one full timestep each.

Furthermore, several factors can destroy this order of convergence, including the quadrature rules used, or the accuracy of the solution of the split equations.

Carrayrou et al. (2004) conduct a broader comparison of split operator approaches concerning mass balance errors [CMB04]. They investigated a multicomponent model with linear reaction mechanisms and flux boundary conditions in a semiinfinite domain, where analytical solutions can be deduced. They advocated for a symmetric iterative scheme, or the Strang splitting, which were also superior in terms of efficiency, i.e., necessary time step lengths and computational effort per time step.

It should be noted, that it is also possible to construct higher order schemes, but at the price of problems concerning consistency, the correct incorporation of boundary conditions, or stability [HV03].

5.2 Fully Implicit Solution Strategy

The simultaneous solution of the fully coupled system of N_S species equations – also termed global implicit approach – has not been very popular in the hydrogeochemical literature albeit it appears to be straightforward and accurate in the sense that it avoids splitting errors (cf. Section 5.1.1). Some authors, among them Yeh and Tripathi in their influential paper [YT89], clearly favoured operator splitting in the form of the sequential iterative approach, mainly due to its easy modular applicability and alleged CPU time and memory savings. However, as already stated in Section 5.1.1, the SIA may encounter convergence problems which lead to restrictive time step sizes and many iterations such that the advantage of smaller systems drops away (cf. the reviews [vdLD01, SM96b, SCA01]).

In this section we seek for an accurate global implicit approach while enhanc-

ing the efficiency by applying a modified Newton’s method (Section 5.2.1), and a flexible componentwise linear solver (Section A.1) that can exploit weak couplings inherent in the problem at hand. The global implicit approach has been applied 1995 by White [Whi95] and 1998 by Saaltink et al. [SAC98].

[MFB02] is a rare paper that also deals with unsaturated media, and with multicomponent transport including equilibrium and kinetic reactions according to the mass action law in up to three dimensions.

Otherwise the treated reaction type is often restricted to simpler systems, e.g. sorption isotherms (see [KMB03] and the references therein).

5.2.1 Newton’s Method and Variants

The nonlinear system of equations (4.27) that results from the discretization of our model equations (see (4.16) – (4.26)) is solved with the help of Newton’s method, which reads in general form [Kel95]:

Definition 5.11 Let a nonlinear problem $f(\mathbf{c}) = \mathbf{0}$ with $f : U \subset \mathbb{R}^N \rightarrow \mathbb{R}^N$, and an initial iterate $\mathbf{c}^{(0)}$ be given. Then *Newton’s method* consists of solving

$$Df(\mathbf{c}^{(k)}) \boldsymbol{\delta}^{(k)} = -f(\mathbf{c}^{(k)}), \quad (5.27)$$

with the functional matrix $Df(\mathbf{c}) = (\partial_j f_i(\mathbf{c}))_{ij}$ and the correction vector $\boldsymbol{\delta}^{(k)}$, what leads to the new iterate

$$\mathbf{c}^{(k+1)} := \mathbf{c}^{(k)} + \boldsymbol{\delta}^{(k)}, \quad k = 0, 1, \dots \quad (5.28)$$

In other words, we may write $\mathbf{c}^{(k+1)} := \mathbf{c}^{(k)} - Df(\mathbf{c}^{(k)})^{-1} f(\mathbf{c}^{(k)})$, while keeping in mind that the inverse Jacobian of course is not calculated explicitly. Newton’s method has the advantage of locally quadratic convergence under some assumptions like the Lipschitz continuity of Df (see, e.g., [Deu04, KA03] for details).

To enlarge the range of convergence Newton’s method is modified here according to Armijo’s rule (cf. [Kel95]). This means that the step from the k th iterate $\mathbf{c}^{(k)}$ to $\mathbf{c}^{(k+1)}$ in the Newton direction $-Df(\mathbf{c}^{(k)})^{-1} f(\mathbf{c}^{(k)})$ is not taken with factor 1, but with a reduced step length, if necessary. The criterion for the step length reduction is an insufficient decrease in the (Euclidean) norm of the residual $\|f\|$, e.g., if

$$\|f(\mathbf{c}^{(k+1)})\| > (1 - \alpha\lambda)\|f(\mathbf{c}^{(k)})\|,$$

with $\alpha \in (0, 1)$ and $\lambda \in (0, 1]$. The algorithm for this damped version of Newton’s method with the above monotonicity test is given in Table 5.1.

Table 5.1: Algorithm for the damped version of Newton’s method with monotonicity test and Armijo’s rule.

1. Set $\mathbf{c}^{(0)}$, $\alpha \in (0, 1)$, $\lambda = 1$, $k = 0$.
2. Solve $Df(\mathbf{c}^{(k)}) \boldsymbol{\delta}^{(k)} = -f(\mathbf{c}^{(k)})$.
3. While $\|f(\mathbf{c}^{(k)} + \lambda \boldsymbol{\delta}^{(k)})\| > (1 - \alpha \lambda) \|f(\mathbf{c}^{(k)})\|$ set $\lambda = \lambda/2$.
4. $\mathbf{c}^{(k+1)} := \mathbf{c}^{(k)} + \lambda \boldsymbol{\delta}^{(k)}$.
5. If $\|f(\mathbf{c}^{(k+1)})\| < \varepsilon_a$ or $\|f(\mathbf{c}^{(k+1)})\| < \varepsilon_r \|f(\mathbf{c}^{(0)})\|$: converged.
else: $k := k + 1$, go to 2.

Practically a maximum number of reduction steps in 4. should be defined, as well as a maximum number of Newton iterations k_{\max} . Then a restart with another $\mathbf{c}^{(0)}$ is suggested. It can be shown [Kel95, ch. 8.2] that the fast convergence of the method is preserved for sufficiently large iteration numbers.

The application of Newton’s method requires the assembling of the Jacobian at each iteration step, what may be very memory and time consuming, in particular in higher dimensions. To avoid this, variants of the method have been developed, where the entire Jacobian is updated only periodically, or where only local parts of the Jacobian are updated in the matrices’ regions of nonconvergence.

After analysing the structure of the Jacobian in the case of reactive multicomponent transport problems in Section 5.2.2 we will deal with *modified Newton methods* that use a modified Jacobian or an altered function f : Instead of $\mathbf{c}^{(k+1)} := \mathbf{c}^{(k)} - Df(\mathbf{c}^{(k)})^{-1} f(\mathbf{c}^{(k)})$ set:

$$\mathbf{c}^{(k+1)} := \mathbf{c}^{(k)} - (Df(\mathbf{c}^{(k)}) + \Delta(\mathbf{c}^{(k)}))^{-1} (f(\mathbf{c}^{(k)}) + \epsilon(\mathbf{c}^{(k)})) . \quad (5.29)$$

Then (under standard assumptions [Kel95]) $\exists C > 0$:

$$\|\mathbf{e}^{(k+1)}\| \leq C (\|\mathbf{e}^{(k)}\|^2 + \|\Delta(\mathbf{c}^{(k)})\| \|\mathbf{e}^{(k)}\| + \|\epsilon(\mathbf{c}^{(k)})\|) \quad (5.30)$$

with $\mathbf{e}^{(k)} := \mathbf{c}^{(k)} - \mathbf{c}^*$, where \mathbf{c}^* is the desired root.

In Section 5.2.3 we want to take advantage of modifications of the Jacobian such that $\|\Delta(\mathbf{c}^{(k)})\|$ is small (in order to preserve the convergence properties), and the matrix $(Df(\mathbf{c}^{(k)}) + \Delta(\mathbf{c}^{(k)}))$ is reducible to decouple the corresponding equations and gain computation time.

5.2.2 Structure of the Jacobian

Motivation Preliminary investigations show the importance of effective algorithms for the solution of such systems. The size of the Jacobian depends quadratically upon the number of species N_S in multicomponent problems. The full matrix has dimensions $(N + 1)N_S \times (N + 1)N_S$, but due to the local support of the finite element ansatz functions (4.15), we have only relations to adjacent elements in the dispersion term (4.18) and the convection term (4.21), thus we have a maximum of $3N_S \times (N + 1)N_S$ nonzeros. Furthermore couplings through reactions (which generate nonzero entries) do only occur among few species such that the number of nonzeros is even less.

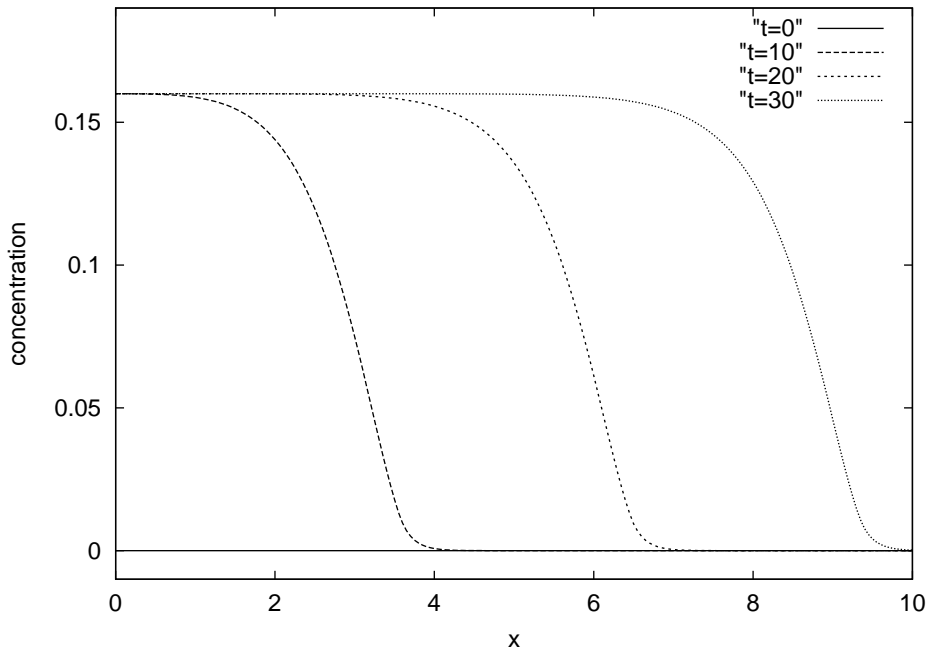


Figure 5.2: Concentration profiles at selected time points ($t = 0, 10, 20, 30$) for the solute in the nonlinear model problem.

To motivate the decoupling strategies of Section 5.2.3 a model problem in 1D with 16 uncoupled species is presented. The (for all species identical) solution that is shown in Figure 5.2 can be obtained by solving one 16 species problem (denoted $1 \times (16)$), or – without loss of information in this case – by solving 16 single species problems ($16 \times (1)$). Table 5.2 shows that for few coupled species, the assembling of the Jacobian predominates the computational load, which is for all cases approximately identical. But for a growing number of

coupled species, the solver becomes important (see also Figure 5.3). The fact that the assembling time remains constant in all cases although the system size grows with N_S^2 is the result of an efficient implementation strategy that avoids assembling of zeros and takes into account the couplings among the species (see Section A.2). With a growing number of species the linear solver dominates the total computation time already in the 1D examples (here we use a direct sparse matrix solver, see A.1). Table 5.2 thus shows that here a reduction of the complexity pays off: A speed-up of the overall computation time of a factor > 9 is achieved through the linear solver that is more than 90 times faster in the uncoupled case.

Table 5.2: CPU Time [s] for solving a nonlinear model problem with 16 uncoupled species in different problem configurations. 200 elements, 1500 time steps, solute transport with nonlinear sorption, average Newton steps per time step: 2.23. Configuration: $a \times (b)$ denotes that the solver treats a subsets of b coupled species each.

configuration	matrix entries		Linear		Speed Up LS
	per node	Assemble	Solver	Total	
$1 \times (16)$	256	256.1	2331.8	2591.8	-
$2 \times (8)$	128	255.0	629.5	888.5	3.7
$4 \times (4)$	64	256.5	184.7	445.1	12.6
$8 \times (2)$	32	258.9	62.5	325.6	37.3
$16 \times (1)$	16	253.4	25.6	283.1	91.1

Matrix Structure The general structure of the Jacobian resulting from 1D finite element discretizations (of conforming, but also mixed type) with linear ansatz functions can be illustrated as follows. Recall from Section 4.3 that the assembling of the global matrix is organised such that indexing of the degrees of freedom for species and nodes is done nodewise (in the order of the elements), and at each node block matrices J_{kl} ($k, l = 0, \dots, N$; $N+1 : \#$ of grid points) of dimension $N_S \times N_S$ can be associated to the diagonal, and sub-, and superdiagonal blocks:

$$\begin{array}{l}
 \text{NODE 0} \\
 \text{NODE 1} \\
 \vdots \\
 \text{NODE N-1} \\
 \text{NODE N}
 \end{array}
 \begin{pmatrix}
 J_{00} & J_{01} & & & 0 \\
 J_{10} & J_{11} & J_{12} & & \\
 & \ddots & \ddots & \ddots & \\
 & & \ddots & \ddots & J_{N-1,N} \\
 0 & & & J_{N,N-1} & J_{N,N}
 \end{pmatrix}. \quad (5.31)$$

The block matrices J_{kk} contain the partial derivatives $\frac{\partial f_{i,k}}{\partial c_{j,k}}$ of the problem

with $i, j = 1, \dots, N_S$, and analogously for J_{kl} with $k \neq l$, where only diagonal terms of the submatrix do not vanish (transport terms):

$$J_{kl} = \begin{pmatrix} \frac{\partial f_{1,k}}{\partial c_{1,l}} & & 0 \\ & \ddots & \\ 0 & & \frac{\partial f_{N_S,k}}{\partial c_{N_S,l}} \end{pmatrix}, \quad J_{kk} = \begin{pmatrix} \frac{\partial f_{1,k}}{\partial c_{1,k}} & \dots & \frac{\partial f_{1,k}}{\partial c_{N_S,k}} \\ \vdots & \ddots & \vdots \\ \frac{\partial f_{N_S,k}}{\partial c_{1,k}} & \dots & \frac{\partial f_{N_S,k}}{\partial c_{N_S,k}} \end{pmatrix}. \quad (5.32)$$

Referring to the nonlinear system (4.27) resulting from the discretization the problem reads at time t_n

$$f(\mathbf{c}^n) = A\mathbf{c}^n + \mathbf{g}(\mathbf{c}^{n,T}) - \mathbf{r}, \quad (5.33)$$

with linear part A containing the contributions of the forms (4.16), or (4.25), for mobile or immobile species, respectively, and, if present, the dispersive parts (4.18), the boundary contributions (4.19) and (4.20), and the convective terms (4.21). The nonlinear part \mathbf{g} subsumes the various reactions in (4.22), and the right-hand side \mathbf{r} gathers the evaluations of the last time step (4.17) and (4.25), respectively, and prescribed nonhomogeneous boundary conditions (4.23) and (4.24).

The off-diagonal entries in the Jacobian block J_{kk} of this problem contain the partial derivatives of f according to the species concentrations at the same spatial node. The only terms that couple the species among each other are the reaction rates in \mathcal{R} , they make the simultaneous solution of the equation system for all species necessary. In detail, those matrix entries for the conforming finite element discretization of Chapter 4 are the following for the off-diagonal entries ($i, j \in \{1, \dots, N_S\}$, $i \neq j$) in the inner diagonal blocks ($k \in \{1, \dots, N-1\}$):

$$\frac{\partial f_{i,k}}{\partial c_{j,k}} = \frac{\tau_n(|\Omega_k| + |\Omega_{k+1}|)}{2} \frac{\partial \mathcal{R}_i}{\partial c_j}, \quad (5.34)$$

For the first and last node we only have

$$\frac{\partial f_{i,0}}{\partial c_{j,0}} = \frac{\tau_n|\Omega_1|}{2} \frac{\partial \mathcal{R}_i}{\partial c_j}, \quad \text{and} \quad \frac{\partial f_{i,N}}{\partial c_{j,N}} = \frac{\tau_n|\Omega_N|}{2} \frac{\partial \mathcal{R}_i}{\partial c_j}. \quad (5.35)$$

Here, \mathcal{R}_i stands for the complete reaction term, that may consist of contributions of N_R single reactions (see also Chapter 2), i.e. for the mobile species

$$\mathcal{R}_i = \Theta \sum_{r=1}^{N_R} \nu_{ir} R_r, \quad (5.36)$$

and analogously for the immobile species, omitting Θ . As often only few species are coupled by one reaction, this submatrix J_{kk} can be sparse and/or reducible. In such a case we may seek to solve some components independently of others. Examples, including the sparsity patterns of the Jacobian, are given in Section 6.2. We will have a closer look at the reaction terms in the following paragraph and Section 5.2.3.

Partial Derivatives of the Reaction Terms In particular, the general multiplicative Monod model of Section 2.4.5 and the kinetic reaction term of Section 2.5 provide multiple connections among the species.

The Monod model results in different partial derivatives of the r th reaction term R_r ($r \in \{1, \dots, N_R\}$) in the degraded species' and the microbial species' equation, where the additional growth restriction term has to be respected. For a degraded species (with index $i \in I_r^1$, recall Definition 2.11) the sum over the microbiological reaction terms was given in (2.26), and the partial derivatives of one such reaction rate R_r (2.25) that we repeat here,

$$R_r = \mu_{\max_r} c_{B_r} \prod_{k \in I_r^1} \left(\frac{c_k}{K_{M_k} + c_k} \right) \prod_{k \in I_r^2} \left(\frac{K_{I_k}}{K_{I_k} + c_k} \right),$$

according to another degraded species ($j \in I_r^1 \setminus I_r^2$) reads

$$\begin{aligned} \frac{\partial \nu_{ir} R_r}{\partial c_j} &= \nu_{ir} \mu_{\max_r} c_{B_r} \prod_{k \in I_r^1 \setminus \{j\}} \left(\frac{c_k}{K_{M_k} + c_k} \right) \prod_{k \in I_r^2} \left(\frac{K_{I_k}}{K_{I_k} + c_k} \right) \frac{K_{M_j}}{(K_{M_j} + c_j)^2} = \\ &= \nu_{ir} \mu_{\max_r} c_{B_r} \prod_{k \in I_r^1} \left(\frac{c_k}{K_{M_k} + c_k} \right) \prod_{k \in I_r^2} \left(\frac{K_{I_k}}{K_{I_k} + c_k} \right) \frac{K_{M_j}}{(K_{M_j} + c_j)^2} = \\ &= \nu_{ir} R_r \frac{K_{M_j}}{c_j (K_{M_j} + c_j)}. \end{aligned} \quad (5.37)$$

According to an exclusively inhibitory species ($j \in I_r^2 \setminus I_r^1$) we get

$$\begin{aligned} \frac{\partial \nu_{ir} R_r}{\partial c_j} &= \nu_{ir} \mu_{\max_r} c_{B_r} \prod_{k \in I_r^1} \left(\frac{c_k}{K_{M_k} + c_k} \right) \prod_{k \in I_r^2 \setminus \{j\}} \left(\frac{K_{I_k}}{K_{I_k} + c_k} \right) \frac{-K_{I_j}}{(K_{I_j} + c_j)^2} = \\ &= \nu_{ir} R_r \frac{-1}{K_{I_j} + c_j}. \end{aligned} \quad (5.38)$$

If $j \in I_r^1 \cap I_r^2$, then

$$\frac{\partial \nu_{ir} R_r}{\partial c_j} = \nu_{ir} R_r \left(\frac{K_{M_j}}{c_j (K_{M_j} + c_j)} - \frac{1}{K_{I_j} + c_j} \right). \quad (5.39)$$

The partial derivative according to the microbial species of the reaction gives

$$\frac{\partial \nu_{ir} R_r}{\partial c_{B_r}} = \nu_{ir} \mu_{\max_r} \prod_{k \in I_r^1} \left(\frac{c_k}{K_{M_k} + c_k} \right) \prod_{k \in I_r^2} \left(\frac{K_{I_k}}{K_{I_k} + c_k} \right). \quad (5.40)$$

Note that the partial derivatives according to the inhibitory species are relevant for the equations of the degraded and microbial species, but not for the equation of the inhibitory species itself, because it is not transformed by the reaction.

In the equation of the microbial species with index $i = B_r \in I^3$, we have to account for the additional growth restriction term (see (2.27)) and thus also for the partial derivatives according to the other microbial species ($B_m \in I^3$, $B_m \neq B_r$):

$$\frac{\partial \nu_{ir} R_r}{\partial c_{B_m}} = \nu_{ir} \left(-\frac{1}{c_{B_{\max}}} \right) R_r. \quad (5.41)$$

Furthermore,

$$\frac{\partial \nu_{ir} R_r}{\partial c_{B_r}} = \nu_{ir} \left(1 - \frac{\sum_{j=1}^{N_{\text{Sbio}}} c_{B_j} - c_{B_r}}{c_{B_{\max}}} \right) \left(\mu_{\max_r} \prod_{k \in I_r^1} \left(\frac{c_k}{K_{M_k} + c_k} \right) \prod_{k \in I_r^2} \frac{K_{I_k}}{K_{I_k} + c_k} \right). \quad (5.42)$$

For the partial derivatives according to the other species, we only have to add the restriction term to the term (5.37), when $j \in I_r^1 \setminus I_r^2$, to (5.38), if $j \in I_r^2 \setminus I_r^1$, and to (5.39), if $j \in I_r^1 \cap I_r^2$.

The second important nonlinear reaction rate stems from the kinetic reaction according to the mass action law (2.30) and had been regularised (see (2.45)) for $c_i < \tilde{c}$. Remember the four cases defined by (2.44). In detail, we get for the partial derivatives according to an educt species ($\nu_{jr} > 0$):

$$\frac{\partial \nu_{ir} R_r}{\partial c_j} = -\nu_{ir} k_r^f \nu_{jr} c_j^{(\nu_{jr}-1)} \prod_{k \in M_1, k \neq j} c_k^{\nu_{kr}} \prod_{k \in M_2} \tilde{c}^{\nu_{kr}} \frac{c_k}{\tilde{c}}, \quad \text{for } j \in M_1, \quad (5.43)$$

$$\frac{\partial \nu_{ir} R_r}{\partial c_j} = -\nu_{ir} k_r^f \tilde{c}^{\nu_{jr}} \frac{1}{\tilde{c}} \prod_{k \in M_1} c_k^{\nu_{kr}} \prod_{k \in M_2, k \neq j} \tilde{c}^{\nu_{kr}} \frac{c_k}{\tilde{c}}, \quad \text{for } j \in M_2. \quad (5.44)$$

Differentiation according to a product species with $\nu_{jr} < 0$ yields

$$\frac{\partial \nu_{ir} R_r}{\partial c_j} = -\nu_{ir} k_r^b \nu_{jr} c_j^{(-\nu_{jr}-1)} \prod_{k \in M_3, k \neq j} c_k^{-\nu_{kr}} \prod_{k \in M_4} \tilde{c}^{-\nu_{kr}} \frac{c_k}{\tilde{c}}, \quad \text{for } j \in M_3, \quad (5.45)$$

$$\frac{\partial \nu_{ir} R_r}{\partial c_j} = -\nu_{ir} k_r^b \tilde{c}^{-\nu_{jr}} \frac{1}{\tilde{c}} \prod_{k \in M_3} c_k^{-\nu_{kr}} \prod_{k \in M_4, k \neq j} \tilde{c}^{-\nu_{kr}} \frac{c_k}{\tilde{c}}, \quad \text{for } j \in M_4. \quad (5.46)$$

Remark 5.12 All of the above terms (5.37) – (5.46) are vanishing, if

- a) stoichiometric coefficients $\nu_{ir} = 0$, i.e. the species concentration c_i is not changed by the r th reaction,
- b) one of the concentrations c_i with $\nu_{ir} \neq 0$ is vanishing.

Furthermore, the terms are small, for small rate constants k_r^f , k_r^b , μ_{\max_r} , i.e., slow kinetic reactions (assuming that the concentrations are not growing unboundedly).

In the following section the neglect of terms (5.37) – (5.46), the decoupling of species equations, and the consequences on computation time and performance of Newton’s method will be investigated.

5.2.3 Process Preserving Decoupling Strategies

As we have seen in Section 5.1, operator splitting bears an inherent splitting error by treating coupled physicochemical processes as if they were independent. Avoiding this shortcoming, we want to pursue the global implicit approach of simultaneously solving the coupled equations. In this context possibilities are sought to enhance the efficiency of the technique without destroying the process preserving character of the implicit method.

‘Correct’ Newton’s Method

First we briefly discuss the case, where in fact no couplings between some groups of species exist, and thus no terms have to be neglected in the Jacobian to benefit from this property. This issue corresponds to the question of reducibility of the Jacobian matrix, if the reaction network is such that species are effectively uncoupled, or if – in the course of the evolution of the solution – some concentrations vanish, and thus the involved reactions become obsolete. The matrix graph is no longer connected in this case, and subsystems can be solved separately. In these cases we still apply the standard method of Newton in its proposed form with line search according to Armijo’s rule (Table 5.1), with the only difference that the linear solver operates on a sequence of subsets of the equation system without loss of accuracy. We estimate the number of floating point operations saved by this technique, on the basis of a Gaussian elimination of a band matrix that needs $2np^2$ flops, where n is the dimension of the matrix, and p the bandwidth [GL96].

Lemma 5.13 *Let $N + 1$ be the number of spatial nodes, and N_S the total number of components. Let further on the system be reducible in p independent parts of size $N_i \leq N_S$, $i = 1, \dots, p$, $p \geq 1$, where $\sum_{i=1}^p N_i = N_S$. The full system matrix has dimensions $(N + 1)N_S \times (N + 1)N_S$ with a maximum of $3N_S \times (N + 1)N_S$ non-zero entries, the bandwidth is $2N_S - 1$. Suppose the linear equation system is solved with a Gaussian band matrix solver. Define $f_f := \#\{\text{flops}\}$ for solving the full system at once, $f_p := \#\{\text{flops}\}$ for solving the system in parts. Then the computational saving for solving the system in p decoupled parts of size $(N + 1)N_i \times (N + 1)N_i$, $i = 1, \dots, p$, with $3N_i \times (N + 1)N_i$ non-zero entries, is equal to*

$$f_f - f_p = 8(N + 1) \left(\sum_{\substack{i,j,k=1 \\ \setminus \{i=j=k\}}}^p N_i N_j N_k - \sum_{\substack{i,j=1 \\ i \neq j}}^p N_i N_j \right). \quad (5.47)$$

In the case of parts of equal size, i.e., $N_i = N_S/p$, $i = 1, \dots, p$, the computational effort reduces by a factor of

$$\frac{f_p}{f_f} = \frac{(2N_S/p - 1)^2}{(2N_S - 1)^2}. \quad (5.48)$$

Proof: As the floating point operations for solving the full system are $f_f = 2(N + 1)N_S(2N_S - 1)^2$, simple arithmetics yield the first proposition

$$\begin{aligned} f_f - f_p &= 2(N + 1)N_S(2N_S - 1)^2 - 2(N + 1) \sum_{i=1}^p N_i(2N_i - 1)^2 = \\ &= 2(N + 1) \left(4N_S^3 - 4N_S^2 + N_S - \sum_{i=1}^p (4N_i^3 - 4N_i^2 + N_i) \right) = \\ &= 8(N + 1) \left(\left(\sum_{i=1}^p N_i \right)^3 - \left(\sum_{i=1}^p N_i \right)^2 - \sum_{i=1}^p (N_i^3 - N_i^2) \right) = \\ &= 8(N + 1) \left(\sum_{\substack{i,j,k=1 \\ \setminus \{i=j=k\}}}^p N_i N_j N_k - \sum_{\substack{i,j=1 \\ i \neq j}}^p N_i N_j \right). \end{aligned}$$

If now $N_i = N_S/p$ we obtain the theoretical speed-up factor

$$\frac{f_f}{f_p} = \frac{N_S(2N_S - 1)^2}{\sum_{i=1}^p \frac{N_S}{p} \left(\frac{2N_S}{p} - 1 \right)^2} = \frac{(2N_S - 1)^2}{\left(\frac{2N_S}{p} - 1 \right)^2},$$

what proves the assertion. □

Example 5.14 For illustration, take the case of a reaction system implying the matrix structure (5.49) for the Jacobian diagonal blocks (cf. 5.32), where three parts, i.e. three groups of species, can be solved independently of the others: (1 and 2), (0, 3, 5, 6), and (4,7):

$$J_{kk} = \begin{pmatrix} * & & * & * & * \\ & * & * & & \\ & * & * & & \\ * & & * & * & * \\ & & & * & & * \\ * & & * & * & * \\ * & & * & * & * \\ & & & * & & * \end{pmatrix}. \quad (5.49)$$

In this example, computational savings according to (5.47) are

$$f_f - f_p = 8(N+1)(N_S^3 - N_S^2 - \sum_{i=1}^3 (N_i^3 - N_i^2)) = 8(N+1)(448 - 56) = 3136(N+1)$$

operations. Further examples are given in Section 6.2.

To benefit from such a reducible matrix without changing the structure of the whole finite element problem, a flexible linear solver is needed that is able to solve an arbitrary number of arbitrary subsystems of arbitrary size – without rearranging matrices, right-hand sides and solution vector. This task has been realized with the help of pointer lists containing the information on the indices of the subsets, and by rewriting all loops of the solver acting on these pointer lists, see Appendix A.1 for some details about the implementation. It should be noted that by this technique, CPU time for the fully coupled problem, when we do not profit from solving smaller systems, augmented by approximately 20 %, because loops over pointer lists are computationally more expensive than linear loops acting on local variables. In principal this strategy can only be promising when the computational effort for linear solving time outweighs assembling time, i.e., for many species (cf. Figure 5.3).

Modified Newton's Method

In order to obtain a reducible Jacobian, where the decoupled solution algorithm can be applied, we may neglect small off-diagonal coupling terms

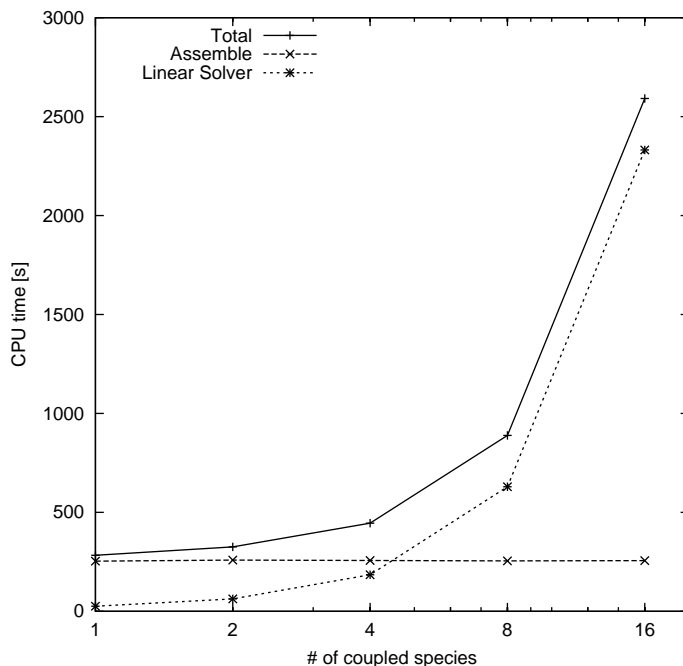


Figure 5.3: Comparison of computational effort for assembling and linear solving with growing number of coupled species for a nonlinear model problem (see also Section 5.2.2).

in J_{kk} ($\forall k = 0, \dots, N$) [RVV00]. This corresponds to a modified Newton's method (cf. Section 5.2.1) which can result in a deterioration of the convergence properties, because the approximation of the 'correct' problem is worse, and as a consequence more Newton steps become necessary to achieve the desired level of accuracy. Here a trade-off has to be made between the inferior convergence of Newton's method (see Table 5.3) and the speed-up achieved by solving smaller systems (see Table 5.2).

Table 5.3 illustrates for two examples, that this inferior convergence behaviour does not appear immediately. The parameter δ denotes the threshold below which matrix entries are being ignored ($\delta = 0$: the 'exact' system is solved) – without taking profit from eventual decouplings here. Evidently the tolerance when quadratic Newton convergence is destroyed is problem-dependent: 10^{-2} for the EDTA example of Section 6.1, 10^{-5} for an example of PHREEQC (Nr. 11 in [PA99]). As already demonstrated in the previous sections the efficiency of decoupling depends on the number of species, the time scales of the reactions, the number of grid points, and the dimensionality of the problem.

Table 5.3: Simplification of Jacobian: neglecting off-diagonal terms. Effect on number of Newton steps and time for solving.

threshold δ	Newton steps	Ass. time	LS time	Total
EDTA-example:				
0.0	210	1.34	1.86	3.20
1.0E-9	210	1.28	0.95	2.23
1.0E-5	210	1.21	1.00	2.21
1.0E-2	213	1.26	1.00	2.26
1.0E-1	508	2.38	2.49	4.89
Phreeqc-example:				
0.0	106	2.26	2.70	4.99
1.0E-6	106	2.20	3.33	5.59
1.0E-5	146	2.58	4.08	6.71
1.0E-4	372	4.94	9.37	14.45
1.0E-3	467	5.94	11.73	17.79

Figure 5.4 shows which situation has to be avoided in principle. The error reduction in one time step is given (l_2 -norm of the residual) for the fully coupled and a decoupled strategy, the problem is the EDTA reaction of Section 6.1. In the left ($\tau=0.5$) both variants possess approximately quadratic convergence. But only a slight enlargement of the time step size to $\tau = 0.7$ leads to a dramatic deterioration of the decoupled method (right graphics, Figure 5.4). In this case we only allowed one line search step, otherwise no sufficient improvement of the error could be achieved at all. In Section 6.2 we investigate the performance for some numerical and practical examples, the gains in CPU time are summarized in Figure 5.5 at the end of this section.

As the componentwise sparse block matrix solver (Section A.1) does not require any rearranging of the equation system to profit from decoupled subsystems, it is a promising and flexible tool to adaptively change solution strategies potentially in every time step without additional cost. Only the criterion for neglecting terms has to be evaluated. If such a criterion is based on a concentration threshold $c_i < \varepsilon$ it is very cheap to evaluate, and we can save in addition the evaluation of the corresponding rate contributions R_r , where $\nu_{ir} \neq 0$. If it is based on the matrix entries ($\tau|\Omega_k|/2 \partial R_r/\partial c_i$) the reactive terms are evaluated as usual, but eventually not added to the Jacobian. The assembling time thus remains the same.

Figure 5.5 subsumes the results of the numerical examples in this section

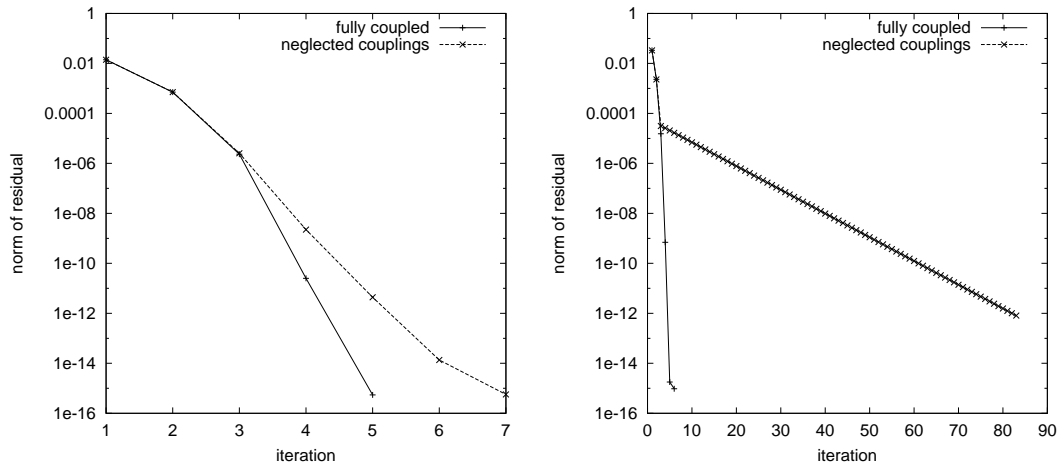


Figure 5.4: l_2 -norm of the residual for the Newton iterations, left: timestep $\tau = 0.5$, right: $\tau = 0.7$.

(idealized case with 16 species) and also of those presented in Section 6.2: the artificial six and twelve species problem, and the EDTA scenario. Maximum observed speed-ups in CPU times are presented, i.e. CPU time of the fully coupled case over CPU time for decoupled case. The speed-up ranges from 5 (EDTA-example) up to 93 (idealized 16 species case) for the linear solver, and from 2 (EDTA) up to 9 (16 species) for the total computation time in the presented examples. This demonstrates the potential of the decoupling method and also shows that the increase in CPU time by operating on pointer lists is easily compensated.

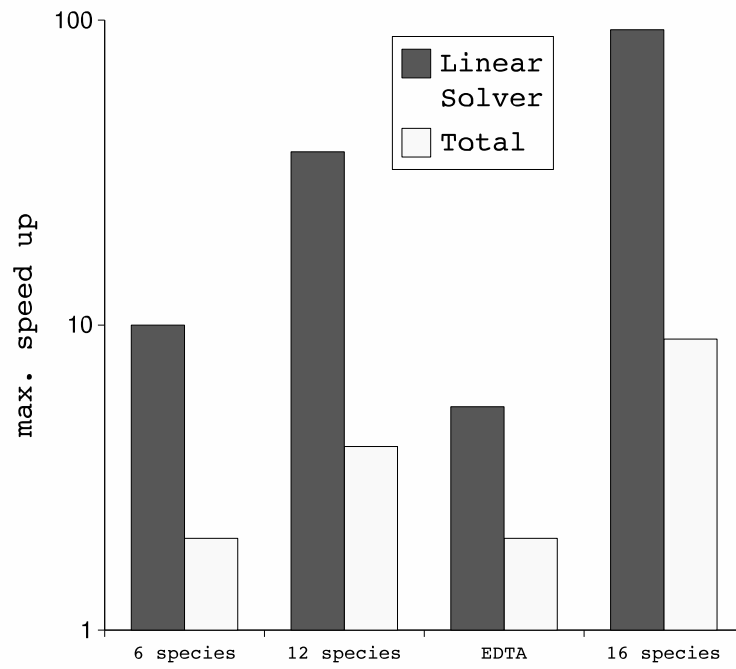


Figure 5.5: Summary of the maximum speed-up factors (CPU time fully coupled : CPU time decoupled) of several test cases.

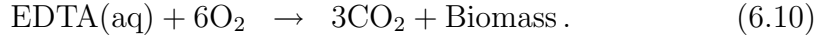
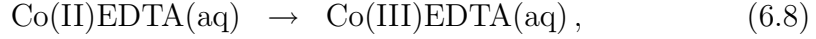
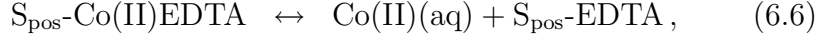
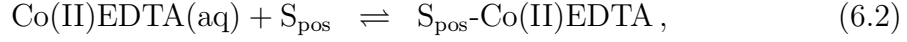
Chapter 6

Numerical Examples of Reactive Multicomponent Transport

In this chapter several numerical examples serve to verify the implementation of the multicomponent reaction model (Section 6.1) and to demonstrate the efficiency of the decoupling techniques by artificial examples as well as the EDTA problem (Section 6.2). Finally the simulation tool is applied in a real case study concerning column experiments investigating the anaerobic degradation of propylene glycol (Section 6.3), where the understanding of the underlying processes benefits from the interplay between model and data.

6.1 The EDTA Example Problem

This problem deals with reactions in groundwater and sediments of the metal complexant EthyleneDiamineTetraacetic Acid (EDTA). Some of these complexes, e.g. the cobalt (Co)–EDTA complexes are harmful contaminants found in groundwater systems near military sites [SZC⁺98]. The species and reactions we want to consider here are taken from [CGS98] and [FYB03], where the example served to test implementations of reactive multispecies models. The example takes into account the interactions of 15 species in ten biogeochemical reactions including fast adsorption/desorption, slow kinetics of oxydation and dissolution, and biodegradation. Thus we deal with a heterogeneous mixed equilibrium/kinetic problem. The reaction system according to [CGS98] and [FYB03] is given by



As indicated by the different arrow symbols, reactions (6.1) – (6.5) are fast, heterogeneous sorption/desorption reactions, reactions (6.6) – (6.8) are slow kinetic reactions, and reactions (6.9) and (6.10) are irreversible biodegradation reactions of the Monod type (2.22) (see page 22) without inhibition terms. In both reactions, oxygen acts as electron acceptor. An analysis of the stoichiometric matrix shows that we have 9 independent chemical reactions. E.g., for the last reaction we can write (6.10) = (6.4) + (6.7) + (6.9). The corresponding equilibrium constants K , forward and backward reaction rates k^f and k^b , maximum growth rates μ_{max} , and Monod constants K_M are:

$$(6.1) : \quad K = \frac{k^f}{k^b} = 12.0,$$

$$(6.2) : \quad K = \frac{k^f}{k^b} = 25.0,$$

$$(6.3) : \quad K = \frac{k^f}{k^b} = 9.0,$$

$$(6.4) : \quad K = \frac{k^f}{k^b} = 25.0,$$

$$(6.5) : \quad K = \frac{k^f}{k^b} = 2.5,$$

$$(6.6) : \quad k^f = 1.0 [\text{h}^{-1}], k^b = 1.0 \cdot 10^{-3} [\text{h}^{-1}],$$

$$(6.7) : \quad k^f = 2.5 [\text{h}^{-1}], k^b = 0.0 [\text{h}^{-1}],$$

$$(6.8) : \quad k^f = 1.0 \cdot 10^{-3} [\text{h}^{-1}], k^b = 0.0 [\text{h}^{-1}],$$

$$(6.9) : \quad \mu_{\text{max}} = 2.5 \cdot 10^{-4} [\text{h}^{-1}], K_{M_1} = 1.0 \cdot 10^{-5}, K_{M_2} = 1.0 \cdot 10^{-5} [\text{mMl}^{-1}],$$

$$(6.10) : \quad \mu_{\text{max}} = 2.5 \cdot 10^{-2} [\text{h}^{-1}], K_{M_1} = 1.0 \cdot 10^{-5}, K_{M_2} = 1.0 \cdot 10^{-5} [\text{mMl}^{-1}].$$

The equilibrium reactions have been simulated here with the help of fast kinetic reactions, setting backward reaction rates of 1000 $[\text{h}^{-1}]$ and choosing the appropriate forward reaction rate to attain the desired equilibrium constant K . Simulations with different ratios showed that this is a reasonable

approximation of the equilibrium state at the given time scales, what was verified by calculation of reference solutions with smaller step sizes and faster rates, where no differences could be observed.

The initial concentrations of the following species differed from zero:

Co(II)EDTA(aq) (0.032 mM l^{-1}), dissolved O_2 (0.256 mM l^{-1}), biomass (0.02 mM l^{-1}), and the charged surface sites S_{pos} (0.016 mM l^{-1}), and S_{neg} (0.0011 mM l^{-1}).

The results of the batch simulation coincide with those of [CGS98] and the calculations by [FYB03] with BIOGEOCHEM, and are given in Figure 6.1. This example serves among various other tests as an additional verification of the correct implementation of the algorithms in RICHY.

Due to the above selection of initially present species, at first only the fast

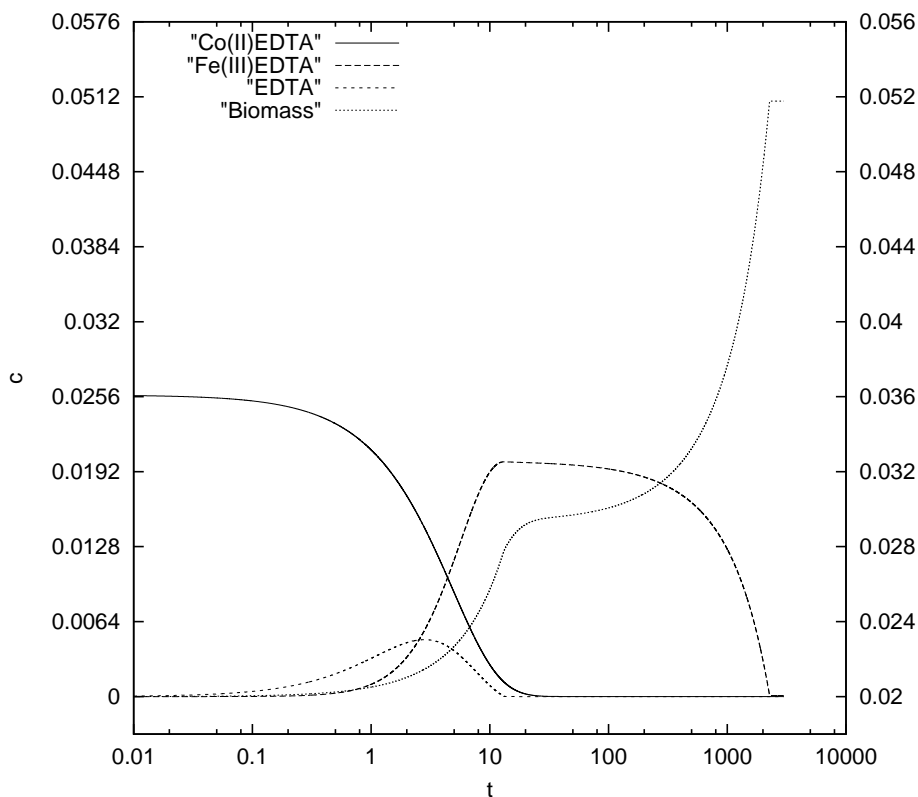


Figure 6.1: Results for the EDTA-example of [CGS98]. Concentrations [mM/l] of species Co(II)-EDTA, Fe(III)-EDTA, EDTA, and biomass over time [h]. Second y-axis refers to the concentration of the biomass, intervals of the labels on the axes are chosen such that they correspond to Figure 1 in [FYB03].

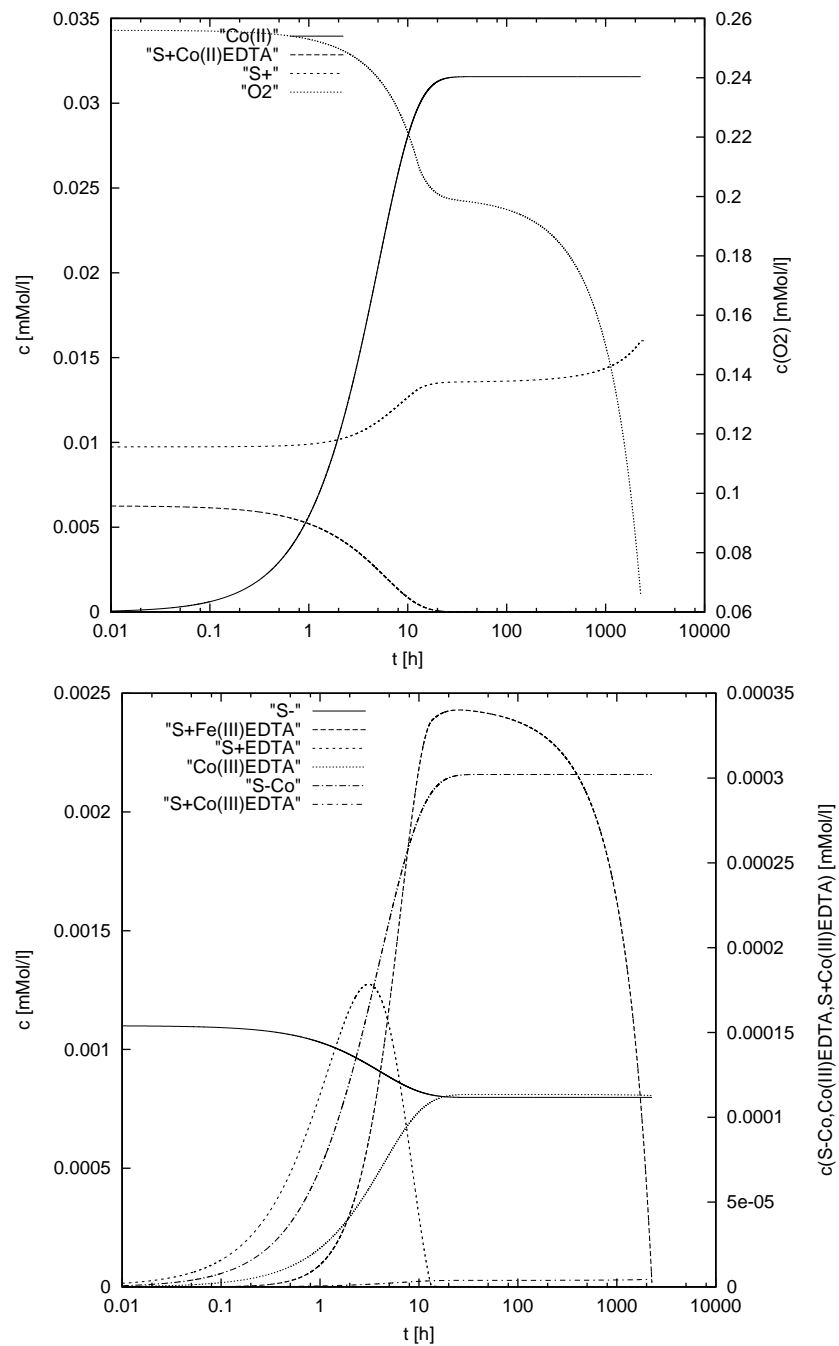


Figure 6.2: Results for the EDTA-example of [CGS98]. Concentrations [mM/1] of species over time [h]. $S_{\text{pos-Co(III)EDTA}}$ does not exceed 5.0×10^{-6} [mM/1]. Note the secondary y-axes for some species.

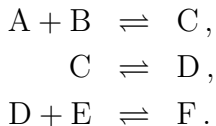
reaction (6.2) and the kinetic reaction (6.8) can occur. The immediate generation of $S_{\text{pos}}\text{-Co(II)EDTA}$ via (6.2) triggers off the kinetic reaction (6.6). On the other hand, in (6.8) Co(II)EDTA is produced, which immediately enables reaction (6.5).

EDTA and Fe(III)EDTA are first produced via the reactions (6.3) and (6.4), respectively, before they are degraded. The proceeding of the degradation reactions is reflected by the growing biomass concentration. The growth stops when all the Fe(III)EDTA is consumed (see Figure 6.1 for $t > 2000$). We refer to [CGS98] for further physicochemical interpretations.

6.2 Efficiency of Solution Strategies

6.2.1 Selective Coupling: Academic Examples

To investigate systematically the potential of the decoupling algorithm, first two academic test problems are presented, which are motivated by Robinson et al. (2000) [RVV00]. The first one consists of a simple reaction system with six virtual species A, \dots, F that interact via the following reaction system:



The degree of coupling between these species is determined by the Damköhler numbers (recall Section 2.7) for the reaction / transport ratio, which will vary from 1 (kinetic) up to 1000 (quasi-equilibrium).

The given CPU times [s] in Table 6.1 stem from a scenario with 1D stationary flow, 100 elements, and 3000 time steps of size $\Delta t = 0.01$. Initially present in the column is only species E at 100 mg/1, at the left boundary species A and B are constantly set to 1 mg/1 (Dirichlet condition), and all other boundary conditions are homogeneous Neumann conditions.

We observe that already in that small, six species example, the splitting of the 6×6 matrices in two blocks of 3×3 matrices results in a speed-up of factor 3 in the linear solver if $Da = 1$ for the second reaction, irrespective of the other rates. Total CPU time reduces by one third, while Newton convergence is not deteriorated.

If, however, all reaction couplings are ignored, only scenarios with $Da \leq 10$ converge at the given fixed time step size, while an effective gain in computation time (speed-up of factor 10 in linear solver and 2 overall, see Table 6.1) can only be observed in the purely kinetic (1,1,1) case.

Table 6.1: Performance of the six species example for different decouplings and Damköhler numbers. Total number of Newton steps (NS), Newton steps per time step (NS/TS), and CPU times for assembling, linear solver, and overall in [s].

Scenario (Da)	Configuration	NS	NS / TS	Ass.	LS	Tot.
(1000,1,1000)	(ABCDEF)	4021	1.3	67	96	165
(1000,1,1000)	(ABC)(DEF)	4040	1.4	67	30	98
(1000,1,1000)	(A)(B)...(F)	not	conv.			
(100,1,100)	(ABCDEF)	3354	1.1	67	87	155
(100,1,100)	(ABC)(DEF)	3940	1.3	67	29	98
(100,1,100)	(A)(B)...(F)	not	conv.			
(10,1,10)	(ABCDEF)	3354	1.1	63	83	147
(10,1,10)	(ABC)(DEF)	3816	1.3	69	30	101
(10,1,10)	(A)(B)...(F)	8978	3.0	133	16	153
(1,1,1)	(ABCDEF)	3000	1.0	58	74	133
(1,1,1)	(ABC)(DEF)	3000	1.0	57	22	80
(1,1,1)	(A)(B)...(F)	3938	1.3	58	7	66
(1000,1000,1000)	(ABCDEF)	4152	1.4	66	94	161
(1000,1000,1000)	(ABC)(DEF)	10265	3.4	125	72	200
(1000,1000,1000)	(A)(B)...(F)	not	conv.			

Note that in the not converging, completely decoupled cases (A)(B)...(F) convergence still can be achieved by decreasing the time step sizes, but in this example the resulting overall computation time has not been favourable for the decoupled case. This underlines once more the importance of an at least partially coupled process-preserving solution strategy.

In this 'few species example', assembling time is roughly the same as solving time. It can be expected that the gain in a reaction system with more species is greater, because linear solving will dominate due to the assembling techniques (see Section A.2) that allow only an $\mathcal{O}(N_S)$ effort for that part of the solution process. The size of the above system has been doubled, including an additional coupling of the two halves. The twelve species problem reads



Table 6.2: Performance of the twelve species example for different decouplings and Damköhler numbers. Total number of Newton steps (NS), Newton steps per time step (NS/TS), and CPU times for assembling, linear solver, and overall in [s].

Scenario (Da)	Configuration	NS	NS / TS	Ass.	LS	Tot.
(1000,1,1000,1000,1,1000)	(ABC...L)	4051	1.3	155	702	860
(1000,1,1000,1000,1,1000)	(ABC)...(JKL)	4091	1.4	150	59	212
(1000,1,1000,1000,1,1000)	(A)(B)...(L)	not	conv.			
(1,1,1,1,1,1)	(ABC...L)	3000	1.0	143	554	700
(1,1,1,1,1,1)	(ABC)...(JKL)	3000	1.0	133	45	180
(1,1,1,1,1,1)	(A)(B)...(L)	4128	1.4	165	15	182

The diagonal blocks of the Jacobian have the following sparsity pattern:

$$\begin{array}{c}
 \text{A} \\
 \text{B} \\
 \text{C} \\
 \text{D} \\
 \text{E} \\
 \text{F} \\
 \text{G} \\
 \text{H} \\
 \text{I} \\
 \text{J} \\
 \text{K} \\
 \text{L}
 \end{array}
 \left(\begin{array}{cccc|cccc}
 \bullet & \bullet & \bullet & & & & & \\
 \bullet & \bullet & \bullet & & & & & \\
 \bullet & \bullet & \bullet & \bullet & & & \circ & \\
 & & \bullet & \bullet & \bullet & \bullet & & \circ \\
 & & & \bullet & \bullet & \bullet & & \\
 & & & & \bullet & \bullet & \bullet & \\
 & & & & \bullet & \bullet & \bullet & \\
 \hline
 & & & & & \bullet & \bullet & \bullet \\
 & & & & & \bullet & \bullet & \bullet \\
 & & \circ & \circ & & \bullet & \bullet & \bullet & \bullet \\
 & & & & & & \bullet & \bullet & \bullet & \bullet \\
 & & & & & & & \bullet & \bullet & \bullet \\
 & & & & & & & \bullet & \bullet & \bullet
 \end{array} \right) .$$

Only the second reaction couples the two halves, which we suppose to be slow, as indicated by \circ . The result is as expected, we only present two scenarios in Table 6.2. Again, uniformly small reaction rates with $Da = 1$ allow the best reductions in computation time, here the linear solver for the fully coupled problem needs 37 times longer than the uncoupled case (554 instead of 15 s) although the number of Newton steps per time step slightly increases from 1.0 to 1.4. Decoupling here results in an overall CPU time reduction from 700 to 182 (factor 3.8). We can conclude that the decoupling method proves to be powerful for many species (say more than 10) and slow kinetic reactions which can be neglected, irrespective of the speed of the other, coupled reactions. Also remember the idealized 16 species example of Table 5.2, which has been presented in the motivating paragraph of Section 5.2.2, with a maximum speed-up of factor ≈ 93 in the linear solver and 9 in total CPU time.

6.3 An Experimental Study: Degradation of Propylene Glycol

6.3.1 Problem Description

In this section the application of the simulation tool for the interpretation of experiments and field data concerning the transport and degradation of propylene glycol in soils is demonstrated. Propylene glycol (PG) is commonly used as a deicing chemical for airplanes and thus infiltrates soils adjacent to runways in considerable amounts. A mid-size airport uses quantities of deicing fluids in the order of 10 000 tons per year, while between 20 % and 60 % of the applied chemicals are spread to unsealed surfaces by diffusion, wind drift or shearing off the airplanes during take-off [JTKK05]. Thus we deal with an anthropogenic contamination problem with important public relevance, because operating licenses of airports do also depend on environmental restrictions.

PG is environmentally harmful due to its high biological and chemical oxygen demand during its transport and degradation in seepage water, groundwater and rivers, what even may result in methanogenic conditions, and also due to the toxicity of its additives. As the oxygen in the subsoil is rapidly consumed, anaerobic processes become relevant. Anaerobic biodegradation of PG has been investigated by Jaesche et al. (2005) in soil column percolation experiments under dynamic conditions with seepage solutions and airport site material.

The underlying process mechanisms should be identified with the help of the developed simulation tool to transfer the results from the measurements to further situations and time points, and to identify controlling factors of the processes. The reaction partners are Fe and Mn hydroxides which act as the terminal electron acceptors for the degradation in the calcereous soils of a gravel plane. Both Fe_\circ and Mn_\circ form coatings of the gravels, thus are immobile species.

6.3.2 Data

The experiments and results are described in greater detail in [JTKK05], here we only repeat an extract of the relevant data for the simulations. We concentrate on one soil column of length 15 cm filled with a sandy gravel (denoted subsoil S1) taken at a depth of about 30 cm, and a second column filled with 7.5 cm aquifer material rich of manganese hydroxides (S2a) and 7.5 cm of soil rich of iron hydroxides (S2b), sampled in a depth of 200 cm. Water flow in the second column is orientated such that it percolates through

Table 6.4: Soil and transport parameters of the PG degradation experiments.

Parameter	Soil S1	Soil S2a	Soil S2b
length [dm]	1.5	0.75	0.75
porosity Θ	0.36	0.22	0.22
bulk density ρ_b [kgdm ⁻³]	1.58	2.03	2.03
dispersion length α_l [dm]	5.1E-2	3.2E-2	3.2E-2
initial PG concentration [mg l ⁻¹]	0	0	0
initial Mn _o concentration [mgkg ⁻¹]	48	3157	45
initial Fe _o concentration [mgkg ⁻¹]	251	308	2471

S2a first. The physicochemical parameters and initial concentrations are given in Table 6.4. The columns were saturated, however under varying flow conditions including multiple flow interruptions. Table 6.5 subsumes the imposed boundary conditions of the experiments. The columns were percolated with seepage water from the field site with an additional PG concentration of $c_{1,\text{in}}(t) = 500 \text{ mg/l}$. This corresponds to a flux boundary condition ($D\partial_x c_1 - qc_1 = q_{\text{in}}(t)c_{1,\text{in}}(t)$). The outflow condition is a free outlet (homogeneous Neumann condition). In soil sciences, time units are frequently expressed as pore volumes, more precisely the time that is needed to exchange completely the fluid volume in the saturated column. One pore volume for S1 corresponds to a time of approximately 25.9 h, whereas in S2 it is equivalent to approximately 14.7 h at the initial flow rates of Figure 6.3, which were $q_{\text{in}}(0) = 0.0105 \text{ dm/h}$ for S1, and $q_{\text{in}}(0) = 0.0226 \text{ dm/h}$ for S2.

Biodegradation parameters are depending on the reaction partners and on site conditions, because the pore size distribution influences the bioavailability of the reaction partners, for example. Experiments with a solution of pure water and PG showed no substantial degradation of PG, whereas biodegrada-

Table 6.5: Boundary conditions for the PG experiments with columns S1 and S2.

	Column S1	Column S2
column inflow	$q_{\text{in}}(t)$: see Figure 6.3	
	$c_{\text{in}}(t) = 500 \text{ mg/l} \forall t$	$c_{\text{in}}(t) = 500 \text{ mg/l} \forall t$
column outflow	$\partial_x c_1(x_{\text{out}}, t) = 0 \forall t$	$\partial_x c_1(x_{\text{out}}, t) = 0 \forall t$

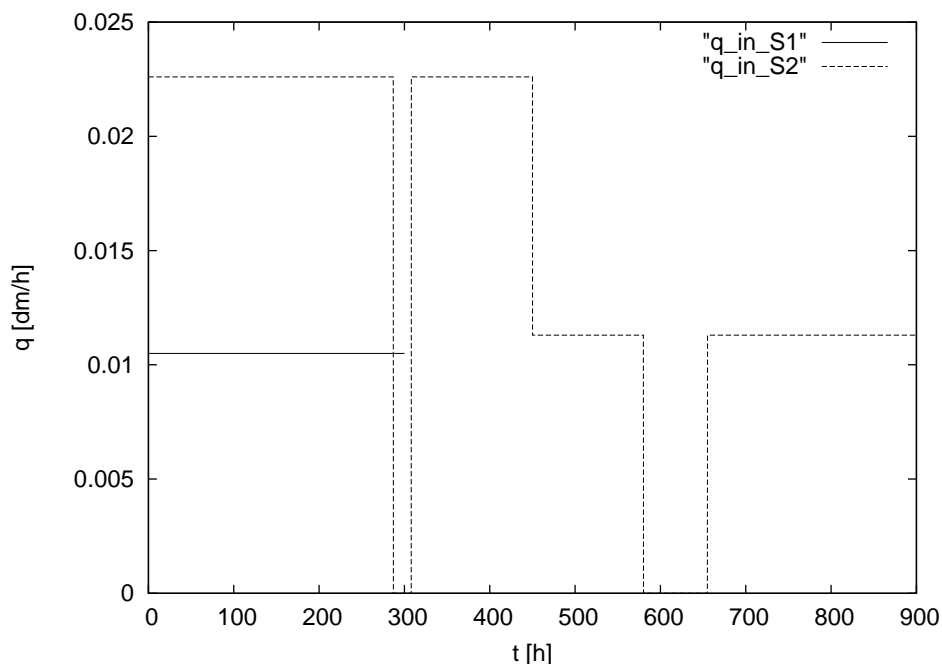


Figure 6.3: Flux $q_{in}(t)$ at inflow $x = 0$ for PG experiments with columns S1 and S2.

tion was obvious when seepage water from the field site was used [JTKK05]. Thus it can be concluded that biomass (natural organic matter) is imported as a part of dissolved organic carbon (DOC) to the subsoil, where it attaches and may grow [WT98, WTKK⁺02]. Initial conditions of the species are given in Table 6.4.

Figure 6.4 shows the breakthrough data of PG for the continuous feed experiment in the S1 column (left) and the stop-flow experiment in the layered S2 column (right). Note that in both cases a complete degradation of PG finally occurs despite the continuous feed during the experiments. Concentrations of Fe_o and Mn_o have been measured in the soil after conduction of the whole experiment which included more than the shown excerpts. The soil has been analysed in layers of approximately 2.5 cm. These concentrations only give an upper bound for the transformed mass in the simulated experiments, they may also be altered by other geochemical processes.

The data will be interpreted and analysed in detail in the following section in conjunction with the derivation of an appropriate model (including its parameters) for the given situation.

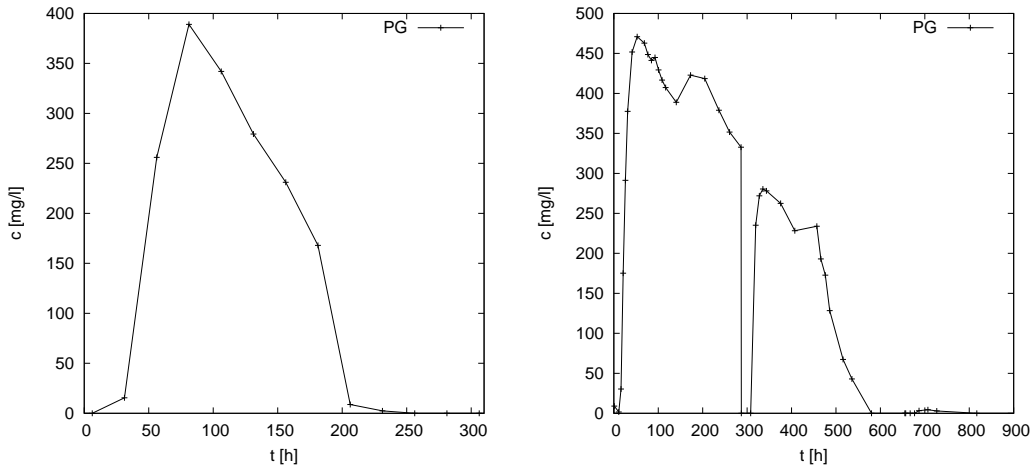


Figure 6.4: Experimental breakthrough concentrations of PG at the outlet $x = 1.5 \text{ dm}$ of column S1 (left) and column S2 (right).

6.3.3 Modelling Approach

Choice of Principal Model Type

The relevant species that are taken into consideration are PG, biomass, and as electron acceptors the Fe_o and, with a minor role, Mn_o species. From energetic reasons, the iron hydroxide is the preferred acceptor. We can easily draw the conclusion that the degradation process is not of zeroth or first order, as the breakthrough curves are not stationary (i.e., reaching a constant value) after 1-2 pore volumes of water and concentration flux under the same inflow conditions (Fig. 6.4). From the same reason, a solute as electron acceptor (like oxygen or nitrate) can be excluded because it would be transported with the fluid out of the column in that period of time and thus a stationary profile must also result after few pore volumes. Comparing PG decay and Fe_o it is obvious that the stoichiometric relation is such that transformation of one mole of PG will require only a fraction of Fe_o , otherwise Fe_o had been used up during the experiments. Compare, e.g., soil S2a with initially 625 mg/l , and finally still $395 - 491 \text{ mg/l}$ (Figure 6.7), while PG concentrations of 500 mg/l are completely consumed during the propagation through the column. This conclusion has been confirmed by molecular considerations afterwards (see below).

The small resurrection of the PG concentration after the flow interruption of 75 hours ($580 < t < 655$, cf. Figures 6.3 and 6.4, right) shows that biomass is dying during that period, otherwise concentrations would stay at the level of before the stop. Therefore we have to include a death rate of first order

in the model formulation.

So prior to any orientating simulation, the data clearly indicate that a complex model of the Monod type with growing biomass and death rate has to be chosen. With the indices 1 for PG, 2 for Fe_o, 3 for Mn_o, and 4 for the biomass, the system of equations to solve thus reads

$$\begin{aligned}\partial_t(\Theta c_1) - \nabla \cdot (\mathbf{D}\nabla c_1 - \mathbf{q}c_1) &= \Theta\nu_{11}R_1(c_1, c_2, c_4) + \Theta\nu_{12}R_2(c_1, c_3, c_4), \\ \partial_t c_2 &= \nu_{21}R_1, \\ \partial_t c_3 &= \nu_{32}R_2, \\ \partial_t c_4 &= \left(1 - \frac{c_4}{c_{\max}}\right) (\nu_{41}R_1 + \nu_{42}R_2) - kc_4.\end{aligned}$$

The reaction rates are given as

$$R_1 = \mu_{\max_1} c_4 \frac{c_1}{K_{M_1} + c_1} \frac{c_2}{K_{M_2} + c_2} \frac{K_{I_3}}{K_{I_3} + c_3}, \text{ and} \quad (6.13)$$

$$R_2 = \mu_{\max_2} c_4 \frac{c_1}{K_{M_1} + c_1} \frac{c_3}{K_{M_3} + c_3} \frac{K_{I_2}}{K_{I_2} + c_2}. \quad (6.14)$$

Model Parameters – Characteristics of the Data

The parameters that are not available are the initial biomass concentration $c_4(x, 0)$, the stoichiometric factors for the biomass ν_{41} and ν_{42} (also known as yield factors), the growth rates for the biomass $\mu_{\max_1}, \mu_{\max_2}$, the maximum biomass concentration c_{\max} , the death rate for the biomass k , the half saturation concentrations K_{M_2} and K_{M_3} , and eventually inhibition constants K_{I_2} and K_{I_3} .

The stoichiometric factor ν_{21} can be derived from molecular considerations that show that approximately 1 mg of Fe_o is needed to transform 18 mg of PG [Totsche, personal communication, 2005]. For Mn_o, a ratio of 1:10 can be deduced in the same way. Thus, $\nu_{11} = \nu_{12} = -1$, $\nu_{21} = -0.056$, and $\nu_{32} = -0.1$ (see also Tables 6.6 and 6.7). The manganese reaction only was considered in some simulations in S2a, as the iron reaction was supposed to dominate.

The unknown parameters should be identified from the data, a task that may admit multiple possible choices leading to the same result. As a starting point, we note that the experimental setting is such that PG is infiltrating at a high concentration level, and that the hydroxides – which are consumed in relatively small amounts – are equally not a limiting factor for the reaction, and it should proceed from this point of view in an optimal range. This means that Monod constants for the substances can be assumed to be rather

moderate, we used concentrations of 50 mg/1 for each of the species at a first stage.

Inhibition concentrations were only included in some final simulations, it can be argued that Fe_o and Mn_o concentrations are varying only at a small extent (they are consumed in relatively small amounts compared to the PG concentration), and thus an additional inhibition term would be more or less constant, so it cannot be distinguished from the growth constant. Thus it suffices to vary μ_{\max} .

The data reveal that the maximum biomass concentration is rather high, or more precisely does not reach its limit during the experiments, because the breakthrough curve is permanently decreasing (until PG even vanishes) in spite of the continuous feed of 500 mg/1 at the inflow. Otherwise we would observe a plateau of the PG concentration.

Finally we remark that despite a fast initial degradation, the concentration thereafter decreases slowly over a long period of time. This suggests a damped growth rate, what we will discuss among other aspects in the next section.

6.3.4 Simulations

For the simulations, some parameters are not directly accessible and had to be derived or estimated from the breakthrough data and further information. We will show, however, that this choice may not be unique, depending on the design of the experiment. This is also an important result a modelling tool can yield, if it is used to optimally design a significant experiment that *allows to identify* the controlling processes. Let us therefore first investigate soil column S1.

Subsoil S1

This part of the experiment was run at stationary flow conditions and continuous feed at the inflow. It is a priori clear that not all of the model parameters in question can be determined from this experiment. Only the iron reaction is relevant here, no inhibition by other species considered.

Analysing the breakthrough curve (Figure 6.4, left), several observations can be made: The **degradation** is **instantaneous** and initially very **high**, because the peak is less than 400 mg/1, what points at an important initial biomass concentration that is active here. However, despite of this high initial activity, the PG concentration afterwards shows a relatively **slow decrease**, what contradicts the assumption of a fast, unlimited exponential growth of the biomass thereafter. This is illustrated in Figure 6.5 (left),

Table 6.6: Degradation parameters of the simulations of soil column S1.

Parameter	Sim01	Sim02	Sim03	Sim04
fixed				
stoichiometric factor ν_{11}	-1.0	-1.0	-1.0	-1.0
stoichiometric factor ν_{12}	0	0	0	0
stoichiometric factor ν_{21}	-0.056	-0.056	-0.056	-0.056
death rate biomass k [1/h]	0.001	0.001	0.001	0.001
varied				
max. growth rate μ_{\max} [1/h]	0.19	0.03	0.25	0.8
Monod constant K_{M_1} for PG [mg/l]	50	50	1000	1000
Monod constant K_{M_2} for Fe _o [mg/l]	50	50	50	50
yield factor ν_{41}	1.0	1.0	0.12	0.12
yield factor ν_{42}	0	0	0	0
max. biomass c_{\max} [mg/l]	5000	600	5000	5000
initial biomass $c_4(x, 0)$ [mg/l]	0.1	35	20	5

where a high growth rate ($\mu_{\max} = 0.19 \text{ h}^{-1}$, see also Table 6.6) is not damped by virtue of other model parameters (Sim01). The right part of the figure shows a first adjustment by damping the reaction rate by a smaller μ_{\max} , a maximum biomass concentration, and – to achieve the initial degradation – a lifted initial biomass concentration (Sim02).

To demonstrate the **non-uniqueness** of the identification problem, a further parameter set is presented, that is based on results obtained from column S2 explained later (Sim03 in Figure 6.6, left). As initial biomass concentration and maximum growth rate are likely to differ for two different soils under different conditions, these two parameters were adjusted. The result is Sim04, that almost coincides with Sim02, although it is based on tremendously different parameters, e.g. a difference in Monod constants for PG of 50 to 1000, or yield factors of 0.12 to 1 (cf. Table 6.6).

The knowledge of the biomass concentrations at the end of the experiment would allow to eliminate a set of parameters, as illustrates the left graphics in Figure 6.7. Whereas the limitation to a maximum biomass concentration of 600 mg/l in Sim02 leads to an almost uniform repartition of the biomass, the higher limit in Sim04 (that is compensated by a smaller yield factor and an unfavourable Monod constant) results in a highly reactive zone at the inflow, and a smaller biomass concentration thereafter. The latter might be considered as the more realistic scenario, as sharp reactive zones are frequently observed in biodegradation problems.

The assumed initial biomass concentrations (Table 6.6) all lie in the range

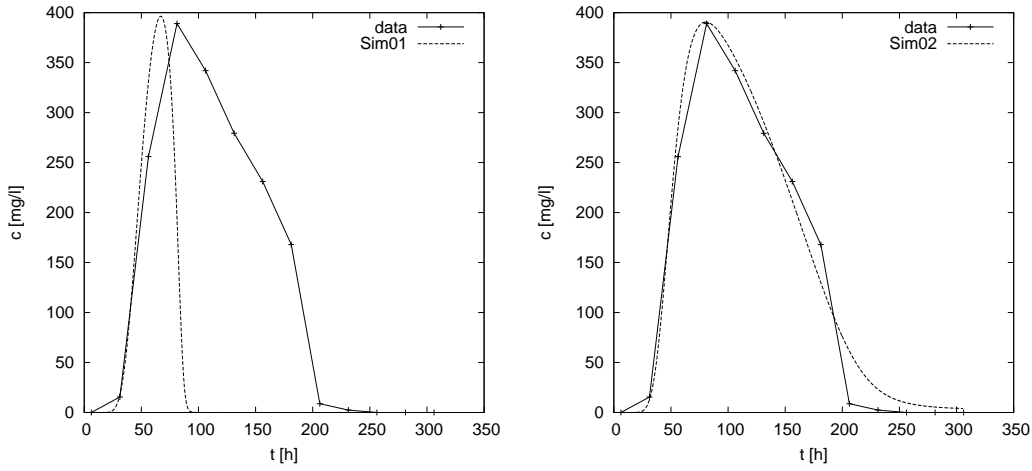


Figure 6.5: Simulation results and experimental breakthrough concentrations of PG at the outlet of column S1, see Table 6.6 for the corresponding biodegradation parameters, left: undamped reaction rate, right: damped by smaller growth rate and maximum biomass concentration.

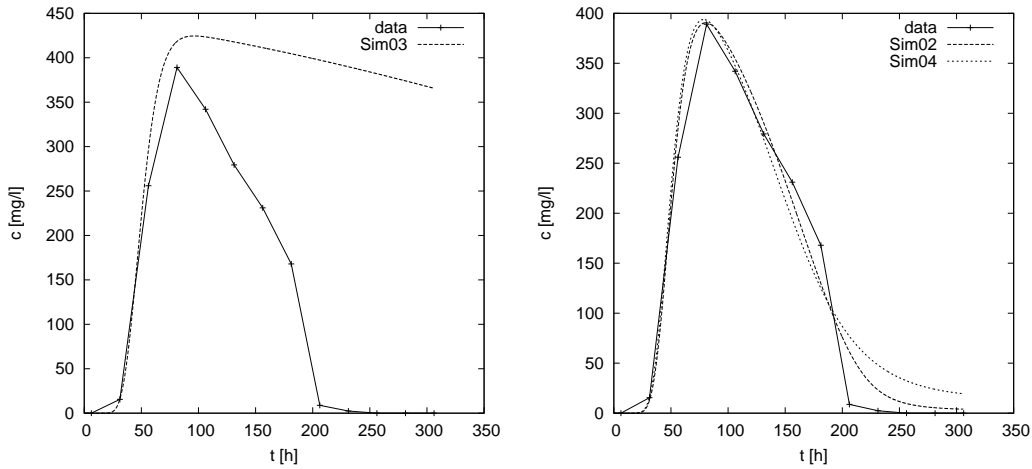


Figure 6.6: Simulation results and experimental breakthrough concentrations of PG at the outlet of column S1 (cf. Table 6.6 for biodegradation parameters), left: unchanged parameters taken over from results of S2, right: same set with adjusted initial biomass and growth rate, compared to set Sim02.

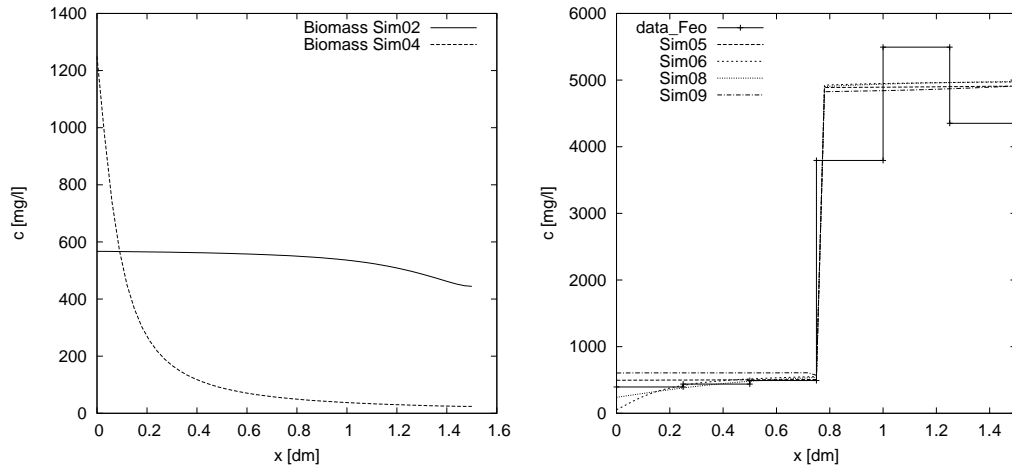


Figure 6.7: Left: Biomass concentrations in S1 at the end ($t = 305$ h) of simulations Sim02 and Sim04 (see Figure 6.6 and Table 6.6); Right: Fe_0 concentrations, data: at the end of all conducted experiments, simulations: after 900 h of simulated single experiment in S2 (see Table 6.7).

of plausible values, assuming that a certain percentage of the imported OC concentration in the seepage water of about 250 mg/l [JTKK05] is biomass that can attach to the soil, however no biomass concentrations in the soil have been determined explicitly.

Subsoil S2

Due to the variations in the fluid flow experiment S2 reveals more information on the underlying processes. Analyzing the data, a striking **increase in the concentrations** at $t = 150$ h can be observed. This behaviour could be explained by a flushing out of large agglomerations of biomass, what can be undermined by turbidity measurements that show unregular peaks. Eventually shocks of the experimental apparatus cannot be excluded, because this increase could also be observed in independent soil columns [Jaesche, personal communication] at the same time. It is astonishing that the decrease of the PG concentration seems delayed at $t > 150$ h, compared to the initial step descent (Figure 6.4). We tried to identify parameters with and without taking into account such an irregular event. If included, it has been modelled by a zeroth order rate in the biomass concentration at $t = 150$ h for several time steps.

Compared to the approximately 300 hours of experiment S1, in S2 the complete degradation is strongly delayed: it takes ≈ 600 hours (cf. Figure 6.4).

Table 6.7: Degradation parameters of the simulations of soil column S2.

Parameter	Sim05	Sim06	Sim07	Sim08	Sim09
fixed					
ν_{11}	-1.0	-1.0	-1.0	-1.0	-1.0
ν_{12}	-1.0	-1.0	-1.0	-1.0	-1.0
ν_{21}	-0.056	-0.056	-0.056	-0.056	-0.056
ν_{32}	-0.1	-0.1	-0.1	-0.1	-0.1
k [1/h]	0.001	0.001	0.001	0.001	0.001
varied					
μ_{\max} [1/h]	0.03	0.25	0.022	0.5	0.03
K_{M_1} for PG [mg/l]	50	1000	50	1000	50
K_{M_2} for Fe _o [mg/l]	50	50	50	50	50
K_{M_3} for Mn _o [mg/l]	-	-	-	-	50
K_{I_3} for Mn _o [mg/l]	-	-	-	-	5000
ν_{41}	1.0	0.12	0.7	0.12	1.0
ν_{42}	-	-	-	-	1.0
c_{\max} [mg/l]	600	5000	2000	500	1000
$c_4(x, 0)$ in S2a/S2b [mg/l]	35/35	20/20	50/100	5/5	30/30

On the one hand, this is due to higher velocities and thus **shorter residence times** in the column. On the other hand the different geochemical and physical conditions may lead to smaller growth rates and/or different maximum biomass capacities.

Table 6.7 subsumes the degradation parameters of the various simulations. Applying a data set determined uniquely from the S1 experiment above (Sim02, see Figure 6.5 and Table 6.6) – without any changes – yields Figure 6.8 (left). The initial decrease is mapped very accurately, while at $t = 300$ h the biomass concentration has reached its maximum, and thus also the degradation rate has reached its maximum, what does not correspond to observed reality (Sim05).

To adjust the model to the registered behaviour, c_{\max} can be raised, however, if the same Monod constants are kept, growth must not occur too early, therefore the growth rate μ_{\max} and the biological yield ν_{41} have been lowered in Simulation Sim07 (cf. Figure 6.8 (right), Table 6.7). The other explanation (just as in Sim02 and Sim04) is a damped rate by a high Monod constant for PG, then combined with a fast growth rate, but low yield. Due to the high growth rate, initial biomass concentrations can assumed to be lower (Sim06), compare the parameters in Table 6.7. Figure 6.8 (right) displays that both assumptions yield acceptable models for the observed data.

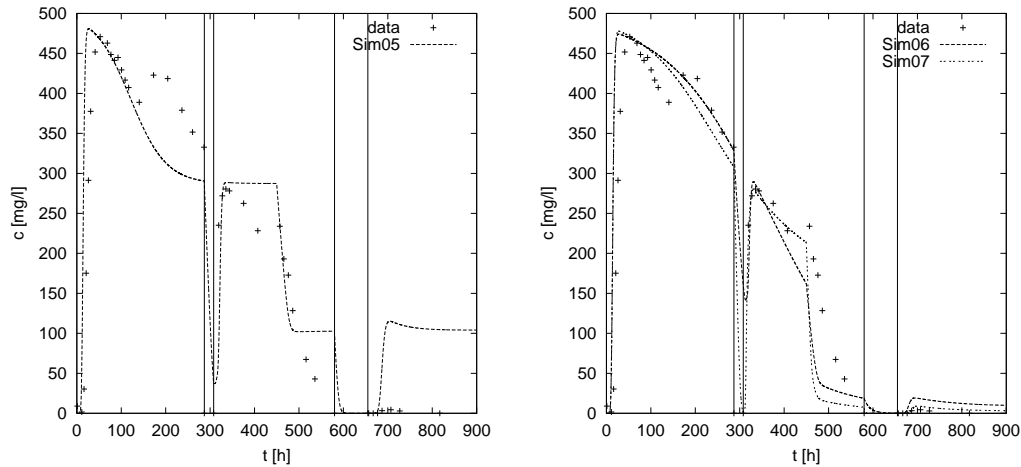


Figure 6.8: Simulation results and experimental breakthrough concentrations of PG at the outlet of column S2 (cf. Table 6.6), left: unchanged parameter set of S1 (Sim02); right: Sim06 and Sim07, similar breakthrough curves – different parameter sets (Table 6.7). Flow interruptions are marked by horizontal lines.

The preceding simulations (Sim05 – Sim07) did not account for the step at $t = 150 \text{ h}$, but sought an average approximation in the time interval $[0, 300]$. If we want to include a **sudden event of biomass reduction**, growth rates have to be adjusted. This has been done in Sim08 for the combination of low yield (0.12), high Monod concentration for PG (1000 mg/l), low maximum biomass concentration (500 mg/l), and high growth rate (0.5 h^{-1}). Nevertheless this combination implies a fast degradation after the first flow interruption (Figure 6.9, left).

Sim09, with a yield of 1.0, low K_{M_1} of 50 mg/l, but high $c_{\max} = 1 \text{ g/l}$, and an additional damping of the iron/PG reaction by an inhibition concentration of 5000 mg/l for Mn_o that applies only in S2a, seems more appropriate. But we note that the distinction between Fe and Mn on the basis of the data remains unclear from this single experiment. The number of parameters of the model should be kept to the necessary minimum at this stage. If we assume that one biomass species is responsible for both degradation pathways, and that sufficient substrates are present, the both cannot be clearly distinguished. This would become relevant if, e.g., reactions are inhibited.

None of the simulations can appropriately account for the data during the **flow reduction** starting at $t = 450 \text{ h}$.

Based on the parameters of Sim07, Sim10 is implemented with a linear decrease in q from $t = 450 \text{ h}$ until the flow interruption at $t = 580 \text{ h}$, and not

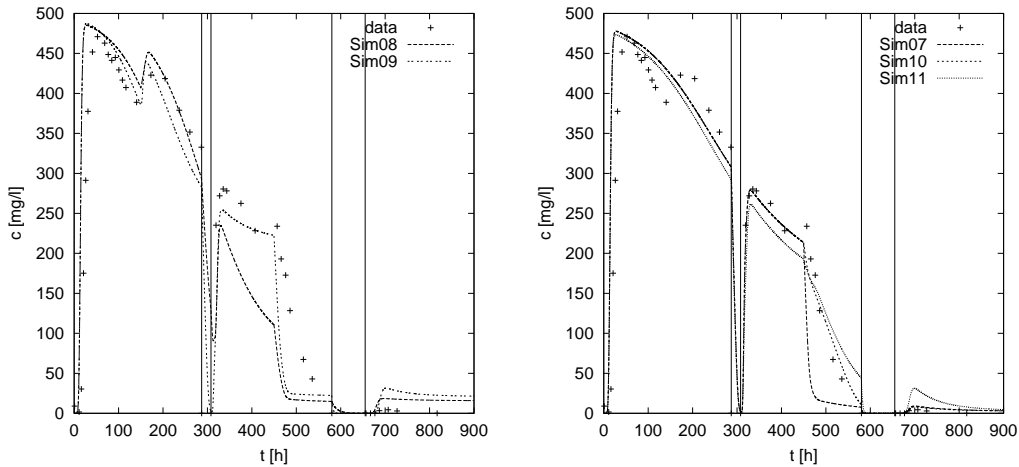


Figure 6.9: PG data and simulation in S2, left: including sudden biomass decrease at $t = 150$ h, right: Sim07, and adjustments to flow reduction by linear flow decline (Sim10), or biomass decrease (Sim11).

instantaneously. Sim11, also based on Sim07, is run with a reduction in concentration of 50 % of the active biomass at $t = 450$ h. It sinks on the average from 1000 mg/l in S2a to 500 mg/l, and from 1800 mg/l in S2b to 900 mg/l. To compensate the loss, initial biomass concentration in S2a has been lifted to 100 mg/l (Sim07: 50 mg/l).

Both, Sim10 and Sim11 give very good matches of the data, it should be noted, however that the linear decrease in q has not been reported, and thus we should speak of a behaviour *as if* q decreased in a linear way. The reduction in biomass is a hypothesis that will be discussed in the following section.

Verifying iron concentrations at the end of the simulations does not allow clear conclusions on the correct parameter set, because measurements are only given as averaged values over layers of 2.5 cm with a high variance [JTKK05], and simulated profiles are quite similar due to the low stoichiometric coefficient (Figure 6.7). We claim that more detailed depth profiles could explain whether biomass grows rather uniformly in the domain, or if a sharp reactive zone with strong Fe_o depletion exists in the first centimeters of the soil, as seen in Sim06 which had the highest c_{\max} .

6.3.5 Discussion and Conclusion

Summarizing the experimental modelling study the following characteristics of the underlying degradation process could be identified:

- Models of zeroth or first order, or with mobile biomass can clearly be excluded here.
- A dynamic degradation with growing biomass is apparent.
- Concentration profiles show that biomass growth is damped, and does not evolve exponentially.
- An important initial microbial activity has to be assumed.
- A microbial death rate can be deduced.

Some aspects could not be answered definitely. Simulations show that damping of microbial growth can be due to a suboptimal PG concentration (i.e., a high half saturation concentration) and a low microbial yield. Or, it can be due to a low biomass concentration limit, then together with a higher yield, and optimal PG offer (e.g., $K_{M_1} = 50 \text{ mg/l}$). The two cases entail maximum growth rates that differ by more than one order of magnitude.

This issue could be clarified by measurements of biomass concentrations, microbial knowledge about the yield factor, or by experiments at different concentration levels to identify the Monod concentrations for PG.

The concentration step at $t = 150 \text{ h}$ can be accounted for under the assumption of a sudden biomass decrease. A repetition of the same experiment could help eliminating erratic events. A possible explanation could also be an unreported concentration rise in the influent.

Another key question for process understanding is the change of the degradation rate with the flow reduction. It could be explained by the following working hypothesis: By reducing velocities an important part of the pore space can be excluded from transport: smaller pores do no longer participate to the flow regime, and thus the corresponding attached biomass can no longer contribute to the degradation process.

It has been demonstrated that distinguished experiments in combination with reactive multicomponent models are an indispensable tool to evaluate the risk of the spreading of biodegradable contaminants in the subsurface. Simulations can indicate which type of measurements are needed to resolve unclear process mechanisms.

Multiple experiments are necessary to identify an unequivocal complex parameter set underlying the anaerobic degradation process. They should be conducted such that some parameters can be fixed, e.g. at high concentrations of substrate and acceptors, then the model is insensitive in terms of Monod constants and the maximum growth rate of the biomass can be identified. Furthermore expert knowledge from microbiology, e.g., may be used

to fix stoichiometric factors also for the biomass (yield factors). Otherwise even such transient flow experiments cannot supply unique parameter identification.

The simulated experiments were conducted at a fixed temperature of 20 °C, however comparisons at 4 °C clearly showed the temperature dependence of the microbial activity [JTKK05]. This aspect could be included in further studies, a parametrization of the temperature dependence is already included in RICHY [Ins05] and can be combined with a simulation of the heat transport in the porous medium.

Appendix A

Implementation Issues

RICHY 1D has meanwhile become a simulation tool applied in engineering associations, research institutes, and university seminars. Therefore implementation in RICHY 1D includes the incorporation of the model components in a graphical user interface, and the generation of an associated practical user's guide and documentation in `html-code` [Ins05] available in the WWW. The source code currently contains about 60 000 lines in the language C.

A.1 Componentwise Linear Sparse Matrix Solver

To handle efficiently multicomponent problems the direct sparse matrix solver in RICHY has been rewritten in order to be capable to decouple subproblems (species equations) and solve them independently of each other. This has been lined out in Section 5.2.3.

Of course in the 1D case with linear finite elements the band-block structure of the Jacobian can be exploited, and we use a Gaussian elimination with pivot search.

For flexible selective couplings of species equations, the solver should be capable to handle an arbitrary number of arbitrary disjoint subsets of species without rearranging the assembled global system. This strategy entails a number of complications for all loops and indices, where it must be dealt with varying blocksizes (number of species) of the parts, fixed blocksizes between spatial nodes (total number of species), and arbitrary increments between succeeding components in the blocks.

In addition the Jacobian in RICHY is efficiently stored as a sparse matrix in form of vectors (corresponding to the rows, more precisely parts of the rows), where the entries are assessed relative to the diagonal, with a struc-

ture variable where one index denotes the row, and the second denotes the offset from the diagonal element (e.g., $A(9,0)$ denotes element $a_{9,9}$, $A(9,-2)$ corresponds to $a_{9,7}$, and so on).

The principal modifications are described in terms of the RICHY source code, where a matrix is organized as a structural variable containing fields as, e.g., $A \rightarrow \text{blocksize}$, where the number of components in one block (the number of species in ADR problems) is stored.

The linear solver is now organized in loops of $A \rightarrow \text{parts}$ that solve only a number of ($A \rightarrow \text{partblocksize}[p]$) components (species) fully coupled in part p . The index of the j th species in part p is kept in an index list (itself a matrix) termed $A \rightarrow \text{partsubcomplist}[p][j]$.

As the simplest case, in diagonal blocks (see (5.32)), replace loops $j = 0, \dots, N_S - 1$ by loops of $j = 0, \dots, A \rightarrow \text{partblocksize}[p] - 1$, and transform matrix indices $A(i, j)$:

$$\begin{aligned} i &\longrightarrow A \rightarrow \text{partsubcomplist}[p][i] \\ j &\longrightarrow A \rightarrow \text{partsubcomplist}[p][j] - A \rightarrow \text{partsubcomplist}[p][i]. \end{aligned}$$

For solving, also off-diagonal entries in the non-diagonal blocks A_{ij} , ($i \neq j$) are needed (fill-ins).

As an example we show the transformation of a loop backwards starting at the last line, where successively all entries from the diagonal to right are being assessed (see (A.1)), except the diagonal entries:

$$\left(\left(\begin{array}{ccc} * & * & * \\ & * & * \\ & & * \end{array} \right) \left\{ \begin{array}{cccc} * & * & * & * \\ * & * & * & * \\ * & * & * & * \\ & * & * & * \\ & & * & * \\ & & & * \end{array} \right\} \left\{ \begin{array}{cccc} * & * & * & * \\ * & * & * & * \\ * & * & * & * \\ * & * & * & * \\ * & * & * & * \\ * & * & * & * \\ * & * & * & * \\ & * & * & * \\ & & * & * \\ & & & * \end{array} \right\} \right). \quad (\text{A.1})$$

The submatrices have blocksize 4 in (A.1). Now suppose we want to solve the linear problem in two parts: equation parts dealing with components (0,3), highlighted with symbol $*$ in (A.2), together, and components (1,2) with symbol \times together:

$$\left(\left(\begin{pmatrix} \cdot & \cdot & * \\ & \times & \cdot \\ & & \cdot \end{pmatrix} \begin{pmatrix} * & \cdot & \cdot & * \\ \cdot & \times & \times & \cdot \\ \cdot & \times & \times & \cdot \\ * & \cdot & \cdot & * \\ & \cdot & \cdot & * \end{pmatrix} \begin{pmatrix} * & \cdot & \cdot & * \\ \cdot & \times & \times & \cdot \\ \cdot & \times & \times & \cdot \\ * & \cdot & \cdot & * \\ * & \cdot & \cdot & * \\ \cdot & \times & \times & \cdot \\ \cdot & \times & \times & \cdot \\ * & \cdot & \cdot & * \\ \cdot & \cdot & \cdot & * \end{pmatrix} \right) \cdot \quad (\text{A.2})$$

Here the remaining matrix entries (\cdot) are ignored, provided that the groups are uncoupled or have negligible coupling terms. Note that diagonal entries are not included in this loop.

In the transformed version the following simple sequential block version must be converted, in particular the loop over at most $3 \times A \rightarrow \text{blocksize}$ matrix entries with equidistant incrementation (1) of the indices has to be split.

```

numinblock = A->blocksize-1;
for validrows=1..3*A->blocksize-1
(
  if (--numinblock<0) ...
  ...
  for i=0..validrows-1 A(numinblock,i+1) ...
)

```

The matrix entries addressed by this loop, starting from the last, are displayed in (A.1). The loop in i above is now split in two loops to account for steps in one block (j -loop of length $A \rightarrow \text{partblocksize}[p]$), and to account for steps between following blocks that are separated by $A \rightarrow \text{blocksize}$ (new k -loop):

```

numinblock = A->partblocksize[p]-1; m=0;
for validrows=1..3*A->partblocksize[p]-1
(
  if (--numinblock<0)      ...  m++;
  ...
  i=0; start=numinblock+1;
  for k=0..m
  (
    for j=start..A->partblocksize[p]-1
    (
      A(A->partsubcomplist[p][numinblock],k*A->blocksize+
        A->partsubcomplist[p][j]-A->partsubcomplist[p][numinblock]) ...
      i++;
      if (i==validrows) break;
    )
    start = 0;
    if (i==validrows) break;
  )
  ...
)

```

This allows in principle an adaptive change of the coupled solution of components in each step of the Newton iteration, i.e., at each call of the linear solver. Thus species with vanishing concentrations can be easily decoupled, or non-existing or very weak couplings in chemical reactions among some species can be accounted for.

A.2 Compressed Data Storage and Efficient Assembling of the Jacobian

In geochemical reaction systems, albeit many species are relevant, typically few of these species are directly coupled with each other via reaction terms. Thus the ($N_S \times N_S$) submatrices (cf. (5.32)) of the Jacobian are sparse, and standard storage schemes and assembling routines would waste space and time with zeros.

An efficient implementation, e.g., with a compressed storage of reactions by pointer lists, should exploit the sparsity of the reaction network. Rules for an efficient implementation include:

- Group identical function evaluations for different species. Partial derivatives of a reaction rate R_r according to species concentration c_j appear in all species equations with $\nu_{ir} \neq 0$. Therefore loops in the assembling of the Jacobian are reaction based, not species based, to avoid multiple evaluations of the same term.

- Store compressed lists of species participating in a reaction to avoid zero rate evaluations. Reaction rates are never evaluated in loops over all species, but only in loops over species *participating* in that reaction, leading to reductions in rate calculation, their derivatives and assembling of the Jacobian entries.
- Distinguish mobile, immobile and microbial species a priori. Those species are treated separately to save computation time in unnecessary loops.

By means of species lists and their stoichiometric coefficients in the reactions (a compressed form of the stoichiometric matrix V , cf. Definition 2.4) and a sophisticated arrangement of loops it could be achieved that the complexity for assembling the global sparse system typically only grows linearly with the number of species, and not quadratically, as it is the case theoretically.

The $\mathcal{O}(N_S)$ can be seen e.g. in the CPU times for assembling of the examples presented in Table 5.2 and Figure 5.3, which remain constant whether one 16 species problem is assembled, or 16 one species problems. Note that the time for assembling only grows (almost) linearly with the number of species, although the size of the Jacobian grows quadratically with N_S . We should also mention that in the case of full matrices, evaluation of pointer lists results in an additional computational effort, compared to a linear index loops over all species. However this case is of minor practical importance for large reaction systems.

Appendix B

Notations

\circ		Hadamard product ($\mathbf{x} \circ \mathbf{y} = (x_i y_i)_{i=1, \dots, n}$)
a_i	[M/L ³]	activity of the i th species
c_i	[M/L ³]	concentration of the i th chemical species
c_{X_i}	[M/L ³]	concentration of the i th microbial species
D	[L ² /T]	diffusion–/dispersion–tensor
ϕ		equilibrium sorption isotherm
φ		nonequilibrium sorption isotherm
I		identity matrix
k_i	[1/T]	rate parameter for nonequilibrium sorption
k^b		backward reaction rate constant of kinetic reaction
k^f		forward reaction rate constant of kinetic reaction
K_j		thermodynamic equilibrium constant of reaction j
K_{M_i}	[M/L ³]	Monod constant (half saturation concentration) of the i th species
K_{I_i}	[M/L ³]	inhibition constant (Haldane concentration) of the i th species
\mathcal{L}		transport operator
μ_i^0		chemical reference potential of the i th species
μ_{\max}	[1/T]	maximum microbial growth rate
N_C		number of basis components
N_E		number of elements
N_R		number of reactions
$N_{R_{\text{bio}}}$		number of biochemical reactions
N_S		number of species
$N_{S_{\text{bio}}}$		number of microbial species
$N_{S_{\text{im}}}$		number of immobile species
$N_{S_{\text{mob}}}$		number of mobile species
\mathcal{N}		number of time steps

$O(\cdot), o(\cdot)$		Landau symbols of asymptotic analysis
$\mathcal{P}_k(\Omega)$		polynomials of maximum degree k over Ω
\mathbf{q}	[L/T]	specific discharge (volumetric flux, Darcy velocity)
R_j	[M/(L ³ T)]	rate of j th reaction
\mathcal{R}		reaction operator
ρ_b	[M/L ³]	bulk density (mass of solids per total volume)
s_i	[M/M]	sorbed concentration of the i th chemical species
Θ	[1]	volumetric water content
t	[T]	time
T	[T]	endtime
Y	[M/M]	yield factor: mass of produced biomass per mass of used substrate

Summary

The scope of this thesis is the development of a versatile hydrogeochemical multicomponent transport model, the evaluation of different solution strategies, and the preparation of an efficient simulation tool that handles the variety of coupled hydraulic, chemical, and biological processes accurately, which are relevant for the fate of contaminant plumes in porous media.

Therefore an existing single species transport model is extended with descriptions for geochemical multispecies reactions in the solid and aqueous phase, and with adequate models for natural degradation processes of organic contaminants that are catalysed by microorganisms. The basic advection-dispersion equation is presented and complemented with complex models for the essential reactive processes, e.g., sorption reactions that also can take into account colloidal carrier substances.

The formulation of stoichiometric reaction mechanisms can be given in a canonical form for arbitrary reaction networks. The range of processes the resulting model deals with exceeds that of many simulation tools, on the one hand through the possibility to couple chemical reactions according to the mass action law (without the limiting assumption of local equilibrium) with biodegradation reactions that follow Monod kinetics and can be limited by a maximum biomass concentration or inhibitory species of arbitrary kind and number. On the other hand the incorporation in RICHY1D offers various advanced model components that can be combined with the reactive transport module, in particular simulations of (also preferential) water flow in the saturated and vadose zone, or of heat conduction in soils, which may have an impact on microbial activities.

The recombination of the partial differential equations, which is necessary if local equilibrium is assumed to eliminate rates, but is also an option to reduce the computational burden, is briefly presented.

For the general reactive multicomponent transport model a weak formulation is depicted that is discretized with the conforming Finite Element Method. In this H^1 -conforming setting also the immobile species equations are incorporated, what nevertheless does not lead to spatial couplings due to the

application of suitable quadrature rules.

The investigation of different solution strategies for the transport-reaction problems focusses on the operator splitting error that stems from the separate treatment of simultaneous processes. With the help of Lie operators and their commutators that express their interrelations, a convenient representation of this error is derived. The error is specified for the chemical and biological reaction terms of relevance, and situations void of splitting errors are characterized. This holds, e.g., for models with linear reaction terms independent of space, and a divergence free flow field; situations, though, that are of limited practical relevance. Thus the global implicit approach is pursued that treats subprocesses simultaneously, while Newton's method with Armijo's rule is used for the solution of the nonlinear problems.

As even in large chemical systems typically only few species are directly coupled in one reaction, the resulting sparse matrix structure in the finite element matrix can be exploited to reduce the computational effort. Through an analysis of the reaction network reducible matrix parts can be identified – even in course of the simulation – and solved separately. This presumes a flexible, component wise linear solver that has been implemented with the help of pointer lists. The reducibility of the Jacobian can also be enforced by the neglect of weak coupling terms which arise when small reaction rate constants or small concentrations occur. This corresponds to a modified Newton's method, then. If the convergence properties of the Newton scheme are not deteriorated substantially, a clear gain in efficiency can be reported. Numerical examples from the literature serve to verify the implementation of the multicomponent reaction systems. Systematic academic examples demonstrate the speed-up by neglecting weak couplings in the Jacobian, but not strong ones, and also the realistic EDTA degradation example can be accelerated by this technique. Finally the simulation tool is applied in a real case study with column experiments concerning the anaerobic degradation of propylene glycol, in order to comprehend the inherent degradation processes. By the analysis of data and scenarios the majority of the degradation mechanisms can be qualitatively detected and quantified. However, also nonuniqueness in the data curves can be demonstrated, what does not allow the identification of all degradation parameters from the experiments. The simulations indicate nevertheless how further experiments have to be designed such that remaining open questions could be answered.

Zusammenfassung

Die vorliegende Arbeit beschäftigt sich mit der Modellierung und numerischen Lösung von reaktiven hydrogeochemischen Mehrkomponenten-Transportproblemen in porösen Medien. Ziel war es dabei, verschiedene Lösungsstrategien zu beurteilen und ein effizientes Simulationswerkzeug bereitzustellen, das die vielfältigen gekoppelten Prozesse auch akkurat simultan im Lösungsalgorithmus behandelt.

Bezüglich der Modellbildung musste dazu ein bestehendes Einkomponenten-Transportmodell erweitert werden um Beschreibungen geochemischer Reaktionen in Fest- und Flüssigphase, sowie um eine adäquate Abbildung natürlicher, von Mikroorganismen katalysierter Abbauprozesse organischer Umweltschadstoffe. Die grundlegende Advektions-Dispersions-Reaktionsgleichung wird erläutert und um komplexe Modelle der wichtigsten reaktiven Prozesse ergänzt, so etwa um Sorptionsprozesse, die auch für kolloidale Träger-substanzen betrachtet werden können. Stöchiometrische Reaktionsmechanismen werden in einem formalen Rahmen präsentiert, welcher eine Darstellung beliebiger Reaktionsnetzwerke in einer kanonischen Form erlaubt.

Das resultierende Modell geht dabei im Umfang der abgebildeten Prozesse über die meisten vergleichbaren Simulationstools hinaus, einerseits durch die flexible Kopplungsmöglichkeit beliebiger chemischer Reaktionen nach dem Massenwirkungsgesetz (ohne die einschränkende Annahme lokalen Gleichgewichts) mit biologischen Reaktionen, welche der Monod-Kinetik folgen und durch eine maximale Biomassenkonzentration beschränkt werden können oder durch inhibierende Spezies jedweder Art und Zahl. Andererseits bietet die Einbettung in RICHY1D vielfältige fortgeschrittene Modellbeschreibungen an, die mit dem obigen reaktiven Transportmodell gekoppelt werden können, insbesondere Modelle des (auch präferenziellen) Wasserflusses in gesättigter und ungesättigter Zone, oder des Wärmetransports in Böden, welcher auch die biologischen Abbauparameter beeinflussen kann.

Die Rekombination der partiellen Differentialgleichungen, welche nötig ist bei Annahme lokalen Gleichgewichts zur Elimination von Raten, aber auch eine Möglichkeit zur Reduktion des Rechenaufwandes ist, wird kurz vorge-

stellt. Für das allgemeine reaktive Mehrkomponenten-Transportmodell wird eine schwache Formulierung entwickelt, welche mittels der Methode der konformen Finiten Elemente diskretisiert wird. Hierbei werden auch immobile Spezies in die H^1 -konforme Darstellung integriert, was durch Anwendung geeigneter Quadraturformeln in einer Raumdimension aber trotzdem keine räumlichen Kopplungen nach sich zieht.

Bei der Untersuchung verschiedener Lösungsalgorithmen für die gekoppelten Reaktions-Transportgleichungen wird vor allem der Verfahrensfehler durch Operator Splitting, der durch die getrennte Behandlung simultaner Prozesse entsteht, näher betrachtet. Mit Hilfe von Lie-Operatoren und deren Kommutatoren ergibt sich eine eingängige Darstellung des Splittingfehlers, der die Beziehungen zwischen den Prozessen beinhaltet. Der Splittingfehler wird insbesondere für die vorliegenden chemischen und biologischen Reaktionsterme im Transportmodell dargelegt, und Situationen mit verschwindendem Splittingfehler charakterisiert. Dies sind etwa Modelle mit linearen, ortsunabhängigen Reaktionstermen und divergenzfreiem Fließfeld, die jedoch für reale Situationen kaum von Relevanz sind.

Umsetzung findet deshalb der global implizite Ansatz, der die Prozesse simultan behandelt, wobei das Newtonverfahren mit Armijo-Regel zur Lösung genutzt wird. Da auch in großen chemischen Reaktionssystemen typischerweise nur wenige Spezies in einzelnen Reaktionen direkt miteinander gekoppelt sind, wird die dünnbesetzte Struktur der Matrixblöcke der FE-Diskretisierung ausgenutzt, um den Aufwand zur Lösung der resultierenden Gleichungssysteme mit dem Newton-Verfahren zu reduzieren.

Durch eine Analyse des Reaktionsnetzwerkes können reduzible Matrixkomponenten – auch während der Simulation – identifiziert werden, und effizient separat gelöst. Dies setzt einen flexiblen, komponentenweisen Gleichungslöser für das linearisierte System voraus, welcher mit Hilfe verzeigerter Listen implementiert wurde. Die Reduzibilität der Jacobimatrix kann auch durch die Vernachlässigung schwacher Kopplungsterme erzwungen werden, welche aufgrund kleiner Reaktionsratenkonstanten oder verschwindender Konzentrationen entstehen können, was einem modifizierten Newton-Verfahren entspricht. Sollte dadurch dessen Konvergenzgeschwindigkeit nicht stark reduziert werden, kann auch hier ein Effizienzgewinn beobachtet werden.

Numerische Beispiele aus der Literatur dienen zur Verifikation der Implementierung und Vergleich mit anderen Realisierungen. Systematische, akademische Beispielrechnungen zeigen den Effizienzgewinn durch die Entkopplung schwach gekoppelter Spezies, und auch das Referenzbeispiel zum EDTA-Abbau kann von dieser Methode profitieren. Schließlich wird das Simulationswerkzeug in einer realen experimentellen Studie mit Säulenversuchen zum anaeroben Abbau von Propylenglykol eingesetzt, um Aufschluss über zugrun-

deliegende Abbauprozesse zu gewinnen. Dabei können durch die Analyse von Szenarien und Daten ein Großteil der Prozessmechanismen qualitativ erklärt und quantifiziert werden, es werden aber auch Uneindeutigkeiten aufgezeigt, die Hinweise auf das Design zukünftiger Experimente geben, um zu einer zweifelsfreien Bestimmung der Reaktionsraten zu gelangen.

Bibliography

- [AM63] R. Aris and R. H. S. Mah. Independence of chemical reactions. *Industrial & Engineering Chemistry Fundamentals*, 2:90–94, 1963.
- [Ama95] H. Amann. *Linear and Quasilinear Parabolic Problems*. Birkhäuser, Basel, 1995.
- [AS89] M. Alexander and K. M. Scow. Kinetics of biodegradation in soil. In B. L. Sawhney and K. Brown, editors, *Reactions and Movement of Organic Chemicals in Soils*, pages 243–269, Madison, 1989. Soil Science Society of America.
- [BB86] R. C. Borden and P. B. Bedient. Transport of dissolved hydrocarbons influenced by oxygen-limited biodegradation, 1. Theoretical development. *Water Resources Research*, 22(13):1973–1982, 1986.
- [BE02] A. Brun and P. Engesgaard. Modelling of transport and biogeochemical processes in pollution plumes: literature review and model development. *Journal of Hydrology*, 256:211–227, 2002.
- [Bea72] J. Bear. *Dynamics of Fluids in Porous Media*. Dover, New York, 1972.
- [Bet96] C. M. Bethke. *Geochemical Reaction Modeling*. Oxford University Press, New York, 1996.
- [BK04] M. Bause and P. Knabner. Numerical simulation of contaminant biodegradation by higher order methods and adaptive time stepping. *Computing and Visualization in Science*, 39:61–78, 2004.

- [BMCH96] D. A. Barry, C. T. Miller, and P. J. Culligan-Hensley. Temporal discretisation errors in non-iterative split-operator approaches to solving chemical reaction/groundwater transport models. *Journal of Contaminant Hydrology*, 22:1–17, 1996.
- [Bra97] D. Braess. *Finite Elemente*. Springer, Berlin, second edition, 1997.
- [BWG98] B. A. Bekins, E. Warren, and E. M. Godsy. A comparison of zero-order, first-order, and Monod biotransformation models. *Ground Water*, 36(2):261–268, 1998.
- [CGS98] A. Chilakapati, T. Ginn, and J. Szecsody. An analysis of complex reaction networks in groundwater modeling. *Water Resources Research*, 34(7):1767–1780, 1998.
- [Cha01] F. H. Chapelle. *Ground-Water Microbiology and Geochemistry*. John Wiley & Sons, New York, second edition, 2001.
- [CHL03] Y. S. Choi, Z. Huan, and R. Liu. Global existence of solutions of a strongly coupled quasilinear parabolic system with applications to electrochemistry. *Journal of Differential Equations*, 194:406–432, 2003.
- [CMB04] J. Carrayrou, R. Mosé, and P. Behra. Operator-splitting procedures for reactive transport and comparison of mass balance errors. *Journal of Contaminant Hydrology*, 68:239–268, 2004.
- [Cui01] S. Cui. Local and global existence of solutions to semi-linear parabolic initial value problems. *Nonlinear Analysis*, 43(3):293–323, 2001.
- [Cur03] G. P. Curtis. Comparison of approaches for simulating reactive solute transport involving organic degradation reactions by multiple terminal electron acceptors. *Computers & Geosciences*, 29:319–329, 2003.
- [CYSM00] A. Chilakapati, S. Yabusaki, J. Szecsody, and W. MacEvoy. Groundwater flow, multicomponent transport and biogeochemistry: development and application of a coupled process model. *Journal of Contaminant Hydrology*, 43:303–325, 2000.
- [Deu04] P. Deuffhard. *Newton Methods for Nonlinear Problems*. Springer, Berlin, 2004.

- [DJTM92] F. M. Dunnivant, P. M. Jardine, D. L. Taylor, and J. F. McCarthy. Cotransport of cadmium and hexachlorobiphenyl by dissolved organic carbon through columns containing aquifer material. *Environmental Science & Technology*, 26:360–368, 1992.
- [dM86] G. de Marsily. *Quantitative Hydrogeology*. Academic Press, San Diego, 1986.
- [dM95] G. de Marsily. *L'Eau*. Flammarion, Paris, 1995.
- [DS98] P. A. Domenico and F. W. Schwartz. *Physical and Chemical Hydrogeology*. John Wiley & Sons, New York, second edition, 1998.
- [EK92] P. Engesgaard and K. L. Kipp. A geochemical transport model for redox-controlled movement of mineral fronts in groundwater flow systems: a case of nitrate removal by oxidation of pyrite. *Water Resources Research*, 28(10):2829–2843, 1992.
- [Eva98] L. C. Evans. *Partial Differential Equations*. American Mathematical Society, Providence, 1998.
- [Fet99] C. W. Fetter. *Contaminant Hydrogeology*. Prentice Hall, Upper Saddle River, second edition, 1999.
- [FR92] J. C. Friedly and J. Rubin. Solute transport with multiple equilibrium-controlled or kinetically controlled reactions. *Water Resources Research*, 28(6):1935–1953, 1992.
- [Fri91] J. C. Friedly. Extent of reaction in open systems with multiple heterogeneous reactions. *AIChE Journal*, 37(5):687–693, 1991.
- [FYB03] Y. Fang, G. T. Yeh, and W. D. Burgos. A general paradigm to model reaction-based biogeochemical processes in batch systems. *Water Resources Research*, 39(4):1083, 2003. doi:10.1029/2002WR001694.
- [GL96] G. H. Golub and C. F. Van Loan. *Matrix Computations*. The Johns Hopkins University Press, Baltimore, third edition, 1996.
- [Hol00] A. Holstad. A mathematical and numerical model for reactive fluid flow systems. *Computational Geosciences*, 4:103–139, 2000.

- [HV03] W. Hundsdorfer and J. Verwer. *Numerical Solution of Time-Dependent Advection-Diffusion-Reaction Equations*. Springer, Berlin, 2003.
- [HWvC98] K. S. Hunter, Y. Wang, and P. van Cappellen. Kinetic modeling of microbially-driven redox chemistry of subsurface environments: coupling transport, microbial metabolism and geochemistry. *Journal of Hydrology*, 209:53–80, 1998.
- [IK98] B. Iglér and P. Knabner. Identification of nonlinear sorption isotherms by soil column breakthrough experiments. *Physics and Chemistry of the Earth*, 23(2):215–219, 1998.
- [Ins05] Institute of Applied Mathematics, University of Erlangen. RICHY’s manual. <http://www.am.uni-erlangen.de/software/RichyDocumentation/>, 2005.
- [ISO01] J. Islam, N. Singhal, and M. O’Sullivan. Modeling biogeochemical processes in leachate-contaminated soils: a review. *Transport in Porous Media*, 43:407–440, 2001.
- [JA95] W. P. Johnson and G. L. Amy. Facilitated transport and enhanced desorption of polycyclic aromatic hydrocarbons by natural organic matter in aquifer sediments. *Environmental Science & Technology*, 29:807–817, 1995.
- [JK03] W. Jäger and H.J. Krebs, editors. *Mathematics - Key Technology for the Future*. Springer, Berlin, 2003.
- [JTKK05] P. Jaesche, K. U. Totsche, and I. Kögel-Knabner. Transport and anaerobic biodegradation of propylene glycol in gravel-rich soil materials. *to appear*, 2005.
- [KA03] P. Knabner and L. Angermann. *Numerical Methods for Elliptic and Parabolic Partial Differential Equations*, volume 44 of *Texts in Applied Mathematics*. Springer, New York, 2003.
- [Kas02] S. Kastner. Mathematische Modellierung und numerische Simulation von Selbstreinigungsprozessen. Master’s thesis, Friedrich-Alexander-Universität Erlangen-Nürnberg, Lehrstuhl für Angewandte Mathematik I, Germany, 2002.

- [Kel95] C. T. Kelley. *Iterative Methods for Linear and Nonlinear Equations*. SIAM, Philadelphia, 1995.
- [KKar] S. Kräutle and P. Knabner. A new numerical reduction scheme for fully coupled multicomponent transport-reaction problems in porous media. *Water Resources Research*, to appear.
- [KM95] J. J. Kaluarachchi and J. Morshed. Critical assessment of the operator-splitting technique in solving the advection-dispersion-reaction equation: 1. First-order reaction. *Advances in Water Resources*, 18(2):89–100, 1995.
- [KMB03] J. K. Kanney, C. T. Miller, and D. A. Barry. Comparison of fully coupled approaches for approximating nonlinear transport and reaction problems. *Advances in Water Resources*, 26:353–372, 2003.
- [KMK03] J. K. Kanney, C. T. Miller, and C. T. Kelley. Convergence of iterative split-operator approaches for approximating nonlinear reactive transport problems. *Advances in Water Resources*, 26:247–261, 2003.
- [Kna91] P. Knabner. *Mathematische Modelle für Transport und Sorption gelöster Stoffe in porösen Medien*. Peter Lang, Frankfurt/Main, 1991.
- [KS96] P. Knabner and E. Schneid. Qualitative properties of a model for carrier facilitated groundwater contaminant transport. In F. Keil et al., editor, *Scientific Computing in Chemical Engineering*, pages 129–135, Berlin, 1996. Springer.
- [KTKK96] P. Knabner, K. U. Totsche, and I. Kögel-Knabner. The modeling of reactive solute transport with sorption to mobile and immobile sorbents; 1. Experimental evidence and model development. *Water Resources Research*, 32(6):1611–1622, 1996.
- [Lic96] P. C. Lichtner. *Reactive Transport in Porous Media*, chapter Continuum formulation of multicomponent-multiphase reactive transport, pages 1–81. Reviews in Mineralogy 34. Mineralogical Society of America, Washington, 1996.
- [LLX03] Y. Li, Q. Liu, and C. Xie. Semilinear reaction-diffusion systems of several components. *Journal of Differential Equations*, 187:510–519, 2003.

- [LSO96] P. C. Lichtner, C. I. Steefel, and E. H. Oelkers, editors. *Reactive Transport in Porous Media*. Reviews in Mineralogy 34. Mineralogical Society of America, Washington, 1996.
- [LV99] D. Lanser and J. G. Verwer. Analysis of operator splitting for advection-diffusion-reaction problems from air pollution modelling. *Journal of Computational and Applied Mathematics*, 111:201–216, 1999.
- [LX03] Y. Li and C. Xie. Quasilinear parabolic systems of several components. *Mathematische Annalen*, 327:395–407, 2003.
- [Mar90] G. I. Marchuk. *Handbook of Numerical Analysis*, volume I, chapter Splitting and Alternating Direction Methods, pages 197–462. Elsevier, Amsterdam, 1990.
- [MCAS04] S. Molins, J. Carrera, C. Ayora, and M. W. Saaltink. A formulation for decoupling components in reactive transport problems. *Water Resources Research*, 40(10):W10301, 2004. doi:10.1029/2003WR002970.
- [Mer05] W. Merz. Global existence result of the Monod model in bioremediation. *Advances in Mathematical Sciences and Applications*, 2005. to appear.
- [MFB02] K. U. Mayer, E. O. Frind, and D. W. Blowes. Multicomponent reactive transport modeling in variably saturated porous media using a generalized formulation for kinetically controlled reactions. *Water Resources Research*, 38(9):1174, 2002. doi:10.1029/2001WR000862.
- [MH93] F. M. M. Morel and J. G. Hering. *Principles and Applications of Aquatic Chemistry*. John Wiley & Sons, New York, 1993.
- [MK95] J. Morshed and J. J. Kaluarachchi. Critical assessment of the operator-splitting technique in solving the advection-dispersion-reaction equation: 2. Monod kinetics and coupled transport. *Advances in Water Resources*, 18(2):101–110, 1995.
- [MN94] W. W. McNab Jr. and T. N. Narasimhan. Modeling reactive transport of organic compounds in groundwater using a partial redox disequilibrium approach. *Water Resources Research*, 30(9):2619–2635, 1994.

- [MR93] C. T. Miller and A. J. Rabideau. Development of split-operator, Petrov–Galerkin methods to simulate transport and diffusion systems. *Water Resources Research*, 29(7):2227–2240, 1993.
- [MT91] D. C. Mangold and C. F. Tsang. A summary of subsurface hydrological and hydrochemical models. *Reviews of Geophysics*, 29(1):51–79, 1991.
- [MZ89] J. F. McCarthy and J. M. Zachara. Subsurface transport of contaminants. *Environmental Science & Technology*, 19:469–502, 1989.
- [PA99] D. L. Parkhurst and C. A. J. Appelo. *User’s Guide to PHREEQC (Version 2)*. U. S. Geological Survey, Denver, Colorado, 1999.
- [PKST02] A. Prechtel, P. Knabner, E. Schneid, and K. U. Totsche. Simulation of carrier facilitated transport of phenanthrene in a layered soil profile. *Journal of Contaminant Hydrology*, 56(3-4):209–225, 2002.
- [QV94] A. Quarteroni and A. Valli. *Numerical Approximation of Partial Differential Equations*. Springer, Berlin, 1994.
- [RG94] J. N. Reddy and D. K. Gartling. *The Finite Element Method in Heat Transfer and Fluid Dynamics*. CRC Press, Boca Raton, 1994.
- [RNG⁺98] H. S. Rifai, C. J. Newell, J. R. Gonzales, S. Dendrou, L. Kennedy, and J. T. Wilson. BIOPLUME III: Natural attenuation decision support system; user’s guide. Technical Report EPA/600/R-98/010, Subsurface Protection and Remediation Division, U. S. Environmental Protection Agency, Ada, 1998.
- [RSK⁺97] M. Reinhard, S. Shang, P. K. Kitanidis, E. Orwin, G. D. Hopkins, and C. A. Lebron. In situ BTEX biotransformation under enhanced nitrate- and sulfate-reducing conditions. *Environmental Science & Technology*, 31(1):28–36, 1997.
- [Rub83] J. Rubin. Transport of reacting solutes in porous media: Relation between mathematical nature of problem formulation and chemical nature of reactions. *Water Resources Research*, 19(5):1231–1252, 1983.

- [RV96] B. E. Rittmann and J. M. VanBriesen. *Reactive Transport in Porous Media*, chapter Microbiological processes in reactive modeling, pages 311–334. Reviews in Mineralogy 34. Mineralogical Society of America, Washington, 1996.
- [RVV00] B. A. Robinson, H. S. Viswanathan, and A. J. Valocchi. Efficient numerical techniques for modeling multicomponent ground-water transport based upon simultaneous solution of strongly coupled subsets of chemical components. *Advances in Water Resources*, 23:307–324, 2000.
- [Saa96] F. Saaf. *A Study of Reactive Transport Phenomena in Porous Media*. PhD thesis, Rice University, Houston, USA, 1996.
- [SAC98] M. W. Saaltink, C. Ayora, and J. Carrera. A mathematical formulation for reactive transport that eliminates mineral concentrations. *Water Resources Research*, 34(7):1649–1656, 1998.
- [SCA00] M. W. Saaltink, J. Carrera, and C. Ayora. A comparison of two approaches for reactive transport modelling. *Journal of Geochemical Exploration*, 69-70:97–101, 2000.
- [SCA01] M. W. Saaltink, J. Carrera, and C. Ayora. On the behaviour of approaches to simulate reactive transport. *Journal of Contaminant Hydrology*, 48:213–235, 2001.
- [Sch98] M. Schirmer. *Investigation of Multiscale Biodegradation Processes: A Modelling Approach*. PhD thesis, University of Waterloo, Canada, 1998.
- [Sch00] E. Schneid. *Hybrid-Gemischte Finite-Elemente-Diskretisierung der Richards-Gleichung*. PhD thesis, Friedrich-Alexander-University Erlangen-Nuremberg, Germany, 2000.
- [SH96] J. E. Saiers and G. M. Hornberger. The role of colloidal kaolinite in the transport of cesium through laboratory sand columns. *Water Resources Research*, 32(1):33–41, 1996.
- [SM96a] K. Spitz and J. Moreno. *A Practical Guide to Groundwater and Solute Transport Modeling*. John Wiley & Sons, New York, 1996.
- [SM96b] C. I. Steefel and K. T. B. MacQuarrie. *Reactive Transport in Porous Media*, chapter Approaches to modeling of reactive

- transport in porous media, pages 83–129. Reviews in Mineralogy 34. Mineralogical Society of America, Washington, 1996.
- [SM96c] W. Stumm and J. J. Morgan. *Aquatic Chemistry*. John Wiley & Sons, New York, 1996.
- [SMFB00] M. Schirmer, J. W. Molson, E. O. Frind, and J. F. Barker. Biodegradation modelling of a dissolved gasoline plume applying independent laboratory and field parameters. *Journal of Contaminant Hydrology*, 46:339–374, 2000.
- [SSC94] J. M. Sanz-Serna and M. P. Calvo. *Numerical Hamiltonian Problems*. Chapman & Hall, London, 1994.
- [SSK98] D. Schäfer, W. Schäfer, and W. Kinzelbach. Simulation of reactive processes related to biodegradation in aquifers 1. Structure of the three-dimensional reactive transport model. *Journal of Contaminant Hydrology*, 31:167–186, 1998.
- [Str68] G. Strang. On the construction and comparison of difference schemes. *SIAM Journal on Numerical Analysis*, 5(3):506–517, 1968.
- [Str03] G. Strang. *Introduction to Linear Algebra*. Wellesley–Cambridge, Wellesley, third edition, 2003.
- [SY98] K. M. Salvage and G. T. Yeh. Development and application of a numerical model of kinetic and equilibrium microbiological and geochemical reactions (BIOKEMOD). *Journal of Hydrology*, 209:27–52, 1998.
- [SZC⁺98] J. E. Szecsody, J. M. Zachara, A. Chilakapati, P. M. Jardine, and A. S. Ferreny. Importance of flow and particle-scale heterogeneity on co(ii/iii)edta reactive transport. *Journal of Hydrology*, 209:112–136, 1998.
- [TDKK97] K. U. Totsche, J. Danzer, and I. Kögel-Knabner. Dissolved organic matter-enhanced retention of polycyclic aromatic hydrocarbons in soil miscible displacement experiments. *Journal of Environmental Quality*, 26:1090–1100, 1997.
- [Tho97] V. Thomée. *Galerkin Finite Element Methods for Parabolic Problems*. Springer, Berlin, 1997.

- [TKKK96] K. U. Totsche, P. Knabner, and I. Kögel-Knabner. The modeling of reactive solute transport with sorption to mobile and immobile sorbents; 2. Model discussion and numerical simulation. *Water Resources Research*, 32(6):1623–1634, 1996.
- [vdLD01] J. van der Lee and L. De Windt. Present state and future directions of modeling of geochemistry in hydrogeological systems. *Journal of Contaminant Hydrology*, 47:265–282, 2001.
- [vdLDLG03] J. van der Lee, L. De Windt, V. Lagneau, and P. Goblet. Module-oriented modeling of reactive transport with HYTEC. *Computers & Geosciences*, 29:265–275, 2003.
- [vGA82] M. Th. van Genuchten and W. J. Alves. Analytical solutions of the one-dimensional convective-dispersive solute transport equation. Technical Report 1661, U. S. Department of Agriculture, 1982.
- [VM92] A. J. Valocchi and M. Malmstead. Accuracy of operator splitting for advection-dispersion-reaction problems. *Water Resources Research*, 28(5):1471–1476, 1992.
- [Ž90] A. Ženíšek. *Nonlinear Elliptic and Evolution Problems and Their Finite Element Approximations*. Academic Press, London, 1990.
- [WD87] M. F. Wheeler and C. N. Dawson. An operator-splitting method for advection-diffusion-reaction problems. Technical Report TR87-09, Department of Computational and Applied Mathematics, Rice University, Houston, 1987.
- [Whi95] S. P. White. Multiphase nonisothermal transport of systems of reacting chemicals. *Water Resources Research*, 31(7):1761–1772, 1995.
- [WMB88] M. A. Widdowson, F. J. Molz, and L. D. Benefield. A numerical transport model for oxygen- and nitrate-based respiration linked to substrate and nutrient availability in porous media. *Water Resources Research*, 24(9):1553–1565, 1988.
- [WT98] H. Weigand and K. U. Totsche. Flow and reactivity effects on dissolved organic matter transport in soil columns. *Soil Sci. Soc. Am. J.*, 62:1268–1274, 1998.

- [WTKK⁺02] H. Weigand, K. U. Totsche, I. Kögel-Knabner, E. Annweiler, H. H. Richnow, and W. Michaelis. Fate of anthracene in contaminated soil – transport and biodegradation under unsaturated flow conditions. *European Journal of Soil Science*, 53:71–82, 2002.
- [XPB99] T. Xu, K. Pruess, and G. Brimhall. An improved equilibrium-kinetics speciation algorithm for redox reactions in variably saturated subsurface flow systems. *Computers & Geosciences*, 25:655–666, 1999.
- [YT89] G. T. Yeh and V. S. Tripathi. A critical evaluation of recent developments in hydrogeochemical transport models of reactive multichemical components. *Water Resources Research*, 25(1):93–108, 1989.
- [YT91] G. T. Yeh and V. S. Tripathi. A model for simulating transport of reactive multispecies components: Model development and demonstration. *Water Resources Research*, 27(12):3075–3094, 1991.
- [ZSD94] A. Zysset, F. Stauffer, and T. Dracos. Modeling of chemically reactive groundwater transport. *Water Resources Research*, 30(7):2217–2228, 1994.

Curriculum vitae

Name: Alexander Prechtel
Adresse: Fleischstr. 11, 96047 Bamberg, Deutschland
Geburtsdatum: 23. Juli 1971
Geburtsort: Kulmbach, Deutschland
Nationalität: deutsch
Familienstand: verheiratet

BILDUNGSWEG

1977–1981 Grundschule Laineck
1981–1990 Graf–Münster–Gymnasium Bayreuth
6/1990 Abitur
1991–1997 Studium der Mathematik an der Universität Bayreuth
Nebenfach: Geoökologie mit Schwerpunkt Hydrologie
8/1997 Diplom in Mathematik
Diplomarbeit in Räumlicher Statistik (Prof. Dr. Dr. h.c. P. J. Huber): Die Schätzung von Variogrammen durch Betrachtung ihrer Integrale
1997–1998 Studium der Hydrogeologie, Hydrologie, Geostatistik und Geochemie an der École Nationale Supérieure des Mines de Paris (Frankreich)
10/1998 Diplom für vertiefte Studien (D.E.A.: Diplome d'Etudes Approfondies) in Hydrogeologie, Hydrologie, Geostatistik und Geochemie
Diplomarbeit (Prof. Dr. P. Chauvet): La pollution d'un site par des hydrocarbures - aspects de la modélisation hydrogéologique et étude géostatistique
seit 4/1999 Promotionsstudium in Mathematik am Institut für Angewandte Mathematik der Friedrich–Alexander–Universität Erlangen–Nürnberg

WEHR- UND ZIVILDIENTST

- 7/1990–4/1991 Panzergrenadierbataillon, Markgrafenkaserne Bayreuth
4/1991–9/1991 Klinik für Rückenmarksverletzte Hohe Warte, Bayreuth

BERUFLICHER WERDEGANG

- 4/1999–12/2000 Wissenschaftlicher Mitarbeiter am Institut
und für Angewandte Mathematik, FAU
2/2001–heute Beschäftigung in folgenden *Drittmittelprojekten*:
- “Einfluss von Tensiden auf die Schadstoffausbreitung und Sanierungsmaßnahmen im Boden” (BMBF–Förderschwerpunkt “Mathematische Verfahren zur Lösung von Problemstellungen in Industrie und Wirtschaft”),
 - “Mathematische Modellsimulation zur Identifizierung der Quellstärke von Schadstoffen und zur Vorhersage des Transports in den Grundwasserleiter” (BMBF–Förderschwerpunkt Sickerwasserprognose),
 - “Modellierung” (BayStMLU, Verbundvorhaben “Nachhaltige Altlastenbewältigung unter Einbeziehung des natürlichen Reinigungsvermögens”),
 - “Modellierung des reaktiven Transports von Schadstoffen in der (un-)gesättigten Bodenzone zur Prognose der natürlichen Selbstreinigung” (BMBF–Förderschwerpunkt “Kontrollierter natürlicher Rückhalt und Abbau von Schadstoffen bei der Sanierung kontaminierter Böden und Grundwässer”)

Lehrveranstaltungen:

- Übungen zur Mathematik für Ingenieure I-III
- Übung zu Numerical Methods for Partial Differential Equations

VERÖFFENTLICHUNGEN

E. Schneid, A. Prechtel and P. Knabner (2000): *A Comprehensive Tool for the Simulation of Complex Reactive Transport and Flow in Soils*. Land Contamination & Reclamation 8, 4, 357-365.

A. Prechtel, P. Knabner, E. Schneid and K. U. Totsche (2002): *Simulation of Carrier Facilitated Transport of Phenanthrene in a Layered Soil Profile*. Journal of Contaminant Hydrology, 56, 3-4, 209-225.

A. Prechtel and P. Knabner (2002): *Accurate and Efficient Simulation of Coupled Water Flow and Nonlinear Reactive Transport in the Saturated and Vadose Zone - Application to Surfactant Enhanced and Intrinsic Bioremediation*. In S. M. Hassanizadeh et al. (eds.): *Computational Methods in Water Resources*, Elsevier, Amsterdam, 687-694.

P. Knabner, S. Bitterlich, R. Iza Teran, A. Prechtel, and E. Schneid (2003): *Influence of Surfactants on Spreading of Contaminants and Soil Remediation*. In: W. Jäger and H. J. Krebs (eds.): *Mathematics - Key Technology for the Future*, Springer, Berlin, 152-161.

Ch. de Fouquet, A. Prechtel, and J.-C. Setier (2004): *Estimation de la concentration en hydrocarbures totaux du sol d'un ancien site pétrochimique: étude méthodologique*. Oil & Gas Science and Technology 59 (3), 275-295.

A. Prechtel, S. Bitterlich, F. Radu, and P. Knabner (2005): *Natural Attenuation: hohe Anforderungen an die Modellsimulation*. Grundwasser, to appear.